

**RHEOLOGICAL PROPERTIES OF NATURAL  
RUBBER LATEX**

**Jatuporn Sridee**

**A Thesis Submitted in Partial Fulfillment of the Requirements for the**

**Degree of Master of Engineering in Polymer Engineering**

**Suranaree University of Technology**

**Academic Year 2006**

**ISBN 974-533-588-6**

# วิทยากระแสของน้ำอย่างธรรมชาติ

นายจตุพร ศรีดี

วิทยานิพนธ์นี้เป็นส่วนหนึ่งของการศึกษาตามหลักสูตรปริญญาวิศวกรรมศาสตรมหาบัณฑิต

สาขาวิชาวิศวกรรมพอลิเมอร์

มหาวิทยาลัยเทคโนโลยีสุรนารี

ปีการศึกษา 2549

ISBN 974-533-588-6

## RHEOLOGICAL PROPERTIES OF NATURAL RUBBER LATEX

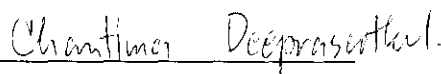
Suranaree University of Technology has approved this thesis submitted in partial fulfillment of the requirements for a Master's Degree.

Thesis Examining Committee



(Asst. Prof. Dr. Yupaporn Ruksakulpiwat)

Chairperson



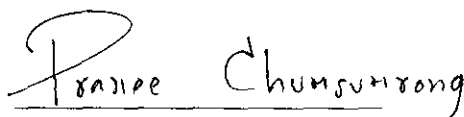
(Asst. Prof. Dr. Chantima Deeprasertkul)

Member (Thesis Advisor)



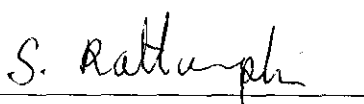
(Asst. Prof. Dr. Chaiwat Ruksakulpiwat)

Member



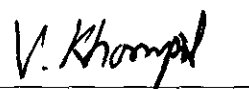
(Asst. Prof. Dr. Pranee Chumsumrong)

Member



(Assoc. Prof. Dr. Saowanee Rattanaphani)

Vice Rector for Academic Affairs



(Assoc. Prof. Dr. Vorapot Khompis)

Dean of Institute of Engineering

จตุพร ศรีดี : วิทยากระแสของน้ำยางธรรมชาติ (RHEOLOGICAL PROPERTIES  
OF NATURAL RUBBER LATEX) อาจารย์ที่ปรึกษา : ผศ. ดร.จันทิมา  
ตีประเสริฐกุล, 101 หน้า. ISBN 974-533-588-6

วิทยานิพนธ์นี้ทำการศึกษาวิทยากระแสของน้ำยางธรรมชาติชั้นชนิดแอมโมเนียสูงที่ผลิตในประเทศไทย ตัวอย่างของน้ำยางธรรมชาติที่ใช้ในการศึกษาถูกเตรียมที่ความเข้มข้นในช่วง 48-68 เปอร์เซ็นต์โดยน้ำหนักของปริมาณของแข็งทั้งหมด โดย 2 วิธีคือ (1) ทำการเจือจางน้ำยางชั้นที่ได้รับโดยตรง และ (2) ทำการเจือจางจากน้ำยางชั้นที่ผ่านการปั่นซ้ำ

จากการศึกษาด้วยเทคนิคการเลี้ยวเบนของแสง พบว่า น้ำยางที่ใช้ในการศึกษามีการกระจายตัวของอนุภาคแบบกระจาย (Polydisperse) และมีค่าเฉลี่ยเส้นผ่านศูนย์กลางโดยปริมาตร ( $D[4,3]$ ) ของน้ำยางธรรมชาติที่เตรียมโดยวิธีที่ (1) อยู่ในช่วง 0.74-0.94 ไมโครเมตร และวิธีที่ (2) 0.81-0.89 ไมโครเมตร และจากเทคนิคไมโครสโคปีแบบอิเล็กตรอนส่องผ่าน (TEM) พบว่า อนุภาคยางมีลักษณะเป็นทรงกลม และมีการกระจายตัวของอนุภาคแบบกระจายเช่นกัน ในช่วงอัตราเฉือนที่ใช้ 3.06-122.58 ต่อวินาที พบว่าน้ำยางธรรมชาติแสดงพฤติกรรมแบบเชิยรทินนิ่ง (shear thinning) เมื่ออนุภาคของยางได้รับแรงเฉือนจะมีการเปลี่ยนรูปร่างและมีการจัดเรียงตัวจากทิศทางของแรงเฉือนที่ได้รับ ทำให้ความหนืดของน้ำยางลดลง น้ำยางที่มีอนุภาคของขนาดใหญ่ให้ความหนืดต่ำกว่าน้ำยางที่มีขนาดอนุภาคเล็ก เนื่องจากอนุภาคใหญ่มีพื้นที่ผิวสัมผัสต่อปริมาตรน้อยกว่าอนุภาคขนาดเล็ก นอกจากนี้พบว่าความหนืดของน้ำยางเพิ่มขึ้นเมื่อปริมาณของแข็งเพิ่มขึ้น โดยเพิ่มขึ้นอย่างช้า ๆ จนถึงปริมาณของแข็งวิกฤต (TSC) ความหนืดจะเพิ่มขึ้นอย่างรวดเร็ว การเพิ่มที่รวดเร็วของความหนืดนี้อาจเกิดจากการเข้าสู่การจัดเรียงตัวของอนุภาคสูงสุด ( $\phi_{max}$ ) ปริมาณของแข็งวิกฤตของน้ำยางจากวิธีที่ (1) อยู่ในช่วง 58-60 เปอร์เซ็นต์โดยน้ำหนักของปริมาณของแข็งและจากวิธีที่ (2) อยู่ในช่วง 59-61 เปอร์เซ็นต์โดยน้ำหนักของปริมาณของแข็ง เมื่อศึกษาผลของอุณหภูมิในช่วง 10-40 องศาเซลเซียส เมื่ออุณหภูมิเพิ่มขึ้นความหนืดของน้ำยางลดลง ขณะที่ความหนืดสัมพัทธ์ของน้ำยางมีค่าเพิ่มขึ้น ซึ่งให้เห็นว่าความหนืดของตัวกลาง (น้ำ) ลดลงเร็วกว่าความหนืดของน้ำยางธรรมชาติเมื่อเพิ่มอุณหภูมิ จากการประยุกต์ใช้สมการของ Mooney และ Krieger-Dougherty กับน้ำยางธรรมชาติชั้น พบว่า สมการทั้งสองสามารถใช้ได้ดีและมีค่าสัมประสิทธิ์สหสัมพันธ์มากกว่า 0.99

สาขาวิชา วิศวกรรมพอลิเมอร์

ปีการศึกษา 2549

ลายมือชื่อนักศึกษา จตุพร ศรีดี

ลายมือชื่ออาจารย์ที่ปรึกษา จันทิมา ตีประเสริฐกุล

ลายมือชื่ออาจารย์ที่ปรึกษาร่วม จ ร

JATUPORN SRIDEE : RHEOLOGICAL PROPERTIES OF NATURAL  
RUBBER LATEX. THESIS ADVISOR : ASST. PROF. CHANTIMA  
DEEPRASERTKUL, Ph.D. 101 PP. ISBN 974-533-588-6

NATURAL RUBBER LATEX CONCENTRATES/ VISCOSITY/ TOTAL SOLIDS  
CONTENT/ TEMPERATURE/ MOONEY/ KRIEGER-DOUGHERTY

In this thesis, the rheological property of high ammonia (HA) natural rubber latex (NRL) concentrates produced in Thailand was investigated. The samples were prepared by two methods; (1) directly diluted from received latex and (2) diluted from re-centrifuged NRL concentrates. The samples were prepared in the range of 48-68 (% by weight) total solids contents (TSC).

From laser diffraction, the z-average diameters ( $D[4,3]$ ) of samples were in the range of 0.74-0.93  $\mu\text{m}$  for directly diluted NRL samples and 0.81-0.89  $\mu\text{m}$  for re-centrifuged NRL samples. All samples showed polydisperse system. TEM micrographs showed the spherical shape and polydisperse rubber particles. At shear rates range of 3.06-122.58  $\text{sec}^{-1}$ , shear thinning behavior was observed in all samples. Large particles gave lower viscosity than small particles because of smaller surface area per unit volume in larger particles. Latex viscosity slowly increased with increasing percent TSC up to the critical total solids content ( $\text{TSC}_c$ ). At upper than the  $\text{TSC}_c$ , viscosity rapidly increased with increasing TSC. The rapid increase of viscosity can be explained by the approach to maximum packing volume ( $\phi_{\text{max}}$ ) of system. The  $\text{TSC}_c$  was in the range of 58-60% TSC for directly diluted NRL and 59-61% TSC for diluted re-centrifuged NRL. The latex viscosity decreased with temperature in the

range of 10 to 40°C. However, the relative viscosity of latex increased with temperature suggesting that viscosity of the medium changes more dramatic than viscosity of the latex itself with temperature. Mooney and Krieger-Dougherty equation showed the good fitting in latex viscosity with the correlation coefficients ( $R^2$ ) higher than 0.99.

School of Polymer Engineering

Academic Year 2006

Student's Signature Jatuporn Sridee

Advisor's Signature Chantima Deeparasitkul

Co-advisor's Signature Chairat Kulsabulpornat

## **ACKNOWLEDGEMENTS**

I received helps and encouragements from many people during my graduate studies. I would like to recognize and sincerely thank them who helped my studies at Suranaree University of Technology a pleasant one and who helped a completion of this degree possible.

Assistant Professor Dr. Chantima Deeprasertkul, my advisor and my teacher, for her guidance, assistance, professional and personal advice, and her supports. Assistant Professor Dr. Chaiwat Ruksakulpiwat, my co-advisor, for his guidance, encouragement and supports. Assistant Professor Dr. Utai Meekum, my teacher, who gave me the opportunity to increase my knowledge in Master degree of polymer engineering. All lecturers and staffs at the School of Polymer Engineering for valuable suggestion, recommendation and make all works to be good memory and success. Good friends in the School of Polymer Engineering for their kindness. This project was partly funded by The Thai Research Fund.

Most importantly, I would like to give the biggest thank to my parents for their love, understanding, supports, suggestion throughout the course of this study at the Suranaree University of Technology.

Jatuporn Sridee

# TABLE OF CONTENTS

	<b>PAGE</b>
ABSTRACT (THAI) .....	I
ABSTRACT (ENGLISH).....	II
ACKNOWLEDGEMENTS.....	IV
TABLE OF CONTENTS.....	V
LIST OF TABLES.....	VIII
LIST OF FIGURES .....	X
SYMBOLS AND ABBREVIATIONS.....	XV
<b>CHAPTER</b>	
<b>I INTRODUCTION</b> .....	<b>1</b>
1.1 General introduction .....	1
1.2 Research objectives.....	5
1.3 Scope and limitation of the study.....	6
<b>II LITERATURE REVIEW</b> .....	<b>7</b>
2.1 Natural rubber latex .....	7
2.2 Particle interaction.....	9
2.3 Factors affecting the viscosity of latex system.....	11
2.3.1 Particle and particle size distribution (PSD) .....	11
2.3.2 Total solids content .....	15

## TABLE OF CONTENTS (Continued)

	<b>PAGE</b>
2.3.3 Temperature.....	15
2.4 Theoretical equations for latex viscosity.....	16
<b>III EXPERIMENTAL</b> .....	<b>20</b>
3.1 General background .....	20
3.2 Materials and chemical reagents .....	20
3.2.1 High ammonia (HA) natural latex concentrates.....	20
3.2.2 Acetic acid.....	21
3.2.3 Osmium tetroxide .....	22
3.2.4 Poly vinyl-formvar .....	22
3.2.5 Polystyrene latex .....	22
3.3 Experimental .....	22
3.3.1 NRL sample preparation .....	22
3.3.2 Determination of total solids content .....	25
3.3.3 Determination of dry rubber content .....	26
3.3.4 Determination of particle size and particle size distribution.....	27
3.3.4.1 Laser diffraction .....	27
3.3.4.2 Transmission electron microscopy (TEM).....	28
3.3.5 Viscosity measurement.....	29
3.3.6 Density measurement.....	33

## TABLE OF CONTENTS (Continued)

	<b>PAGE</b>
<b>IV RESULTS AND DISCUSSIONS</b> .....	35
4.1 Total solids content and dry rubber content.....	35
4.2 Particle size and particle size distribution .....	39
4.2.1 Laser diffraction technique.....	39
4.2.2 Transmission electron microscopy (TEM).....	44
4.3 Flow behavior of natural rubber latex concentrates .....	48
4.4 Effect of particle size and PSD on the latex viscosity.....	55
4.5 Effect of total solids content on the viscosity.....	60
4.6 Effect of temperature on the viscosity.....	69
4.7 Viscosity models .....	76
<b>V CONCLUSIONS</b> .....	88
REFERENCES .....	91
APPENDICES	
APPENDIX A DENSITY AND VISCOSITY OF WATER AT DIFFERENT TEMPERATURES.....	97
APPENDIX B POSTER PRESENTATIONS.....	99
BIOGRAPHY .....	101

## LIST OF TABLES

TABLE	PAGE
2.1 Compositions of the total solids content in natural rubber latex (Crowther, 1982).....	8
2.2 List of methods used to measure PSD and average particle size (Schneider and McKenna, 2002).....	14
3.1 Specification of HA NRL used according to suppliers.....	21
3.2 Abbreviation of HA NRL sample samples .....	25
3.3 Relationship between motor speed (revolution per minutes, rpm) and shear rate ( $\text{sec}^{-1}$ ) of UL-A and SC4-21 sample cups .....	32
3.4 List of experimental shear rate conditions of HA NRL concentrated samples at $25^{\circ}\text{C}$ .....	32
4.1 Total solid contents (TSC) and dry rubber content (DRC) of NRL samples prepared by direct dilution of as received NRL concentrates.....	36
4.2 Total solid contents (TSC) and dry rubber content (DRC) of NRL samples prepared by dilution of re-centrifuged NRL concentrates .....	37
4.3 The summary of z-average diameter ( $D[4,3]$ ), standard deviation ( $\sigma$ ), skewness ( $S_k$ ) and polydispersity ( $P_d$ ) of concentrated NRL samples.....	44

## LIST OF TABLES (Continued)

TABLE	PAGE
4.4 The summary of number of counted particles, z-average diameter ( $D[4,3]$ ), standard deviation ( $\sigma$ ), and polydispersity ( $P_d$ ) of CO <sub>1</sub> , SO <sub>1</sub> , UO <sub>1</sub> and UO <sub>2</sub> samples obtained from TEM .....	48
4.5 The normalized surface area per volume of NRL samples by surface area per volume of CC <sub>1</sub> sample .....	60
4.6 The critical total solids content (TSC <sub>c</sub> ) of NRL samples determined from slope intersection .....	68
4.7 Density of natural rubber latexes .....	77
4.8 Maximum packing volume ( $\phi_{max}$ ), intrinsic viscosity ( $[\eta]$ ) and correlation coefficient ( $R^2$ ) from graph fitting using Mooney equation .....	84
4.9 Maximum packing volume ( $\phi_{max}$ ), intrinsic viscosity ( $[\eta]$ ) and correlation coefficient ( $R^2$ ) from graph fitting using Krieger-Dougherty equation .....	85
4.10 Average maximum packing volume calculated from Mooney equation and Krieger-Dougherty equation .....	87
A.1 Density and viscosity of water at different temperatures (Yaws, 1999) .....	98

## LIST OF FIGURES

FIGURE	PAGE
1.1 Production of natural rubber from main agricultural producers in the world (Rubber Research Institute of Thailand, 2006).....	2
1.2 Production of natural rubber in each rubber category in Thailand (Rubber Research Institute of Thailand, 2006).....	4
1.3 The natural rubber production exported from Thailand (Rubber Research Institute of Thailand, 2006).....	5
2.1 Chemical structure of cis-1,4-polyisoprene in Hevea latex .....	8
2.2 The concentrated silica suspension viscosity data fitted to the theoretical models. The short dash line is drawn according to Einstein equation. The dash-dot line is drawn according to Vand equation with $k_2 = 5$ . The solid line is drawn according to Krieger-Dougherty equation with $\phi_{\max} = 0.631$ and $[\eta] = 3.17$ . The dotted line is drawn according to Mooney model with $\phi_{\max} = 0.631$ and $[\eta] = 3.17$ (Jones et al., 1991) .....	19
3.1 The flow chart of experimental design .....	23
3.2 Schematic of a coaxial cylinder viscometer.....	30
4.1 Particle size distribution of rubber particles in the received NRL concentrates (CO <sub>1</sub> , SO <sub>1</sub> , UO <sub>1</sub> , UO <sub>2</sub> , and UO <sub>3</sub> samples).....	40
4.2 Particle size distribution of rubber particles in the re-centrifuged NRL concentrates (CC <sub>1</sub> , SC <sub>1</sub> , UC <sub>1</sub> , UC <sub>2</sub> and UC <sub>3</sub> samples).....	41

## LIST OF FIGURES (Continued)

FIGURE	PAGE
4.3 TEM micrograph of $220 \pm 6$ nm standard polystyrene taken at different positions.....	45
4.4 TEM micrograph of CO <sub>1</sub> taken at different positions .....	46
4.5 TEM micrograph of SO <sub>1</sub> taken at different positions.....	46
4.6 TEM micrograph of UO <sub>1</sub> taken at different positions .....	47
4.7 TEM micrograph of UO <sub>2</sub> taken at different positions .....	47
4.8 A plot of viscosity at 25°C against shear rate of Chonburi NRL concentrates at various TSC: CO <sub>1</sub> (closed symbols) and CC <sub>1</sub> (opened symbols).....	50
4.9 A plot of viscosity at 25°C against shear rate of Suratthani NRL concentrates at various TSC: SO <sub>1</sub> (closed symbols) and SC <sub>1</sub> (opened symbols).....	51
4.10 A plot of viscosity at 25°C against shear rate of Udonthani lot 1 NRL concentrates at various TSC: UO <sub>1</sub> (closed symbols) and UC <sub>1</sub> (opened symbols).....	52
4.11 A plot of viscosity at 25°C against shear rate of Udonthani lot 2 NRL concentrates at various TSC: UO <sub>2</sub> (closed symbols) and UC <sub>2</sub> (opened symbols).....	53

## LIST OF FIGURES (Continued)

<b>FIGURE</b>	<b>PAGE</b>
4.12 A plot of viscosity at 25°C against shear rate of Udornthani lot 3 NRL concentrates at various TSC: UO <sub>3</sub> (closed symbols) and UC <sub>3</sub> (opened symbols).....	54
4.13 Relative viscosity at various particle sizes as a function of TSC at shear rate of 3.06 sec <sup>-1</sup> and temperature of 25°C: directly diluted samples (closed symbols) and diluted from re-centrifugation NRL (opened symbols).....	56
4.14 Relative viscosity at various particle sizes as a function of TSC at shear rate of 6.13 sec <sup>-1</sup> and temperature of 25°C: directly diluted samples (closed symbols) and diluted from re-centrifugation NRL (opened symbols).....	57
4.15 Relative viscosity at various particle sizes as a function of TSC at shear rate of 12.26 sec <sup>-1</sup> and temperature of 25°C: directly diluted samples (closed symbols) and diluted from re-centrifugation NRL (opened symbols).....	58
4.16 Relative viscosity at various shear rates as a function of TSC of Chonburi NRL at temperature of 25°C: CO <sub>1</sub> (closed symbols) and CC <sub>1</sub> (opened symbols).....	62

## LIST OF FIGURES (Continued)

FIGURE	PAGE
4.17 Relative viscosity at various shear rates as a function of TSC of Suratthani lot 1 NRL at temperature of 25°C: SO <sub>1</sub> (closed symbols) and SC <sub>1</sub> (opened symbols) .....	63
4.18 Relative viscosity at various shear rates as a function of TSC of Udonrthani lot 1 NRL at temperature of 25°C: UO <sub>1</sub> (closed symbols) and UC <sub>1</sub> (opened symbols) .....	64
4.19 Relative viscosity at various shear rates as a function of TSC of Udonrthani lot 2 NRL at temperature of 25°C: UO <sub>2</sub> (closed symbols) and UC <sub>2</sub> (opened symbols) .....	65
4.20 Relative viscosity at various shear rates as a function of TSC of Udonrthani lot 3 NRL at temperature of 25°C: UO <sub>3</sub> (closed symbols) and UC <sub>3</sub> (opened symbols) .....	66
4.21 The determination of critical totals solid content (TSC <sub>c</sub> ) is illustrated .....	67
4.22 Effect of temperature on (a) the viscosity (b) relative viscosity of UO <sub>3,56</sub> at various shear rates .....	71
4.23 Effect of temperature on (a) the viscosity (b) relative viscosity of UO <sub>3,60</sub> at various shear rates .....	72
4.24 Effect of temperature on (a) the viscosity (b) relative viscosity of UC <sub>3,56</sub> at various shear rates .....	73

## LIST OF FIGURES (Continued)

FIGURE	PAGE
4.25 Effect of temperature on (a) the viscosity (b) relative viscosity of UC <sub>3,60</sub> at various shear rates.....	74
4.26 Effect of temperature on (a) the viscosity (b) relative viscosity of UC <sub>3,64</sub> at various shear rates.....	75
4.27 Relative viscosity of CC <sub>1</sub> at shear rate of 3.06 (●) and 12.26 sec <sup>-1</sup> (▲). The dotted lines are drawn according to Mooney equation. The solid lines are drawn according to Krieger-Dougherty equation.....	79
4.28 Relative viscosity of SC <sub>1</sub> at shear rate of 3.06 (●), 12.26 sec <sup>-1</sup> (▲) and 92.68 sec <sup>-1</sup> (■). The dotted lines are drawn according to Mooney equation. The solid lines are drawn according to Krieger-Dougherty equation. ....	80
4.29 Relative viscosity of UC <sub>1</sub> at shear rate of 3.06 (●) and 12.26 sec <sup>-1</sup> (▲). The dotted lines are drawn according to Mooney equation. The solid lines are drawn according to Krieger-Dougherty equation.....	81
4.30 Relative viscosity of UC <sub>2</sub> at shear rate of 3.06 (●), 12.26 sec <sup>-1</sup> (▲) and 92.68 sec <sup>-1</sup> (■). The dotted lines are drawn according to Mooney equation. The solid lines are drawn according to Krieger-Dougherty equation.. ....	82
4.31 Relative viscosity of UC <sub>3</sub> at shear rate of 3.06 (●) and 12.26 sec <sup>-1</sup> (▲). The dotted lines are drawn according to Mooney equation. The solid lines are drawn according to Krieger-Dougherty equation.....	83

## SYMBOLS AND ABBREVIATIONS

### Symbols

$\omega$	=	Angular velocity of spindle (rad/sec) = $(2\pi \times \text{rpm}/60)$
$\rho$	=	Density ( $\text{g}/\text{cm}^3$ )
$\rho_{\text{rubber}}$	=	Density of rubber ( $\text{g}/\text{cm}^3$ )
$\rho_{\text{water}}$	=	Density of water ( $\text{g}/\text{cm}^3$ )
L	=	Effective length of spindle (cm)
$[\eta]$	=	Intrinsic viscosity
$k_2$	=	An adjustable constant ( $k_2$ is between 2.5 to 9)
$m_p$	=	Mass of latex sample in pycnometer
$m_{\text{rubber}}$	=	Mass of rubber in latex sample
$m_{\text{rubber}}$	=	Mass of water in latex sample
$m_0$	=	Mass of initial latex sample
$m_1$	=	Mass of dried latex sample
$\phi_{\text{max}}$	=	Maximum packing volume
$D[1,0]$	=	Mean average diameter by number average
$D[2,0]$	=	Mean average diameter by surface area average
$D[3,0]$	=	Mean average diameter by volume average
$D[3,2]$	=	Mean average diameter by volume/area average
$D[4,3]$	=	Mean average diameter by volume/diameter or z-average diameter

## SYMBOLS AND ABBREVIATIONS (Continued)

### Symbols (continued)

$d_i$	=	Mean class diameter in class $i$
$\bar{d}$	=	Mean diameter by volume average
M	=	Percent of torque from reading (Maximum = 7,187 dynes/cm <sup>2</sup> )
$P_d$	=	Polydispersity index
$R_c$	=	Radius of container (cm)
$R_b$	=	Radius of spindle (cm)
$\eta_r$	=	Relative viscosity of the latex
$V_i$	=	Relative volume in class $i$
rpm	=	Revolution per minute
$S_k$	=	Skewness
$\dot{\gamma}$	=	Shear rate (sec <sup>-1</sup> )
$\tau$	=	Shear stress (dynes/cm <sup>2</sup> )
$\sigma$	=	Standard deviation
$\eta$	=	Viscosity of latex
$\eta_0$	=	Viscosity of the latex medium
V	=	Volt
$v$	=	Volume
$v_p$	=	Volume of density bottom (cm <sup>3</sup> )
$v_{\text{rubber}}$	=	Volume of rubber in latex sample (cm <sup>3</sup> )
$v_{\text{water}}$	=	Volume of water in latex sample (cm <sup>3</sup> )

**SYMBOLS AND ABBREVIATIONS (Continued)****Symbols (continued)**

$\phi$  = Volume fraction

w = Weight

**Abbreviations**

AA = Acrylic acid

BA = Butyl acrylate

CDHF = Capillary hydrodynamic fraction

DCP = Disk centrifuge photosedimentometry

DLS = Dynamic light scattering

DRC = Dry rubber content

EMS = Electron Microscopy Sciences

ISO = International Organization for Standardization

MMA = Methacrylic acid

NRL = Natural rubber latex

PMMA = Poly (methyl methacrylate)

PS = Poly styrene

PSD = Particle size distribution

QELS = Quasielastic light scattering

SEM = Scanning electron microscopy

**SYMBOLS AND ABBREVIATIONS (Continued)****Abbreviations (continued)**

St	=	Styrene
SC4-21	=	Small sample adapter
TEM	=	Transmission electron microscopy
TSC	=	Total solids content
TSC <sub>c</sub>	=	Critical total solids content
UL-A	=	Ultra low viscosity adapter

# CHAPTER I

## INTRODUCTION

### 1.1 General Introduction

Natural rubber latex is obtained principally from rubber-producing trees of the species *Hevea brasiliensis*, of the family Euphorbiaceae which grow in tropical regions. These trees are native plant of Brazil. Hevea rubber was introduced into the tropical Asia in 1876 by Sir Henry Wickman H.N. Ridley (Matthan, 1998). In 1899, Hevea rubber was first cultivated in Trang province, in south of Thailand by Khosimby Na Ranong. With suitable climate, Hevea rubber has been widely cultivated in Thailand. Figure 1.1 presents production of natural rubber from main rubber producers in the world since 1988-2004 (Rubber Research Institute of Thailand, 2006). It can be seen that natural rubber production from Thailand continuously increased. During 1988-1992, the high demand of natural rubber (concentrated latex) was increased because of AIDS infection. In Thailand, World Bank's lending for the rubber replanting promotion activities encouraged the conversion of large areas into rubber plantations. Thai government has converted small traditional rubber estates into large-scale industrial plantations (Matthan, 1998). Thailand becomes the world's largest rubber producer since 1992. In 2004, 34 percent of natural rubber in the world was produced from Thailand.

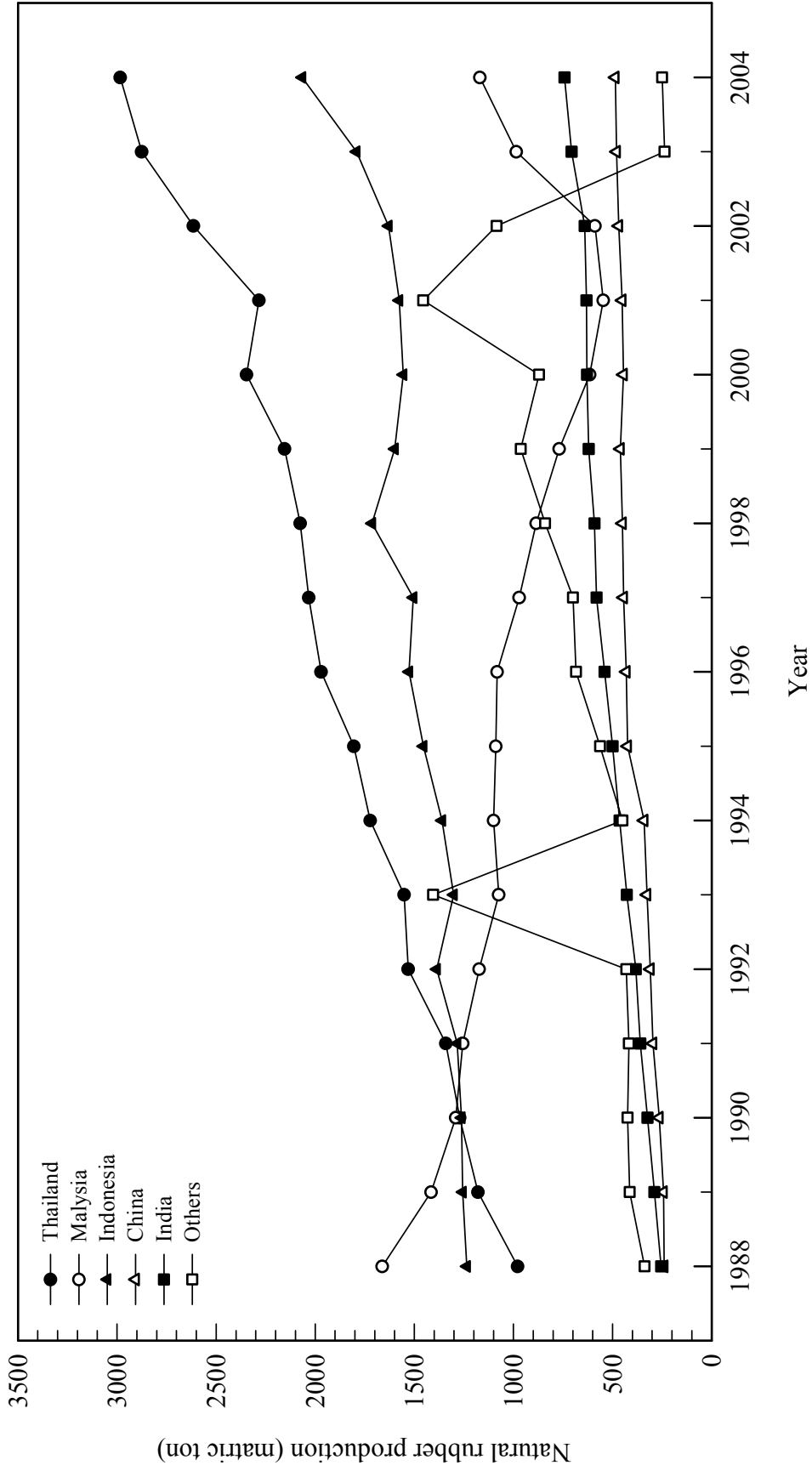


**Figure 1.1** Production of natural rubber from main agricultural producers in the world (Rubber Research Institute of Thailand, 2006)

Natural rubber product in Thailand can be classified into four main categories; ribbed smoked sheet rubber, blocked rubber, concentrated rubber latex and other types. The production of each natural rubber type is shown in Figure 1.2 (Rubber Research Institute of Thailand, 2006). It can be seen that production of blocked rubber, ribbed smoked sheet and concentrated rubber latex were increased while production of others type of rubber was relatively constant. The majority of raw natural rubber production in Thailand is exported. The amount of natural rubber in each rubber category exported from Thailand since 1997-2004 is shown in Figure 1.3 (Rubber Research Institute of Thailand, 2006). It can be seen that an exportation of blocked rubber and concentrated rubber latex were continuously increased while an exportation of ribbed smoked sheet rubber was fluctuated. The export of concentrated natural rubber latex is expected to be increased (Rubber Research Institute of Thailand, 2006). Currently, about 50% of all concentrated latex is consumed by the dipped goods industry (condom, medical and household gloves). Other uses of latex are in carpet backing, thread and adhesives.

Viscosity of latex significantly influences processing conditions and final rubber product properties. Understanding factors affecting viscosity of latex is thus beneficial. Many works have focused on viscosity of synthetic latexes. In this work, we will focus on viscosity of NRL concentrates produced in Thailand.

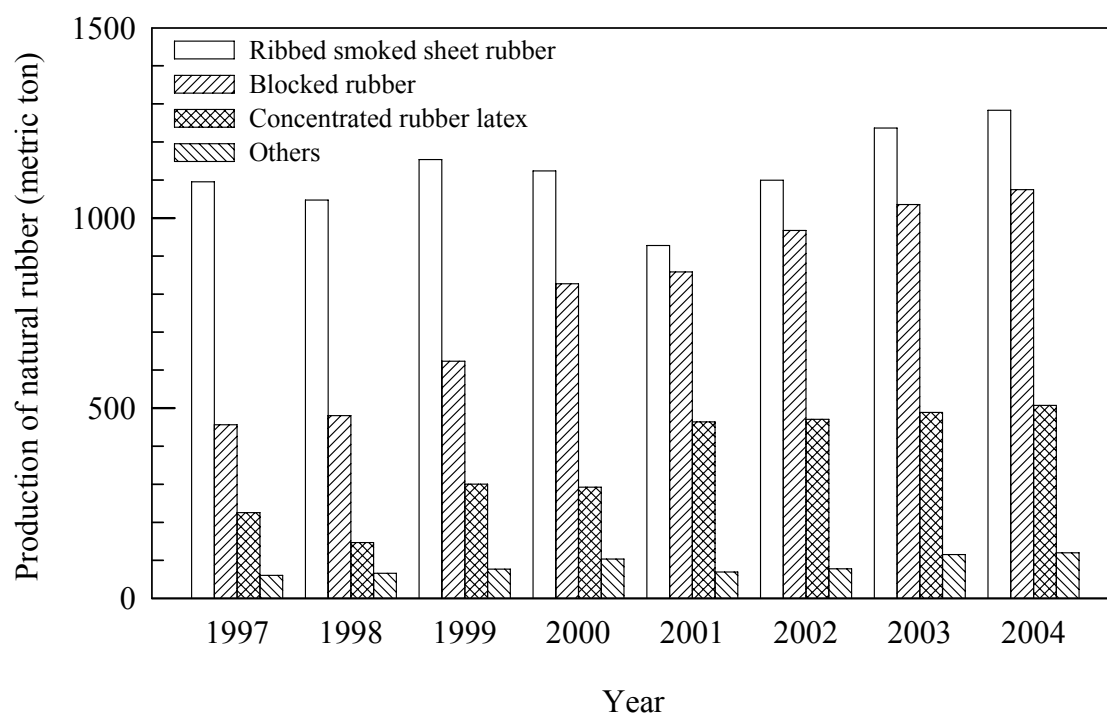


**Figure 1.2** Production of natural rubber in each rubber category in Thailand (Rubber Research Institute of Thailand, 2006)

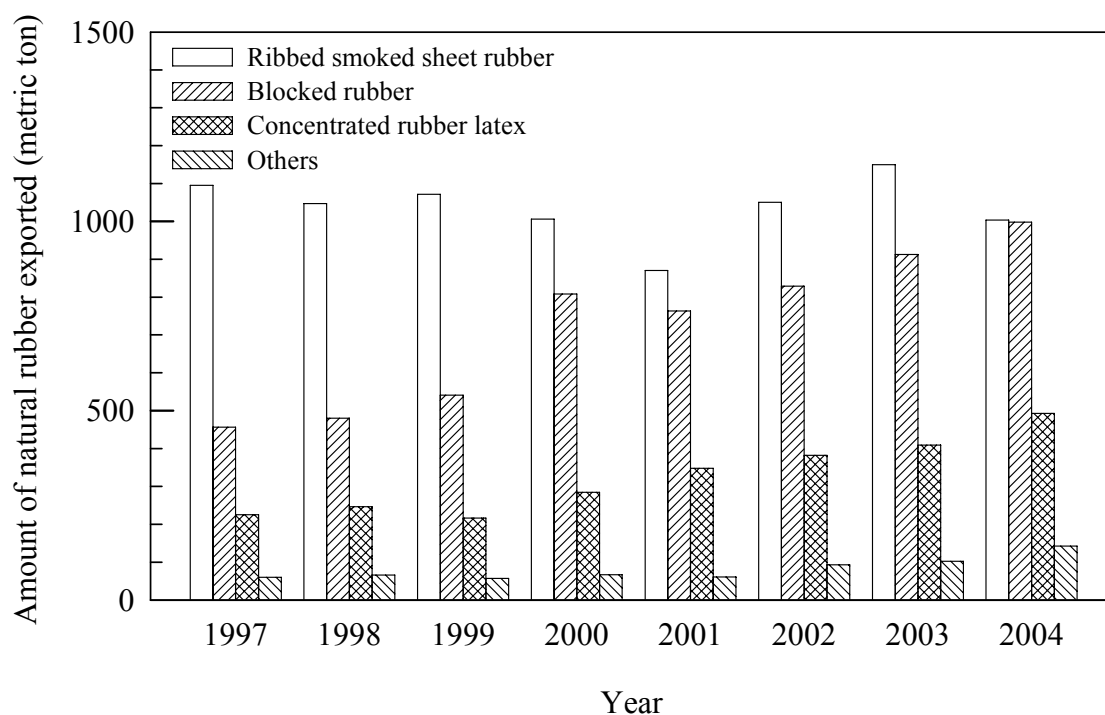


**Figure 1.3** Natural rubber production exported from Thailand (Rubber Research Institute of Thailand, 2006)

## 1.2 Research objectives

This research is aimed to study the rheological properties of concentrated natural rubber latex. High ammonia natural rubber latex concentrates will be used.

The main objectives of this research are;

- (i) To study the flow behavior of high ammonia natural rubber latex concentrate.
- (ii) To study the effect of particle size distribution on viscosity.
- (iii) To study the effect of total solids content on viscosity.
- (iv) To study the effect of temperature on viscosity.

- (v) To study the applicability of Mooney and Krieger-Dougherty equations on latex viscosity.

### **1.3 Scope and limitation of work**

The commercially available high ammonia Hevea rubber latexes (~61.5% TSC) purchased from Thai Hua rubbers Co., Ltd (Udonrthani), Thai eastern rubber Co., Ltd (Chonburi) and Inter rubber latex Co., Ltd (Suratthani) will be used. Total solids content in the range of 50-70 percent (by weight) will be prepared using either dilution or centrifugation. The methods that will be used are shown below.

- (i) Total solids content is determined according to International Standard (ISO) number 124:1997(E).
- (ii) Dry rubber content is determined according to International Standard (ISO) number 126:1995(E).
- (iii) Particle size distribution is determined by light scattering technique or transmission electron microscopy (TEM).
- (iv) Viscosity is measured using Brookfield viscometer (RV model) with coaxial cylinder geometry.

## **CHAPTER II**

### **LITERATURE REVIEW**

The word *Latex* is commonly used to denote a stable colloidal dispersion of a polymeric substance in an aqueous medium. It has sometimes been extended to include stable colloidal dispersions of polymers in non-aqueous media in which the polymer is insoluble (Blackley, 1997). Rubber latex system can be classified into two classes. The synthetic latex is normally obtained from emulsion addition polymerization and condensation polymerization. Natural latex is obtained from plants. Natural rubber latex may be tapped off from part of plants, such as bark, roots, leaves, stems, tubers and fruits. The production of latex is a characteristic feature of many plants, but latex containing rubber in large quantities occurs only in the species of families Moraceae, Euphorbiaceae, Apocynaceae, and Compositae (Matthan, 1998). Nowadays most natural rubber latex is derived from the species *Hevea brasiliensis* of the family Euphorbiaceae (Blackley, 1997).

#### **2.1 Natural rubber latex**

Freshly tapped *Hevea* latex contains not only rubber particles but also non-rubber particles dispersed in an aqueous serum. The ratio of rubber to non-rubber components varies from source to source. The rubber component from *Hevea* rubber tree is an entirely more than 98% of *cis*-1,4-polyisoprene (Figure 2.1) which is unable to crystallize under normal conditions. Therefore it exists as an amorphous, rubbery

material. Natural rubber latex (NRL) typically contains 34% (by weight) of rubber , 2%-3% proteins, 1.5%-3.5% resins, 0.5-1% ashes, 1.0-2.0% sugar 0.1-0.5% sterol glycosides and 55-60 % of water (Cacioli, 1997). The general composition of solid content of NRL is shown in Table 2.1. Hevea latex has a pH of 6.5-7.0 and a density of 0.98 g/cm<sup>3</sup>. Rubber particles varied in size from 0.15 µm to 3 µm (Kroschwitz and Jacqueline, 1990) and molecular weight distribution 10<sup>5</sup>-10<sup>7</sup> g/mol, depending on clone, weather, tapping frequency and other factors (Westall, 1968).

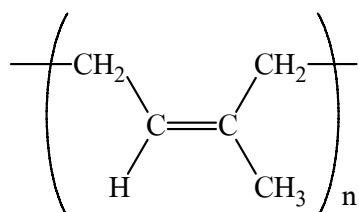


**Figure 2.1** Chemical structure of cis-1, 4-polyisoprene in Hevea latex

**Table 2.1** Compositions of the total solids content in natural rubber latex (Crowther, 1982)

Composition	Percent by weight
cis-1,4-polyisoprene	> 90
Acetone soluble	2.5-4.5
Nitrogen	0.3-0.5
Ash	0.2-0.4

The average rubber content of freshly tapped latex may be in a range of 30 to

45 percent. This fresh latex is not utilized in its original form due to its high water content and susceptibility to bacterial attack. It is necessary both to preserve and concentrate the latex, so that the natural rubber latex is stable and contains 60% or more of rubber. NRL concentrates is differentiated by the method of concentration and type of preservative used. High concentration is achieved by centrifugation (the most common), by creaming, or by evaporation (Tantatherdtam, 2003). Ammonia is normally applied to preserve latex from the bacterial attack. High ammonia (HA) latex, containing 0.7% ammonia in the latex, is still most frequently used material. More than 60 percent of centrifuged latexes are the high ammonia type.

Natural rubber latex concentrates are highly specified materials and are characterized by a number of properties that are significant to the user. The rubber solids content and the alkalinity are considered relatively fixed properties, if properly stored, these properties should remain largely unchanged. In contrast, properties such as potassium hydroxide (KOH) number, volatile fatty acids (VFA) number and latex mechanical stability time (MST) are, time dependent and also depend on the effectiveness of preservation, handling procedures and storage (Tantatherdtam, 2003).

## **2.2 Particle interaction**

Main interparticle forces commonly appearing in colloids are reviewed. There are five main interparticle forces acting in colloidal system (Quemada and Berli, 2002). The first interaction is Van der Waals interaction, which relates the attractive interaction forces between any two bodies of finite mass. Van der Waals forces included the Keesom orientation forces permanent dipoles, Debye induction forces between dipoles and induced dipoles, and London (dispersion) forces between two

induced dipoles (Schramm, 2001). Van der Waals interaction is decreased rapidly and is not relatively important at large distance between center to center of particles.

The second interaction is electrostatic force which arises from the presence of electric charges (either negative or positive) bound at the surface of the particles (Hunter, 1993). Typically, investigation of electrostatic force in colloidal suspension is electric double layer interaction. Electrically charged particles in aqueous media are surrounded by counterions and electrolyte ions, namely, the screening double layer. As two particles approach each other, the overlapping of double layers leads to long-range repulsive forces due to entropic effect (Israelachvili, 1997). The profile of the interaction depends on the ratio between the particle size and the Debye screening length. The electrostatic forces are typically observed in colloidal suspension with electrostatic stabilization.

The third interaction is hydrophilic interaction, also called structural forces. The interactions are relevant for several systems in aqueous media. This interaction arises from highly hydrophilic surfaces that cause molecular order in the adjacent and neighboring water molecules. The superficial hydration leads to a repulsive force between surfaces, which decay exponentially with a characteristic length (Israelachvili, 1997).

The fourth interaction in colloid system is depletion or exclusion interaction. When polymer molecules are added to adjacent surfaces, an attractive force is generally created between the surfaces (Schramm, 2001). The mechanism is involved either bridging or depletion, depending on the net interaction between the particles, macromolecules and the solvent. If particles are relatively large when compared with the polymer, attractive particle-particle forces are arisen by the mechanism of

depletion (Israelachvili, 1997). This interaction is exponentially decaying with a characteristic distance of the order of the segment polymer length.

The fifth interaction is polymer-polymer interaction. This interaction is common to several colloidal systems such as those containing polymer-covered particles (grafted or adsorbed), microgels and star polymers. Some polymers are usually added to stabilize the colloidal suspension. This stabilization is referred to as “steric stabilization”. The interaction relates the thickness of the layer formed by the polymer chains attached to the core and the surface to surface distance between cores (Quemada and Berli, 2002). The steric stabilization strongly depends on temperature. The reason is partly that entropic effects make a greater contribution to the Gibbs free energy change which accompanies the close approach of two particles than electrostatic stabilization (Blackley, 1997).

## **2.3 Factors affecting the viscosity of latex system**

Rheological properties of latex have been widely investigated. Many factors affected to the rheological properties of latex (Blackley, 1997). Here the average size of the latex particles, the distribution of size of latex particles, the concentration of latex particles in latex suspension and temperature are reviewed.

### **2.3.1 Particle size and particle size distribution (PSD)**

Knowledge of particle size and PSD is of primary importance in emulsion systems. The “size” of particle can be referred to its radius or its diameter. The chemical, physical and mechanical properties of emulsion systems are affected by particles size and PSD.

The effect of particle size on the monodisperse latex viscosity was

investigated by Johnson and Kelsey (1958). Three different sizes of polystyrene/butadiene copolymer latexes were employed. At the same total solids content, large particle size gave lower of viscosity than small particles.

Greenwood, Luckman and Gregory (1998) investigated effect of particle size and PSD of two monomodal synthetic polystyrene and their blending. They found that the viscosity of small particle (78 nm) showed higher viscosity than the large particle (360 nm). The viscosity of blend between large particles and small particles was lower than original particles. A minimum in the high shear rate limiting viscosity was found in the range 15-20% by volume of small particles.

The viscosity of aqueous polystyrene latex dispersion from three synthetic batches was investigated by Luckham and Ukeje (1999). TEM was employed to study the number-average particle size and standard deviations of the polystyrene latex. Three synthetic polystyrene latexes showed the same z-average particle size of 400 nm with varying degree of polydispersity, 0.085, 0.301, and 0.485, respectively. The polystyrene particles were stabilized sterically with PEO-PPO-PEO triblock copolymer (Synperonic F127). The results showed that the viscosities of the system exhibit shear thinning behavior at high solid fraction. The degree of shear thinning depends on the breadth of particle size distribution. At the narrowest distribution (polydispersity = 0.085) suspension exhibits the highest degree of shear thinning.

The influence of PSD on the viscosity of synthetic latexes was investigated by Schneider, Claverie, Graillat and McKenna (2002). Three sizes of latex particle were prepared from butyl acrylate (BA), methyl methacrylic acid (MMA) and acrylic acid (AA). The viscosities of trimodal latex blending from large

particles (607 nm), medium particles (340 nm) and small particles (60 nm) were investigated. It was found that at TSC > 65% blending ratio of 10-15% (small particle: 0-10% (medium particle) : 75-80% (large particle) showed the lowest viscosity.

For natural rubber latex, particle sizes are not strictly monodisperse, they do not all have identical size. It is important to know the particle size and PSD in order to control the rheological properties. To measure the particle size and particle size distribution, the most frequently used techniques are microscopic technique, light scattering technique and particle movement technique (Lovell and El-Aasser, 1997).

A comparative study of methods for the particle size and PSD measurements of standard polystyrene latex was studied by Elizalde, Leal and Leiza (2000). Four commercial instruments for measuring the average particle size and PSD were compared by analyzing a wide variety of samples including a series of monodisperse polystyrene latex in submicron range (39-804 nm), and bimodal and trimodal at different weight ratios. Dynamic light scattering (DLS) (N4-PLUS from Coulter), capillary hydrodynamic fraction (CHDF) (CHDF-2000 from Matec Applied Sciences), disk centrifuge photosedimentometry (DCP) (BI-DCP from Brookhaven Instruments) and transmission electron microscopy (TEM) (H-7000 FA from Hitachi) were used. It was found that for monodisperse latexes DLS, CHDF and DCP gave similar particle size which is also comparable to the particle size measured by TEM and reported by the supplier of standard latex. For the polydisperse samples, CHDF and DCP provided the most accurate distributions for the bimodal and trimodal samples analyzed. DLS failed to capture the entire distribution for the bimodal sample and the trimodal sample.

Another comparative study of methods for the particle size and PSD measurements of polymeric suspension was demonstrated by Schneider and McKenna (2002). Particle size and PSD of synthetic poly (BA-MMA) and polystyrene (St) standards were investigated by various methods, as shown in Table 2.2. The technique of cryofracture was employed with scanning electron microscopy (SEM) to give the reference particle size diameter. It was found that all methods gave the same mean particle size diameter for monomodal latexes. However, Lo-C Autosizer gave a much narrower PSD than other techniques. In case of a bimodal latex, multi-angle dynamic light scattering and separative methods offered adequate estimates of the average particle size of population.

**Table 2.2** List of methods used to measure PSD and average particle size (Schneider and McKenna, 2002).

<b>Techniques</b>	<b>Methods</b>	<b>Specific Equipment</b>
Microscopy	Scanning Electron Microscopy	(SEM) Phillips XL 30 FEG
Separative Methods	Capillary Hydrodynamic Fractional (CDHF)	CHDF 2000 (Matec)
	Flow-Field Flow fractionation	(FFF) F-100 from FFFraction, LLC
Dynamic light scattering	Single angle	Lo-C Autosizer (Malvern Instruments) Zetasizer 3000 (Malvern Instruments)
	4-scattering angle detection	N4-PLUS (Coulter)
	Multi-angle variable detection	Zetasizer 5000 (Malvern Instruments)
Static light scattering	Static Light Scatting Light Diffraction coupled with Polarization Intensity Differential Scattering (PIDS-Coulter counter only)	LS 2301 (Coulter) Mastersizer (Malvern Instruments)

### **2.3.2 Total solids content**

Rhode and Smith (1993) studied the viscosity of the preserved field latex (DRC = 24-52%) and concentrated latex (DRC = 56-63%) using Hoppler and pipette viscometers. By assuming shear rate independent viscosity, they found that the relationship between viscosity and DRC depends on DRC. For the preserved field latex, logarithmic viscosity was proportional to tangent of DRC. For the concentrated latex, viscosity was linearly proportional to DRC.

### **2.3.3 Temperature**

Ngothai, Bhattacharya and Coopes (1995) studied the effect of temperature on viscosity of polystyrene latex-gelatin dispersion. The spherical polystyrene latexes with free emulsifier were investigated. The results showed that relative viscosity at shear rate of  $80 \text{ sec}^{-1}$  decreases dramatically with an increase in temperature from 25 to  $90^\circ\text{C}$ . It was explained as a result of decreasing in the interactive forces between particles as the temperature increased or a disappearance of the water bridges due to evaporation. The three main interaction forces are Van der Waals attraction, electrostatic repulsion and the steric forces. In terms of energy calculation, the Van der Waals and electrostatic forces are not really a function of temperature. In the latex system with surfactant added, the most important forces found to depend on temperature is the steric forces.

Varkey, Rao and Thomas (1995) studied the effect of shear rate and temperature on the rheological behavior of natural latex. Hevea latex with a 61.6 percent of TSC and a 60 percent of DRC of Hevea latex were used. NRL showed a decrease in viscosity with an increase in shear rate, indicating shear thinning behavior. In addition, NRL showed a decrease in viscosity with temperature. They

explained that as temperature increases the links between the particles are ruptured. Hence, interactions among the particles are reduced. A recent study on rheological properties of three species of natural rubber latex (*P. argentatum*, *F. elastica*, and *H. brasiliensis*) investigated by Cornish and Brichta (2002) showed that the latex viscosity of three species of NRL increased with increasing rubber particle concentration, but declined with increasing temperature at all DRC.

## 2.4 Theoretical equations for latex viscosity

The viscosity of concentrated colloid suspension is a function of many parameters such as particle size, particle size distribution, concentration, temperature, body thermodynamic and hydrodynamic interparticle interaction. Because of the complicated parameters, a general theory for concentrated colloid suspension is not completely available. However, the existent equation can be made some limiting case. In 1906-1911, Einstein undertook a theoretical analysis of the effect of suspended spherical particles on the viscosity (Lovell and El-Aasser, 1997). For highly dilute suspensions ( $\phi < 0.05$ ) of hard sphere particles, Einstein proposed

$$\eta_r = \frac{\eta}{\eta_0} = 1 + [\eta]\phi \quad (2.1)$$

where  $\eta_r$  = the relative viscosity of the latex

$\eta$  = the viscosity of latex

$\eta_0$  = the viscosity of the latex medium

$[\eta]$  = the intrinsic viscosity of the particles dispersed in the latex

$\phi$  = the volume fraction of spheres relative to the total volume of dispersion.

Assumed that there is no slip between particles and fluid medium, and the fluid medium is a Newtonian and an incompressible fluid, Einstein equation often appears with  $[\eta] = 2.5$  for rigid sphere (Blackley, 1997). Einstein expression is only valid at low to very low value of volume fraction. The equation was extended to higher concentrations by considering interaction between the particles (Vand, 1945):

$$\eta_r = 1 + 2.5\phi + k_2\phi^2 \quad (2.2)$$

where  $k_2 =$  an adjustable constant between 2.5 to 9

This  $k_2\phi^2$  term was contributed to particle-particle interactions or hydrodynamic interaction in semi-dilute, or moderately concentrated solutions. This equation shows good fitting in the data below volume fraction of 0.10 (Lovell and El-Aasser, 1997, Larson, 1999). In 1951, Mooney proposed a new model for monomodal dispersions of hard, nondeformable spheres as followed.

$$\eta_r = \exp\left(\frac{[\eta]\phi}{1 - \phi/\phi_c}\right) \quad (2.3)$$

Mooney introduced the critical packing volume fraction ( $\phi_c$ ) term. This  $\phi_c$  related the particle size distribution to the viscosity (Mooney, 1951). At which relative viscosity approaches infinity, the packing volume corresponded to the maximum packing volume fraction ( $\phi_{max}$ ). Although the Mooney equation was developed to use at higher volume fraction than Vand equation, it is often observed to fit data in range of 0-0.5 volume fraction (Bradna, Stern, Quadrat, and Snuparek, 1996, Horsky, Quadrat, Porsch, Mrkvickova, and Snuparek, 2001, Quadrat, Snuparek, Mikesova, and Horsky, 2005 and Staicu, Micutz and Leca, 2005). In addition, the greater of intrinsic viscosity than 2.5 was also founded (Quadrat et al., 2005). They explained as the large amount of surfactant in system gave stronger repulsive

interaction among the particles in the system that effected to the strength of interactions at particle-water interface. The strength interaction at particle interface in accordance with variation of intrinsic viscosity values. Since, the large amount of surfactant in mixture gave the large values of intrinsic viscosity (Quadrat et al., 2005). In 1959, a well-known equation specifically for polymer latexes was suggested by Krieger and Dougherty (equation 2.4). Krieger-Dougherty equation was developed from Mooney equation to increase efficiency of model for non-dilute system (Krieger and Dougherty, 1959). Small errors in the determination of volume fraction can lead to large errors in the viscosity (Meeker, Poon, Pusey, 1997, quoted in Larson, 1999).

$$\eta_r = \left(1 - \frac{\phi}{\phi_{\max}}\right)^{-[\eta]_{\max} \phi} \quad (2.4)$$

Krieger-Dougherty equation was frequently observed in colloidal latex with volume fraction in range of 0-0.7 (Greenwood, Luckham, and Gregory, 1995, Chu, Guillot, and Guyot 1998, Pishvaei, Graillat, McKenna, and Cassagnau, 2005, Carlsson, Jarnstrom, and Stam, 2006).

Jones, Leary, and Boger (1991) studied the efficiency of the theoretical viscosity model mentioned earlier using dilute and concentrated silica suspension was investigated. Figure 2.5 shows the viscosity data at low volume fraction (triangle,  $\Delta$ ) and high volume fraction (circle, O). The data show that at low volume fraction, the experimental result agrees well with all models. While at high volume fraction of silica suspension, only Krieger-Dougherty model fits the data. Greenwood et al. (1995) studied the rheology of polystyrene and poly (methyl methacrylate) (PMMA) suspension. The experimental results demonstrated that fitting of Krieger-Dougherty equation at low volume fraction has high variation. It indicated that Krieger-

Dougherty equation may be unsuitable to fit the suspension system at low volume fraction.

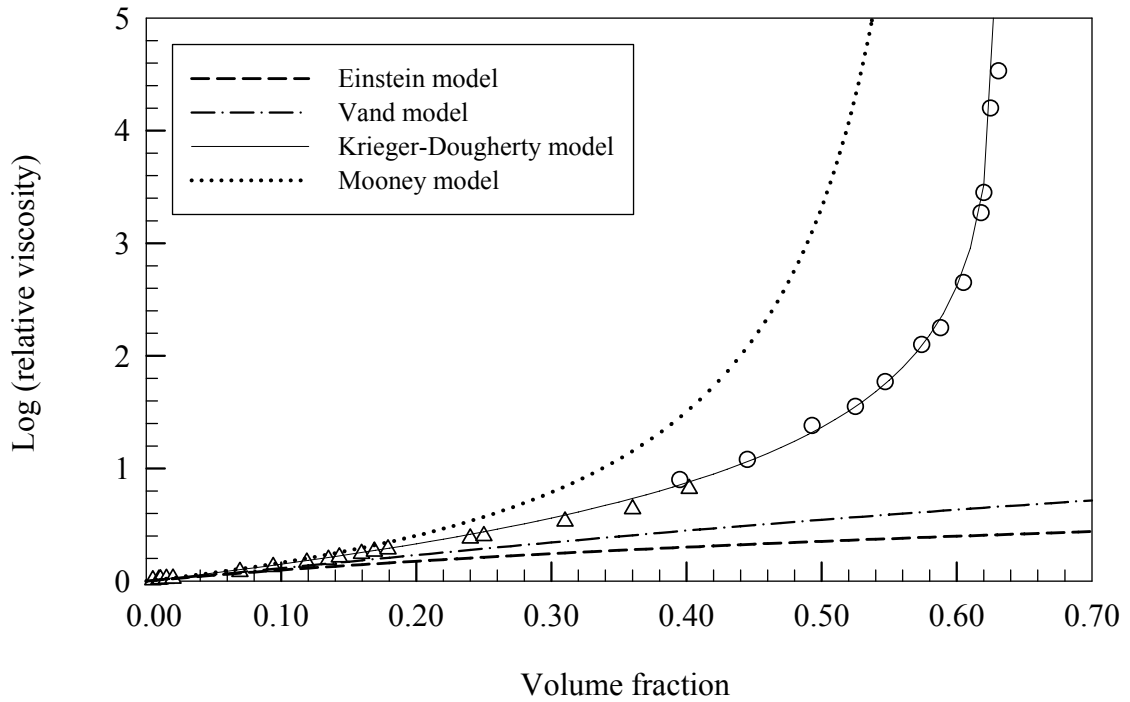


**Figure 2.2** The concentrated silica suspension viscosity data fitted to the theoretical models. The short dash line is drawn according to Einstein equation. The dash-dot line is drawn according to Vand equation with  $k_2 = 5$ . The solid line is drawn according to Krieger-Dougherty equation with  $\phi_{\max} = 0.631$  and  $[\eta] = 3.17$ . The dotted line is drawn according to Mooney model with  $\phi_{\max} = 0.631$  and  $[\eta] = 3.17$ . (Jones et al., 1991)

# **CHAPTER III**

## **EXPERIMENTAL METHODOLOGY**

### **3.1 General background**

The experimental details in this chapter aimed to investigate the viscosity, total solids content (TSC), dry rubber content (DRC), particle size and particle size distribution (PSD) of HA NRL concentrate. *Hevea Brasiliensis* natural rubber latex (RRIM-600 clone) was investigated. The viscosity of NRL was measured by coaxial cylinder geometry viscometer (Brookfield viscometer). Total solids content and dry rubber content were determined according to International Organization for Standardization (ISO) 124:1997(E) and ISO 126:1995, respectively. The average particle size diameter and PSD of rubber particles were determined by laser diffraction technique and transmission electron microscopy (TEM). The flowchart of experimental design is presented in Figure 3.1.

### **3.2 Materials and chemical reagents**

#### **3.2.1 High ammonia (HA) natural latex concentrates**

Five lots of concentrates latex HA NRL from three agricultural sources in Thailand were used. Three lots were purchased from Thai Hua Rubber Public Co., Ltd. (Udonthani, northeastern region of Thailand). One was purchased from Thai Eastern Rubber Co., Ltd. (Chonburi, eastern region of Thailand) and the last was purchased from Inter Rubber Latex Co., Ltd. (Suratthani, southern

region of Thailand). The specification of HA NRL concentrates is shown in Table 3.1. Total solids content in the range of 48-66 percent (by weight) were prepared using either dilution or centrifugation. Sample preparation methods will be described in section 3.3.

**Table 3.1** Specification of HA NRL used according to suppliers

<b>Properties</b>	<b>Chonburi</b>	<b>Surathani</b>	<b>Udornthani lot 1</b>	<b>Udornthani lot 2</b>	<b>Udornthani lot 3</b>
1. TSC, %	62.08	61.50	61.72	61.23	61.77
2. DRC, %	60.19	60.06	60.09	60.09	60.09
3. Non-rubber solid content,%	1.89	1.44	1.63	1.14	1.68
4. NH <sub>3</sub> content (on total weight), %	0.74	0.75	0.69	0.60	0.66
5. NH <sub>3</sub> content (on water phase), %	1.95	1.95	1.80	1.55	1.73
6. pH value	10.51	10.69	10.66	10.48	10.37
7. KOH No.	0.63	0.51	0.48	0.52	0.44
8. VFA No.	0.048	0.019	0.047	0.040	0.021
9. MST, sec	1,050	1,000	656	330	1,227
10. Mg <sup>2+</sup> (on solid), ppm	20.10	26	39.15	39.35	32.99

### 3.2.2 Acetic acid

The 50% by volume of acetic acid solution was purchased from Witayasom Corporation. It was diluted to 5% solution of acetic acid by distilled water before usage.

### **3.2.3 Osmium tetroxide**

The E.M. grade Osmium tetroxide ( $\text{OsO}_4$ ) supplied by Electron Microscopy Sciences (EMS<sup>TM</sup>) was diluted to 4% by weight with distilled water.

### **3.2.4 Poly vinyl-formvar**

Poly vinyl-formvar resin supplied by EMS<sup>TM</sup> and chloroform reagent ( $\text{CH}_2\text{Cl}_2$ ) were used to prepare a film coated on the copper grid. A 0.5% solution of poly vinyl-formvar in chloroform (Bozzola and Russell, 1999) was prepared.

### **3.2.5 Polystyrene latex**

Standard polystyrene latex with diameter of  $220 \pm 6$  nm was used as reference for size calibration in TEM. It was supplied by Duke scientific corporation and directly used without any purification.

## **3.3 Experimental**

### **3.3.1 NRL sample preparation**

The samples used in this study can be classified into two categories: (i) HA NRL concentrated samples were directly diluted from the as received latex and (ii) HA NRL concentrated samples were re-centrifuged and diluted. For (i), five concentrations of 48%, 52%, 56%, 60% and 61.5% TSC (by weight) were prepared. The total solids content of as received HA NRL concentrates from suppliers were determined (as will be described in section 3.3.2). From supplier specification, the received latex concentration is approximately 61.5 percent of TSC. In order to prepare the samples by dilution method, distilled water was added. At each concentration, 200 grams of sample were prepared. To homogenize the latex samples, the sample bottoms were shaken by Ika Orbital shaker (model Digital KS501) at 180

revolutions per minutes (rpm) for 30 minutes and rested at room temperature about 24 hours. The latex samples were kept at 4°C in refrigerator. The cool samples were rested at room temperature about 4 hours before used.

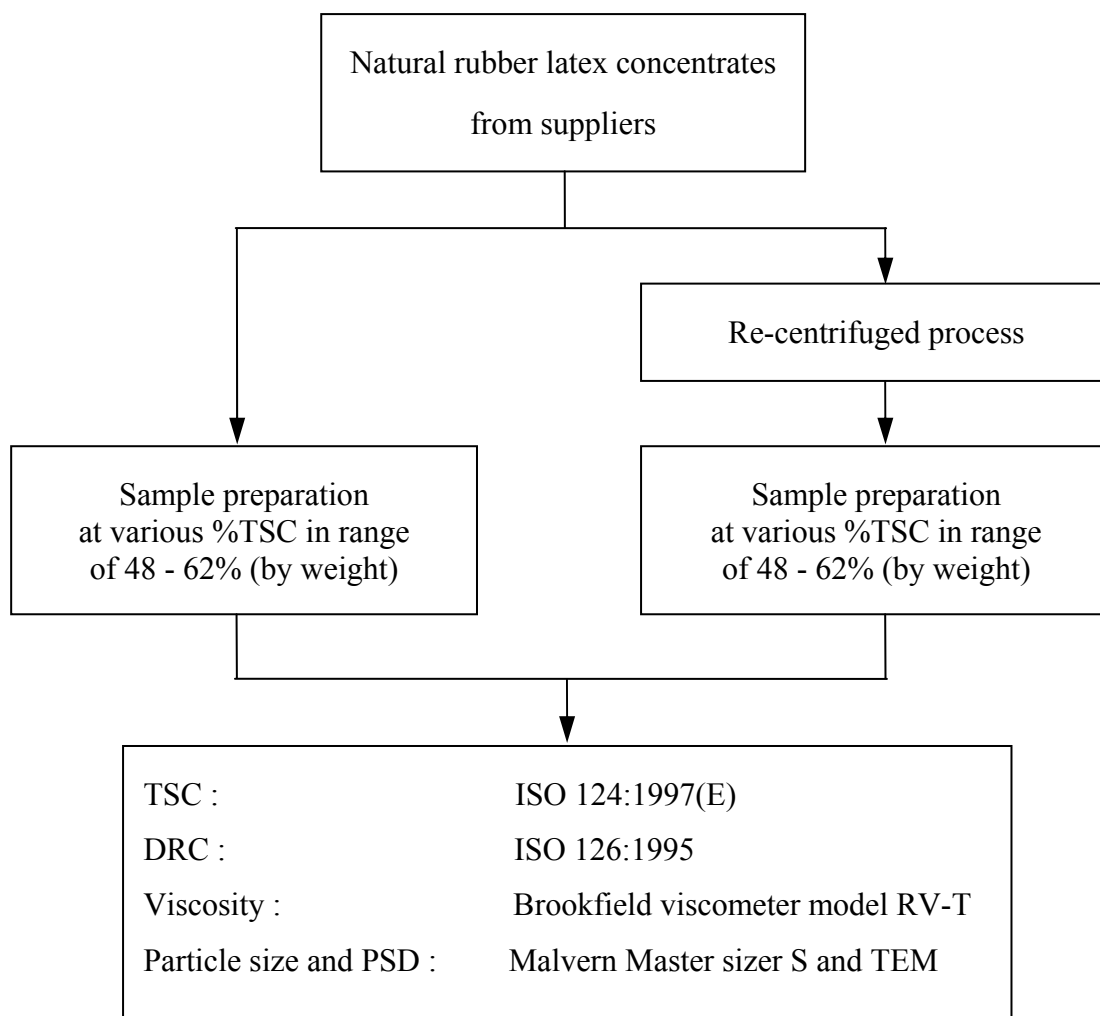


**Figure 3.1** The flow chart of experimental design

For (ii), seven concentrations in range of 48%, 52%, 56%, 60%, 61.5%, 64% and 66% TSC (by weight) were prepared. Sorvall ultra-centrifuge machine (model RC-28S with GSA rotor) was employed. The as received latex was

poured into Sorvall GSA centrifugal tubes and packed into the Sorvall GSA rotor. The centrifuge machine was operated at 9,000 rpm and temperature of 25°C for 45 minutes. After centrifugation, two distinct layers were observed in the centrifugal tubes. Water layer was on the top of centrifugal tubes. It was slowly rinsed off from tubes. TSC of the residual latex layer was determined. The residual latex was diluted by a known amount of distilled water for the specified TSC. The calculated re-centrifuged latex and distilled water were weighted by digital balance and added into the cylindrical bottoms. The sample bottoms were shaken at 180 rpm for 30 minutes to homogenize the latex samples. They were rested at room temperature about 24 hours then kept at 4°C in a refrigerator. The cool samples were released in room temperature about 4 hours before used. The notation was employed to identify each sample as followed;

**AB<sub>C,D</sub>**

where A = source of natural rubber latex concentrate

B = method of sample preparation

C = lot of natural rubber latex

D = total solids content in % (by wt.)

**Table 3.2** Abbreviation of HA NRL samples

<b>A</b>	<b>B</b>	<b>C</b>	<b>D</b>
C = Chonburi	O = directly diluted from supplier	1 = Lot 1	<sub>48</sub> = 48 %
S = Suratthani	C = diluted from re-centrifuged NRL	2 = Lot 2	<sub>52</sub> = 52 %
U = Udornthani		3 = Lot 3	<sub>56</sub> = 56 %
			<sub>60</sub> = 60 %
			<sub>61.5</sub> = 61.5 %
			<sub>64</sub> = 64 %
			<sub>66</sub> = 66 %

### 3.3.2 Determination of total solids content

TSC of latex is defined as the percentage by mass of the whole non-volatile under specified conditions. The rubber latex was dried in an open atmosphere at an elevated temperature. The TSC of natural rubber latex was determined according to International Standard (ISO) number 124:1997(E) (Latex, rubber - Determination of total solids content). An empty flat-bottom dish was weighed. A  $5.0 \text{ g} \pm 1 \text{ g}$  of latex sample ( $m_0$ ) was added in each flat-bottom dish. The sample dish was placed into the oven at temperature of  $105^\circ\text{C} \pm 5^\circ\text{C}$  to evaporate the volatile materials. After 10 hours of drying time, the sample dish was removed from the oven and cool down to ambient temperature in a desiccator. The dried latex dish was weighed and placed into the oven again. This schematic method was repeated in every two hours of drying time after the first weighed. When the constant weight ( $m_1$ ) of dried rubber was obtained (approximately 20 hours), TSC of samples was calculated as following

$$\text{TSC} = \frac{m_1}{m_0} \times 100 \quad (3.1)$$

For each NRL, five samples were repeated to calculate the average TSC of each NRL.

### 3.3.3 Determination of dry rubber content

Dry rubber content is defined as the percentage by mass of coagulated latex under specified conditions of colloidal destabilization. The DRC of natural rubber latex was determined according to ISO number 126:1995(E) (Latex, rubber - Determination of dry rubber content). A  $5.0 \text{ g} \pm 1 \text{ g}$  of latex sample ( $m_0$ ) was weighted in the flat-bottom dish. The latex sample in the dish was diluted by distilled water to 20% TSC (by weight). To homogenize the latex samples with distilled water, the sample dish was slowly swirled. A  $0.5 \text{ g/dm}^3$  of acetic acid solution was filled into the measuring pipette. The acetic solution was slightly poured down from the pipette to inside the edge of the dish and slowly rotated the dish. The acid reacted with rubber latex, thus the coagulation occurred. The coagulated latex below the surface of the acid was pressed by a spatula until it obtained a uniform sheet of rubber not exceeding 2 mm in thickness. The coagulated rubber was soaked by water until the water was no longer acidic to litmus. The sample dish was placed in the oven at temperature of  $70^\circ\text{C} \pm 5^\circ\text{C}$  to evaporate the volatile materials. After 10 hours of drying time, the sample dish was removed from the oven and cooled down to ambient temperature in a desiccator. The dried latex dish was weighed and placed into the oven again. This schematic method was repeated in every two hours of drying time after the first weighed. When the constant weight ( $m_1$ ) of dried rubber was obtained (approximately 20 hours), DRC of samples was calculated as following

$$\text{DRC} = \frac{m_1}{m_0} \times 100 \quad (3.2)$$

For each NRL, five samples were repeated to calculate the average DRC of each NRL.

### **3.3.4 Determination of Particle size and particle size distribution**

Particle size and PSD are important characteristics of the latex system. Other properties of the latex were influenced by PS and PSD (Hunter, 1992). In this experiment, laser light scattering diffraction and transmission electron microscopy (TEM) were employed to investigate the particle size and PSD of HA NRL concentrates. Laser light scattering diffraction is based on the fact that diffraction angle is inversely proportional to particle size (Rawle, 2000). Transmission electron microscopy is the most direct and reliable method for the measurement of the particle. The details of the experimental are described below.

#### **3.3.4.1 Laser diffraction**

Laser diffraction is based on the scientific phenomenon of particles in laser light scattering. The large particles are scattered at small forward angles while small particles are scattered at wider angles (Stimson, 2000). The light scattering from a laser beam are collected by a detector and transferred to computer to analysis. Malvern Mastersizer S was employed to investigate the particle size and PSD of HA NRL concentrates. A laser beam was generated by Helium-Neon source. Wet dispersion analysis was conducted. QSpec (small volume sample handling unit) was used as the dispersant tank. The laser beam was warmed up for 15 minutes to reach the required energy level and a Sizer program was turned on. A 120 ml of distilled water as the dispersant medium was added into the dispersant tank. The ultrasonification speed, stirrer speed and pump speed were set at 80 percent. The distilled water was pumped into the flow cell where the laser beam passed. The

experimental background was collected. To measure the particle size and PSD of latex, a few drops of 60% TSC of latex samples were added into the dispersant tank (in range of 10-30% obscuration, see on the Sizer program). Wait for 15 second before the measurement. The particle size data were transferred from the detector to computer and analyzed by Sizer program. The presentation model was chosen to obtain the correct size based on the light optical constants of the sample and dispersant. Refractive indices of rubber latex (polyisoprene) and distilled water are 1.53 and 1.33, respectively. A  $D[4,3]$  (mean average diameter by volume/diameter or z-average diameter or De Broucker mean), skewness ( $S_k$ ) and polydispersity ( $P_d$ ) of data were reported in Sizer Table results. The statistics of the distribution and average diameters  $D[4,3]$  were calculated from the raw data according to British Standard BS2955:1993. Three measurements were carried out for each sample.

### **3.3.4.2 Transmission electron microscopy (TEM)**

Electromagnetic radiations originating from a filament are converged onto a thin specimen by means of a condenser lens system. An illumination transmitted through the specimen is focused into an image and magnified by a series of intermediate and projector lenses until the final image is viewed on the fluorescent screen (Bozzola and Russell, 1999). In this study, TEM (Hitachi JEOL 2010, 80 kV) was employed. Rubber latex sample was diluted by distilled water to 5% of TSC. A 4% (by weight) osmium tetroxide ( $\text{OsO}_4$ ) solution was used to stain the rubber particle to increase phase contrast (Nopnit, 1985). A 2 ml of diluted rubber latex sample was mixed with one drop of  $\text{OsO}_4$  solution in test tube and slowly shaken. The test tube sample was kept in the dark room overnight. The test tube was slowly shaken again before latex sample was dropped on the copper

grid. Only one drop of stained latex sample was dropped on brilliant side of copper grid (Mesh no. 100) covered by poly vinyl-formvar film. The sample was then dried in a desiccator over night. The dried sample was placed on the grid holder and inserted into specimen exchanger. High vacuum or low pressure system was required to reduce the effect of light diffraction. Wait about 15 minutes to reach the required pressure. In this experiment, lanthanum hexaboride ( $\text{LaB}_6$ ) filament was used to generate the electron beam. The instrument was operated at an accelerating voltage of 80 kV. TEM micrograph was captured by TEM camera connected to computer. At least 200 rubber particles were required for the particle size and PSD calculation for each sample condition. Standard polystyrene latex with diameter of  $220 \pm 6$  nm (Duke scientific corporation) was used as reference for the particle size in TEM measurement.  $\text{CO}_1$ ,  $\text{SO}_1$ ,  $\text{UO}_1$  and  $\text{UO}_2$  were selected to represent the morphology and particle size of samples.

### 3.3.5 Viscosity measurement

The viscosity of natural rubber latex was measured by using Brookfield viscometer (RV model) with coaxial cylinder geometry as shown in Figure 3.2. In this study, ultra low viscosity adapter (UL-A) and small sample adapter (SC4-21) were used as sample cup. The UL-A with cylindrical spindle radius ( $R_b$ ) of 1.2575 cm, cylindrical container with radius ( $R_c$ ) of 1.3810 cm and effective length of (L) 9.2370 cm was employed. The SC4-21 with cylindrical spindle radius ( $R_b$ ) of 0.8380 cm, cylindrical container with radius ( $R_c$ ) of 0.9525 cm and effective length of (L) 6.4770 cm was employed. The viscous drag on the cylinder causes an angular deflection of the torque spring which is proportional to the viscosity of the fluid. Therefore the viscosity was indicated by means of a pointer and scale. The 16 ml of

HA NRL sample was poured into the cup. The sample cup was placed into the water jacket assembly. The water jacket was maintained at set temperature of 10, 15, 20, 25, 30, 35 and 40°C. The cylindrical spindle was carefully inserted into the sample cup to avoid air being trapped. The required shear rates were 0.61, 1.23, 3.06, 6.13, 12.26, 24.52, 61.29, 92.68 and 122.58  $\text{sec}^{-1}$ . The motor speed of rotor was set to obtain the required shear rate, relationship between motor speed and shear rate is shown in Table 3.4. When the sample temperature was reached to set temperature, switch on the viscometer motor. The percent of torque was read from the pointer at equilibrium. Repeat the procedure five times. The shear rate, shear stress and viscosity of latex sample were calculated using equations (3.3), (3.4) and (3.5), respectively.

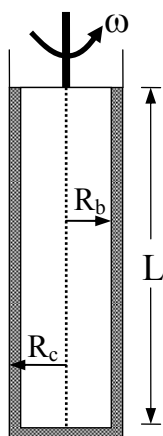


**Figure 3.2** Schematic of a coaxial cylinder viscometer

$$\dot{\gamma} = \left( \frac{2 R_c^2}{R_c^2 - R_b^2} \right) \omega \quad (3.3)$$

$$\tau = \frac{M}{2 \pi R_b^2 L} \quad (3.4)$$

$$\eta = \frac{\tau}{\dot{\gamma}} \quad (3.5)$$

Where:  $\dot{\gamma}$  = shear rate ( $\text{sec}^{-1}$ )

$\tau$  = shear stress ( $\text{dynes/cm}^2$ )

$R_c$  = radius of container (cm)

$R_b$  = radius of spindle (cm)

$L$  = effective length of spindle (cm)

$M$  = percent of torque from reading (maximum = 7,187  $\text{dynes/cm}^2$ )

$\omega$  = angular velocity of spindle ( $\text{rad/sec}$ ) =  $(2\pi \times \text{rpm}/60)$

$\eta$  = viscosity (poise)

Rheological properties were focused on the behavior of HA NRL concentrated samples at 25°C and a range of shear rates shown in Table 3.4. To study the effect of temperature on the viscosity of HA NRL concentrates, seven temperatures were applied on viscosity measurement. UO<sub>3,56</sub>, UO<sub>3,60</sub>, UC<sub>3,56</sub>, UC<sub>3,60</sub> and UC<sub>3,64</sub> were selected to represent the viscosity data at temperature of 10, 15, 20, 25, 30, 35 and 40°C. At each temperature, viscosity of NRL samples at shear rates of 3.06, 6.13, 12.26, 24.52, 61.29 and 122.58  $\text{sec}^{-1}$  was investigated. Five measurements were repeated for each sample condition.

**Table 3.3** Relationship between motor speed (revolution per minutes, rpm) and shear rate ( $\text{sec}^{-1}$ ) of UL-A and SC4-21 sample cups

Motor speed of rotor (rpm)	Shear rate, $\dot{\gamma}$ ( $\text{sec}^{-1}$ )	
	UL-A	SC4-21
100	122.58	92.68
50	61.29	46.34
20	24.52	18.34
10	12.26	9.27
5	6.13	4.63
2.5	3.06	2.32
1	1.23	0.93
0.5	0.61	0.46

**Table 3.4** List of experimental shear rate conditions of HA NRL concentrates samples at 25°C

Sample	Shear rate ( $\text{sec}^{-1}$ )								
	122.58	92.68	61.29	24.52	12.26	6.13	3.06	1.23	0.61
CO <sub>1</sub>	X	O	X	X	X	X	X	O	O
CC <sub>1</sub>	X	O	X	X	X	X	X	O	O
SO <sub>1</sub>	X	X	X	X	X	X	X	O	O
SC <sub>1</sub>	X	X	X	X	X	X	X	O	O
UO <sub>1</sub>	X	X	X	X	X	X	X	X	X
UC <sub>1</sub>	X	X	X	X	X	X	X	O	O
UO <sub>2</sub>	X	X	X	X	X	X	X	X	X
UC <sub>2</sub>	X	X	X	X	X	X	X	O	O
UO <sub>3</sub>	X	O	X	X	X	X	X	O	O
UC <sub>3</sub>	X	O	X	X	X	X	X	O	O

X = tested, O = untested

### 3.3.6 Density measurement

The density of latex samples was measured by using pycnometer with the volume ( $v_p$ ) of 1.51 cm<sup>3</sup>. The empty pycnometer and the cover were weighed. The latex sample was added into the Pyrex<sup>®</sup> pycnometer. Wait a minute to rinse of latex from the cover and cleaned the pycnometer by using blotting paper. The pycnometer was soaked in water bath at 25°C for 5 minutes and cleaned by blotting paper again. The pycnometer was weighed to calculate the weight of latex sample. Density of rubber latex samples were calculated according to equation 3.6

$$\text{Density } (\rho) = \frac{\text{Mass } (m)}{\text{Volume } (v)} \quad (3.6)$$

The rubber latex in pycnometer was identified into two fractions as rubber phase (include non rubber component) and water phase. Thus, the latex volume in pycnometer ( $v_p$ ) composed of volume of rubber phase ( $v_{\text{rubber}}$ ) and volume of water phase ( $v_{\text{water}}$ ), the relation is shown in equation (3.7). Latex weight in pycnometer ( $m_p$ ) composed of weight of rubber phase ( $m_{\text{rubber}}$ ) and weight of water phase ( $m_{\text{water}}$ ), the relation is shown in equation (3.8).

$$v_p = v_{\text{rubber}} + v_{\text{water}} \quad (3.7)$$

$$m_p = m_{\text{rubber}} + m_{\text{water}} \quad (3.8)$$

Equation 3.9 showed the expression of weight of rubber in term of latex weight in pycnometer and equation 3.10 showed the expression of weight of water in term of latex weight in pycnometer.

$$m_{\text{rubber}} = \frac{m_b \times \text{TSC (\% by weight)}}{100} \quad (3.9)$$

$$m_{\text{water}} = m_b - \frac{m_b \times \text{TSC (\% by weight)}}{100} \quad (3.10)$$

Equation 3.10 was substituted into equation 3.6 to obtain volume of water in terms of TSC and weight of rubber latex as showed in equation 3.11. Then it can be found the volume of rubber in term of TSC and weight of rubber latex as showed in equation 3.12.

$$v_{\text{water}} = \frac{m_{\text{water}}}{\rho_{\text{water@25}^\circ\text{C}}} = \frac{m_p - \frac{m_p \times \text{TSC (\% by weight)}}{100}}{1.028 \text{ g/cm}^3} \quad (3.11)$$

$$v_{\text{rubber}} = v_b - \frac{m_p - \frac{m_p \times \text{TSC (\% by weight)}}{100}}{1.028 \text{ g/cm}^3} \quad (3.12)$$

The equation 3.6 was substituted by equation 3.9 and 3.12 to obtain the density of rubber. Three samples were repeated for each sample condition.

$$\rho_{\text{rubber}} = \frac{\frac{m_p \times \text{TSC (\% by weight)}}{100}}{1.51 - \frac{m_p - \frac{m_p \times \text{TSC (\% by weight)}}{100}}{1.028}} \quad (3.13)$$

## CHAPTER IV

### RESULTS AND DISCUSSIONS

#### 4.1 Total solids content and dry rubber content

The natural rubber latex samples were prepared by two methods, direct dilution of as received NRL concentrates and dilution of re-centrifuged NRL concentrates. By direct dilution, five samples with different total solids content (by weight) were prepared. By dilution of re-centrifuge NRL concentrates, seven samples with different total solids content (by weight) were prepared. Total solids content and dry rubber content of NRL samples prepared by direct dilution of as received NRL concentrates are summarized in Table 4.1. Table 4.2 shows the total solids content and dry rubber content of NRL samples prepared by diluted from re-centrifuged NRL concentrates. Due to the difficulty in exactly weighing sticky latex, TSC of each sample may not be exactly the same as specified, e.g. the true TSC of UO<sub>3,48</sub> is 47.77 ± 0.01. Measured TSC (true TSC) was used for all calculations.

**Table 4.1** Total solids content (TSC) and dry rubber content (DRC) of NRL samples prepared by direct dilution of the received NRL concentrates

Sources	NRL samples	TSC (% by weight)	DRC (% by weight)
Chonburi	CO <sub>1,48</sub>	48.05 ± 0.02	46.84 ± 0.14
	CO <sub>1,52</sub>	51.99 ± 0.02	50.88 ± 0.12
	CO <sub>1,56</sub>	56.01 ± 0.07	54.88 ± 0.43
	CO <sub>1,60</sub>	60.04 ± 0.05	58.98 ± 0.13
	CO <sub>1,61.5</sub>	61.65 ± 0.04	60.31 ± 0.20
Suratthani	SO <sub>1,48</sub>	48.09 ± 0.04	47.11 ± 0.03
	SO <sub>1,52</sub>	51.97 ± 0.12	50.89 ± 0.04
	SO <sub>1,56</sub>	56.14 ± 0.04	54.87 ± 0.04
	SO <sub>1,60</sub>	59.97 ± 0.04	58.78 ± 0.04
	SO <sub>1,61.5</sub>	61.16 ± 0.05	60.04 ± 0.19
Udonthani Lot 1	UO <sub>1,48</sub>	48.01 ± 0.33	46.63 ± 0.07
	UO <sub>1,52</sub>	52.61 ± 0.06	51.31 ± 0.10
	UO <sub>1,56</sub>	55.97 ± 0.03	54.63 ± 0.06
	UO <sub>1,60</sub>	60.10 ± 0.08	58.56 ± 0.15
	UO <sub>1,61.5</sub>	61.34 ± 0.06	59.84 ± 0.06
Udonthani Lot 2	UO <sub>2,48</sub>	47.94 ± 0.04	46.80 ± 0.04
	UO <sub>2,52</sub>	52.08 ± 0.01	50.77 ± 0.05
	UO <sub>2,56</sub>	56.07 ± 0.04	54.64 ± 0.19
	UO <sub>2,60</sub>	60.07 ± 0.02	58.77 ± 0.23
	UO <sub>2,61.5</sub>	61.47 ± 0.04	59.77 ± 0.15
Udonthani Lot 3	UO <sub>3,48</sub>	47.77 ± 0.01	47.66 ± 0.09
	UO <sub>3,52</sub>	51.69 ± 0.01	51.11 ± 0.01
	UO <sub>3,56</sub>	55.92 ± 0.19	55.10 ± 0.05
	UO <sub>3,60</sub>	59.64 ± 0.03	58.92 ± 0.01
	UO <sub>3,61.5</sub>	61.54 ± 0.02	59.68 ± 0.01

**Table 4.2** Total solids content (TSC) and dry rubber content (DRC) of NRL samples prepared by dilution of re-centrifuged NRL concentrates

Sources	NRL samples	TSC (% by weight)	DRC (% by weight)
Chonburi	CC <sub>1,48</sub>	47.97 ± 0.02	47.38 ± 0.07
	CC <sub>1,52</sub>	51.98 ± 0.02	51.28 ± 0.12
	CC <sub>1,56</sub>	55.97 ± 0.03	55.39 ± 0.15
	CC <sub>1,60</sub>	60.01 ± 0.01	59.27 ± 0.20
	CC <sub>1,61.5</sub>	61.57 ± 0.02	60.62 ± 0.09
	CC <sub>1,64</sub>	63.94 ± 0.14	63.11 ± 0.06
	CC <sub>1,66</sub>	66.08 ± 0.02	65.53 ± 0.13
Suratthani	SC <sub>1,48</sub>	48.92 ± 0.19	47.87 ± 0.36
	SC <sub>1,52</sub>	51.68 ± 0.01	50.82 ± 0.25
	SC <sub>1,56</sub>	55.75 ± 0.31	55.22 ± 0.03
	SC <sub>1,60</sub>	60.22 ± 0.01	59.38 ± 0.50
	SC <sub>1,61.5</sub>	61.97 ± 0.02	61.20 ± 0.06
	SC <sub>1,64</sub>	64.67 ± 0.02	63.98 ± 0.14
	SC <sub>1,66</sub>	66.16 ± 0.07	65.58 ± 0.10
Udonthani Lot 1	UC <sub>1,48</sub>	48.00 ± 0.04	47.05 ± 0.10
	UC <sub>1,52</sub>	52.03 ± 0.13	51.15 ± 0.99
	UC <sub>1,56</sub>	56.00 ± 0.06	55.15 ± 0.15
	UC <sub>1,60</sub>	59.99 ± 0.03	59.10 ± 0.10
	UC <sub>1,61.5</sub>	61.17 ± 0.07	60.15 ± 0.48
	UC <sub>1,64</sub>	64.46 ± 0.03	63.66 ± 0.03
	UC <sub>1,66</sub>	64.98 ± 0.01	64.20 ± 0.20

**Table 4.2** Total solids content (TSC) and dry rubber content (DRC) of NRL samples prepared by dilution of re-centrifuged NRL concentrates (continued)

Sources	NRL samples	TSC (% by weight)	DRC (% by weight)
Udonthani Lot 2	UC <sub>2,48</sub>	47.74 ± 0.05	46.71 ± 0.24
	UC <sub>2,52</sub>	51.80 ± 0.04	50.70 ± 0.05
	UC <sub>2,56</sub>	55.64 ± 0.02	54.23 ± 0.08
	UC <sub>2,60</sub>	59.67 ± 0.03	58.58 ± 0.20
	UC <sub>2,61.5</sub>	60.89 ± 0.41	59.82 ± 0.08
	UC <sub>2,64</sub>	63.50 ± 0.02	62.56 ± 0.09
	UC <sub>2,66</sub>	65.42 ± 0.05	64.20 ± 0.06
Udonthani Lot 3	UC <sub>3,48</sub>	47.66 ± 0.09	46.92 ± 0.13
	UC <sub>3,52</sub>	51.85 ± 0.02	51.01 ± 0.08
	UC <sub>3,56</sub>	56.33 ± 0.13	55.35 ± 0.08
	UC <sub>3,60</sub>	59.57 ± 0.07	58.84 ± 0.06
	UC <sub>3,61.5</sub>	61.13 ± 0.03	60.57 ± 0.03
	UC <sub>3,64</sub>	63.85 ± 0.02	63.34 ± 0.12
	UC <sub>3,66</sub>	65.56 ± 0.04	64.49 ± 0.19

## **4.2 Particle size and particle size distribution**

### **4.2.1 Laser diffraction technique**

The particle size and PSD data from light scattering technique are presented in terms of particle frequency (% by volume) and rubber particle size diameter. Figure 4.1 shows the particle size distribution of CO<sub>1</sub>, SO<sub>1</sub>, UO<sub>1</sub>, UO<sub>2</sub>, and UO<sub>3</sub> samples. As seen, the shape of PSD of CO<sub>1</sub>, UO<sub>1</sub>, UO<sub>2</sub>, and UO<sub>3</sub> samples is relatively the same while the shape of slightly broader distribution at large size is observed for the SO<sub>1</sub>. The particle size distribution of the CC<sub>1</sub>, SC<sub>1</sub>, UC<sub>1</sub>, UC<sub>2</sub>, and UC<sub>3</sub> samples is shown in Figure 4.2. Large particles were found at the bottom of centrifugal tube and small particles were found at the top of centrifugal tube. Thus, the small particles are possibly removed resulting in narrower size distribution. The difference in size distribution is caused by the re-centrifugation process. In the centrifugation process, the particle size and particle size distribution depend on the density of the particle, density of the fluid medium, operating speed and time of centrifugation (Rippel, Lee, Leite and Galembeck, 2003). The similar distributions of studied Hevea NRL were investigated by Cornish and Brichta (2002) and Sanguansap, Suteewong, Saendee, Buranabunya, and Tangboriboonrat (2005).

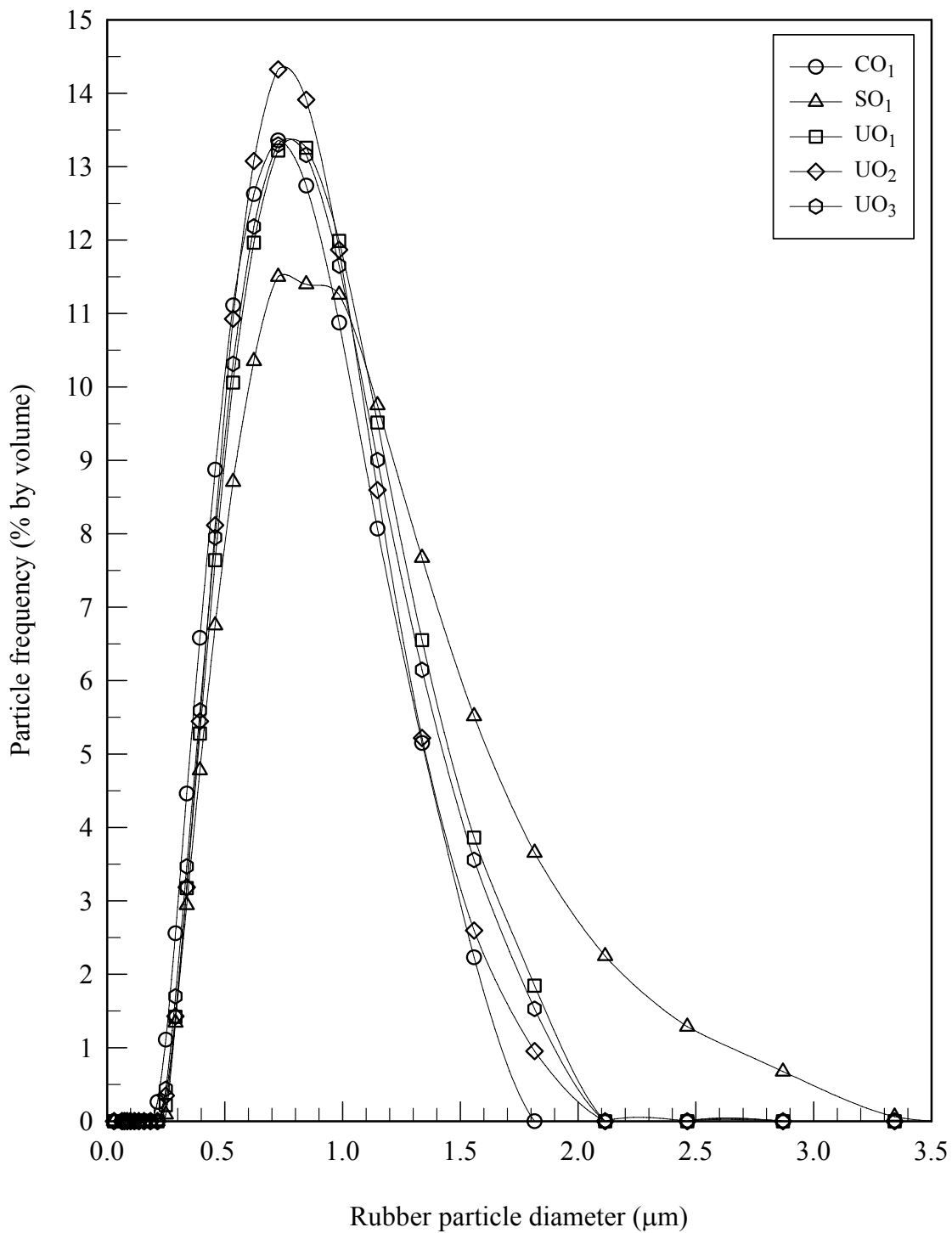


**Figure 4.1** Particle size distribution of rubber particles in the received NRL concentrates (CO<sub>1</sub>, SO<sub>1</sub>, UO<sub>1</sub>, UO<sub>2</sub>, and UO<sub>3</sub> samples)

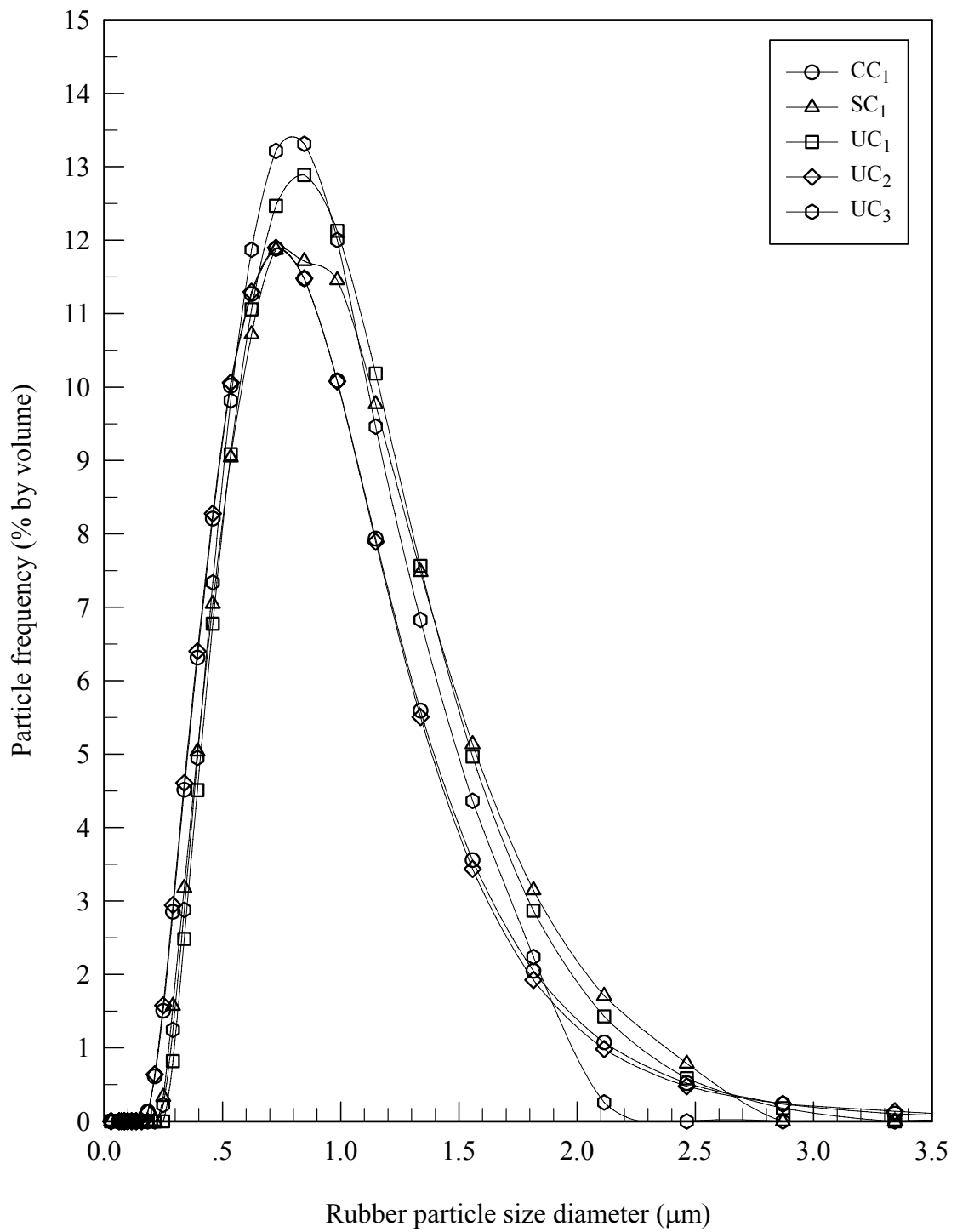


**Figure 4.2** Particle size distribution of rubber particles in the re-centrifuged NRL concentrates (CC<sub>1</sub>, SC<sub>1</sub>, UC<sub>1</sub>, UC<sub>2</sub> and UC<sub>3</sub> samples)

Particle size and particle size distribution are important in the study of latex or colloid system. Many statistical terms of average diameter were commonly used for polydisperse latex such as the average diameter by number average ( $D[1,0]$ ), surface area average ( $D[2,0]$ ), volume average ( $D[3,0]$ ), volume/area average ( $D[3,2]$ ) and volume/diameter average ( $D[4,3]$ ) (Blackley, 1997). In our NRL system, the volume/diameter average or z-average diameter was selected since the rheological properties depend on the distribution of volume of particles with respect to diameter. Average particle diameter was calculated in terms of mean diameter by volume/diameter average ( $D[4,3]$ ) according to equation (4.1) (Hunter, 1993). The distribution of diameter was displayed in terms of standard deviation ( $\sigma$ ) as computed by equation (4.2) (Hunter, 1993).

$$D[4,3] = \left[ \frac{\sum V_i d_i^4}{\sum V_i d_i^3} \right] \quad (4.1)$$

$$\sigma = \left( \frac{\sum V_i (d_i - \bar{d})^2}{\sum V_i} \right)^{1/2} \quad (4.2)$$

where  $V_i$  = relative volume of particle in class  $i$

$d_i$  = mean class diameter of particle in class  $i$

$\bar{d}$  = mean diameter of particle by volume/diameter average ( $D[4,3]$ )

By definition, the standard deviation is the root-mean-square deviation about the mean value. It does not provide an indicator of the statistical error about the mean of multiple measurements. If the distribution is unimodal and not too skewed, the standard deviation will give a reasonable indication of dispersity. But in case of un-normal distribution as in this experiment, the particle distributions were discussed in terms of skewness ( $S_k$ ) and polydispersity index ( $P_d$ ). The skewness is referred to

the degree of asymmetry in particle size distribution. The skewness value is defined as (Press, Teukolsky, Vettering and Flannery, 2002):

$$S_k = \frac{\sum V_i (d_i - \bar{d})^3}{\sigma^3 \sum V_i} \quad (4.3)$$

The polydispersity index,  $P_d$ , is defined by:

$$P_d = \left( 1 + \frac{\sigma^2}{\bar{d}^2} \right)^{1/2} \quad (4.4)$$

The values of z-average diameter average, standard deviation, skewness and polydispersity of concentrated NRL samples are summarized in Table 4.3. SO<sub>1</sub> showed the highest z-average diameter (0.93 μm) and standard deviation (0.48). For NRL concentrates without recentrifugation, the z-average diameter of rubber particle is in the order of SO<sub>1</sub> > UO<sub>1</sub> > UO<sub>3</sub> > UO<sub>2</sub> > CO<sub>1</sub>. Relatively the same standard deviation values were found on UO<sub>1</sub>, UO<sub>3</sub>, UO<sub>2</sub> and CO<sub>1</sub> samples. Z-average diameter and standard deviation of the re-centrifuged samples except SC<sub>1</sub> are higher than their counterparts. All latex samples showed the positive skewness values meaning that average diameter is greater than the median diameter. For normal distribution or monodisperse system, skewness is zero (Hall, 2000, Pongvichai, 2004). The increase of skewness value in re-centrifuged samples indicated the shift of z-average diameter to right positive value. The polydispersity is a measure of the breadth of the PSD: in the hypothetical case of a completely monodisperse,  $P_d = 1$ . A large value of  $P_d$  means a broad PSD (Hunter, 1992). The polydispersity index greater than one was found in all latex samples suggesting that the latex systems are the polydisperse system. The increasing values of  $D[4,3]$  of re-centrifuged samples can be explained by the removal of small particles in re-centrifugation process during

sample preparation (Rippel et al., 2003).

**Table 4.3** The summary of z-average diameter ( $D[4,3]$ ), standard deviation ( $\sigma$ ), skewness ( $S_k$ ) and polydispersity ( $P_d$ ) of concentrated NRL samples

NRL samples	$D[4,3]$ , ( $\mu\text{m}$ )	$\sigma$	$S_k$	$P_d$
CO <sub>1</sub>	0.74	0.30	0.65	1.08
SO <sub>1</sub>	0.93	0.48	1.34	1.13
UO <sub>1</sub>	0.82	0.34	0.78	1.08
UO <sub>2</sub>	0.78	0.31	0.82	1.08
UO <sub>3</sub>	0.80	0.34	0.80	1.08
CC <sub>1</sub>	0.81	0.44	2.00	1.14
SC <sub>1</sub>	0.89	0.43	1.09	1.11
UC <sub>1</sub>	0.89	0.41	1.20	1.10
UC <sub>2</sub>	0.80	0.42	1.66	1.13
UC <sub>3</sub>	0.83	0.35	1.84	1.09

#### 4.2.2 Transmission electron microscopy (TEM)

TEM was employed to investigate the morphology and particle size of NRL samples. Monodisperse polystyrene (Duke<sup>®</sup> scientific) with particle size diameter of  $220 \pm 6$  nm was used as TEM reference. The TEM micrograph of standard polystyrene is shown in Figure 4.3. As it is shown, PS particles are spherical and monomodal in size. Two hundred polystyrene particles were counted. The z-average diameter and standard deviation were calculated according to equations (4.1) and (4.2), respectively. From the calculation, the z-average diameter is  $217.44 \pm 9.41$  nm, which is close to the certification size from the Duke<sup>®</sup> scientific.

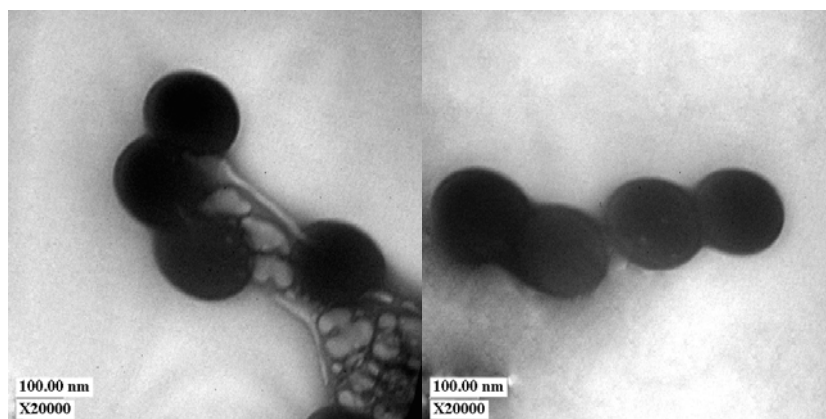


**Figure 4.3** TEM micrographs of  $220 \pm 6$  nm standard polystyrene taken at different positions

$CO_1$ ,  $SO_1$ ,  $UO_1$  and  $UO_2$  samples were selected to investigate the morphology and particle size. Their TEM micrographs are shown in Figure 4.4, 4.5, 4.6 and 4.7, respectively. All micrographs displayed the various size of rubber particle in each rubber cloud. The overlapping of particles was seen in all figures. The different sizes of rubber particles randomly dispersed in each rubber cloud. As it is observed in all micrographs, NRL particles are spherical and polydisperse. This morphology confirmed the polydispersity of NRL latex samples. This TEM micrograph agreed with TEM micrograph of freeze-fractured surface of NRL in the study of Rouilly, Rigal and Gilbert (2004). The z-average diameter and standard deviation from TEM were calculated according to equation (4.1) and (4.2), respectively. The summary of number of counted particles, z-average diameter and polydispersity index of  $CO_1$ ,  $SO_1$ ,  $UO_1$  and  $UO_2$  samples are shown in Table 4.4.

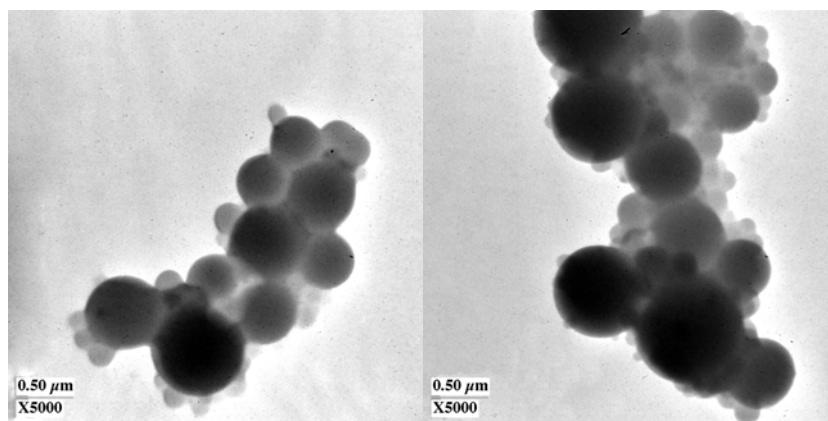


**Figure 4.4** TEM micrograph of CO<sub>1</sub> taken at different positions

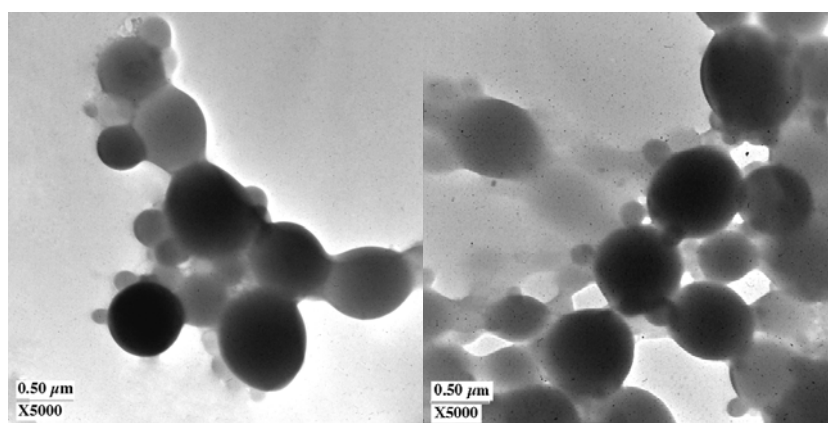


**Figure 4.5** TEM micrograph of SO<sub>1</sub> taken at different positions

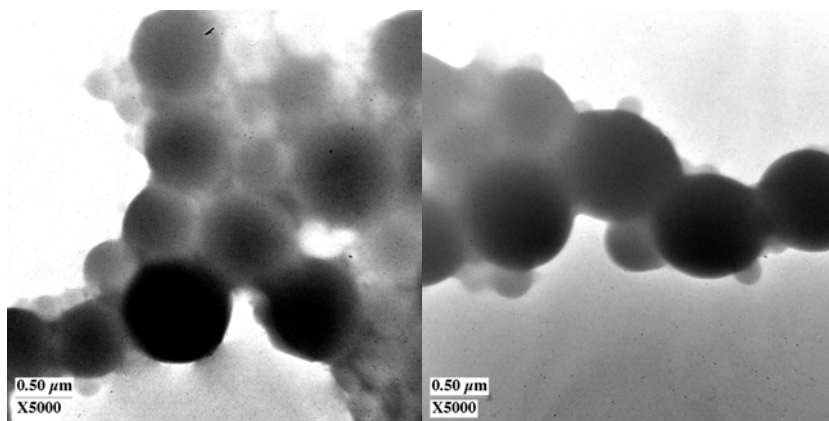


**Figure 4.6** TEM micrograph of  $\text{UO}_1$  taken at different positions

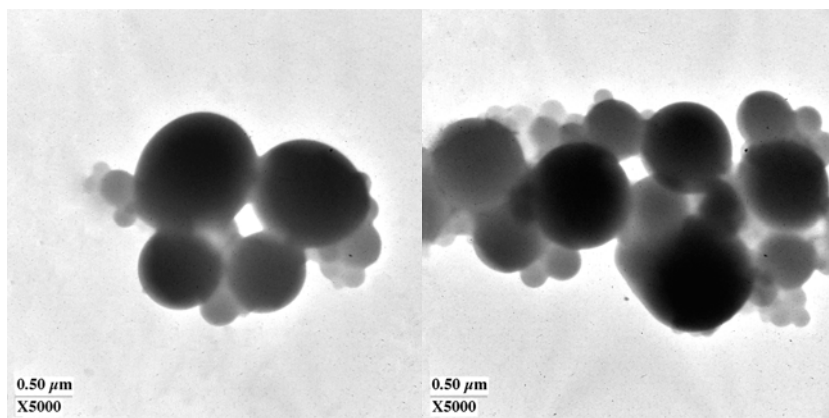


**Figure 4.7** TEM micrograph of  $\text{UO}_2$  taken at different positions

**Table 4.4** The summary of number of counted particles, z-average diameter ( $D[4,3]$ ), standard deviation ( $\sigma$ ), and polydispersity ( $P_d$ ) of CO<sub>1</sub>, SO<sub>1</sub>, UO<sub>1</sub> and UO<sub>2</sub> samples obtained from TEM

<b>NRL samples</b>	<b>Number of counted particles</b>	<b><math>D[4,3]</math>, (<math>\mu\text{m}</math>)</b>	<b><math>\sigma</math></b>	<b><math>P_d</math></b>
CO <sub>1</sub>	712	1.10	0.34	1.05
SO <sub>1</sub>	400	1.18	0.35	1.04
UO <sub>1</sub>	580	1.20	0.36	1.04
UO <sub>2</sub>	855	1.28	0.47	1.07

Higher number of particles counted provides more accurate particle size obtained from TEM. Due to the change in shape upon long exposure to electron beam, number of NR particles counted is limited. Thus TEM results will be used to only depict the shape of natural rubber particles.

### **4.3 Flow behavior of natural rubber latex concentrates**

Plots of viscosity against shear rate at 25°C of NRL concentrates from Chonburi, Suratthani, Udornthani lot 1, Udornthani lot 2 and Udornthani lot 3 are illustrated in Figure 4.8, 4.9, 4.10, 4.11 and 4.12, respectively. In each figure, the viscosity behavior of both sample preparations is presented. The directly diluted samples from the received latex are presented by closed symbols. The diluted samples from the re-centrifuged latex are presented by opened symbols. In the range of shear rates studied, shear thinning behavior is observed in all latex samples. Latex viscosity decreased when the applied shear rate was increased. This flow behavior

was explained by flow of time-independent inelastic fluids (Hunter, 1993). At low shear rates, Brownian motion of the rubber latexes made them to rotate and they interfere strongly with one another so the viscosity is high. As the shear rate increased, the rubber latexes were became deformable and aligned with the direction of flow, so that they interfere less with one other and the viscosity decreased. Shear thinning behavior is normally observed in both synthetic latex (Berend and Richtering, 1995, Ngothai et al., 1995, Varkey et al., 1995, Chu et al., 1998, Luckham and Ukeje, 1999, Mewis and Vermant, 2000) and natural latex system (Varkey et al., 1995). Generally, flow behavior of colloid system is classified into three parts; Newtonian plateau at low shear rate, shear thinning behavior at intermediate shear rate, and finally, Newtonian behavior at high shear rate (Goodwin, 1982 quoted in Rodriguez and Kaler, 1992). In this study, only shear thinning behavior at intermediate shear rate is found.

At the same TSC, NR latexes from both preparation methods do not show significant difference in viscosity. Besides the difference in particle size and PSD (will be discussed in 4.4). The small difference in viscosity may also result from non equivalence in percent of TSC. It suggests that the re-centrifugation of NRL concentrates does not affect the viscosity.

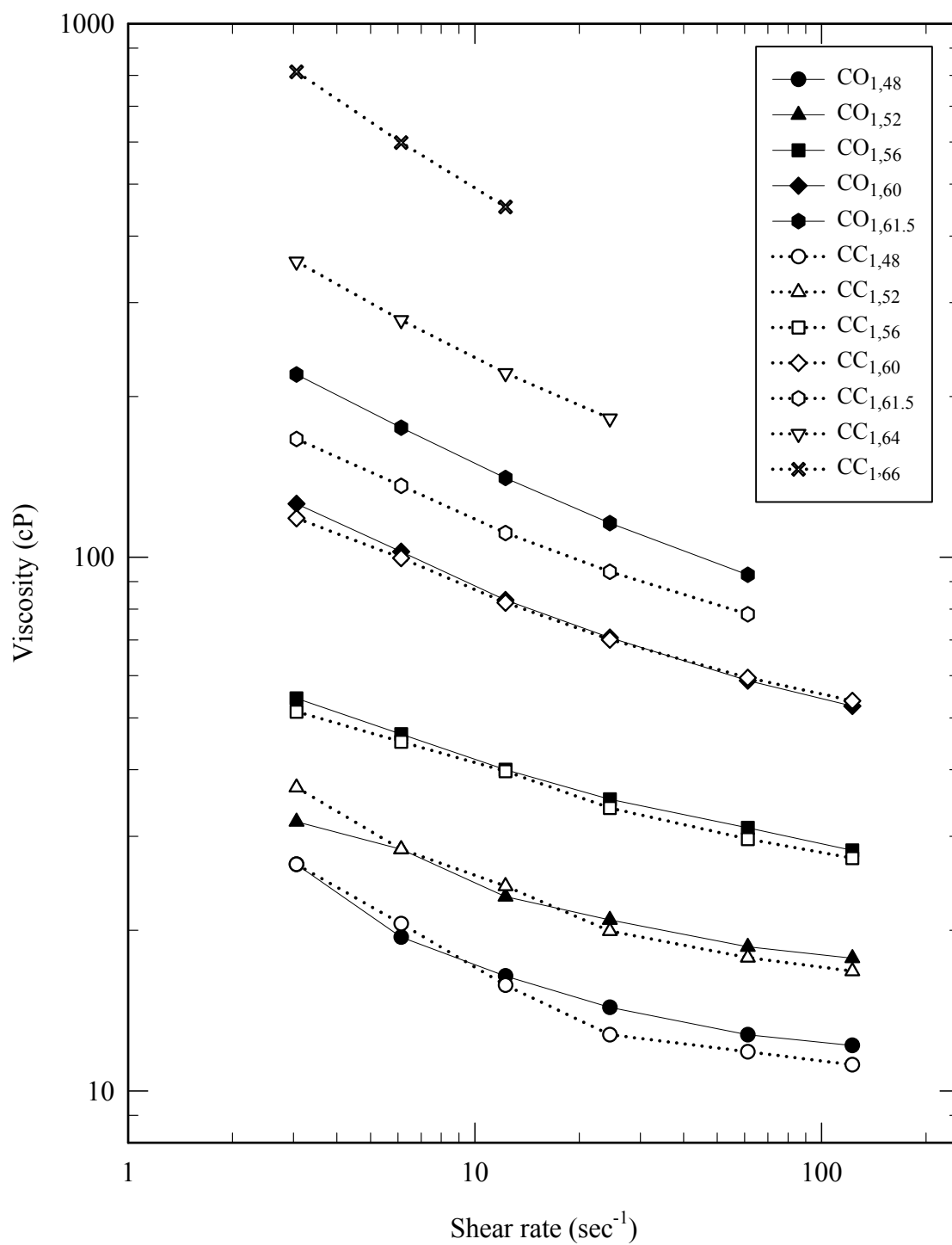


**Figure 4.8** A plot of viscosity at 25°C against shear rate of Chonburi NRL concentrates at various TSC: CO<sub>1</sub> (closed symbols) and CC<sub>1</sub> (opened symbols)

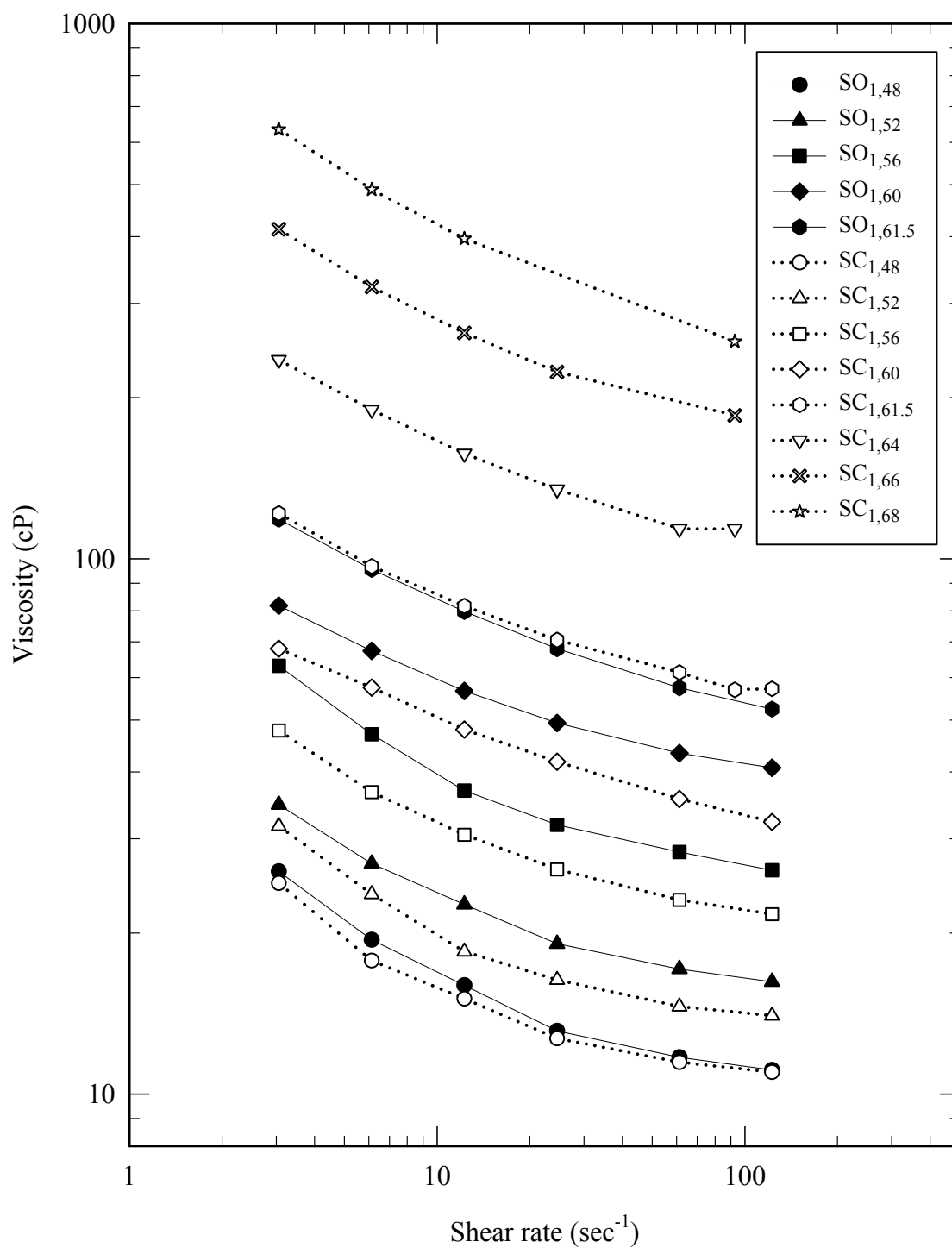


**Figure 4.9** A plot of viscosity at 25°C against shear rate of Suratthani NRL concentrates at various TSC: SO<sub>1</sub> (closed symbols) and SC<sub>1</sub> (opened symbols)

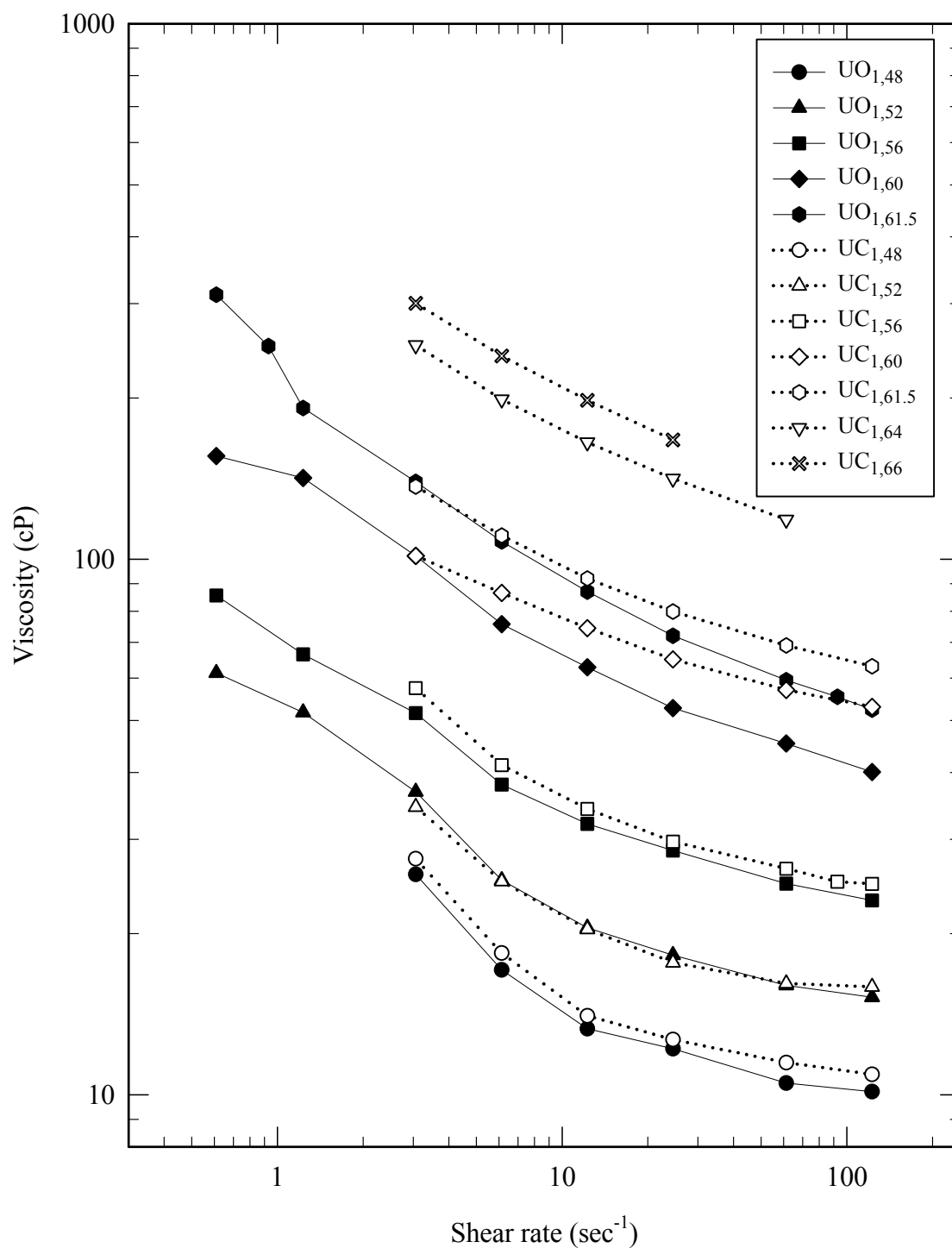


**Figure 4.10** A plot of viscosity at 25°C against shear rate of Udornthani lot 1 NRL concentrates at various TSC: UO<sub>1</sub> (closed symbols) and UC<sub>1</sub> (opened symbols)

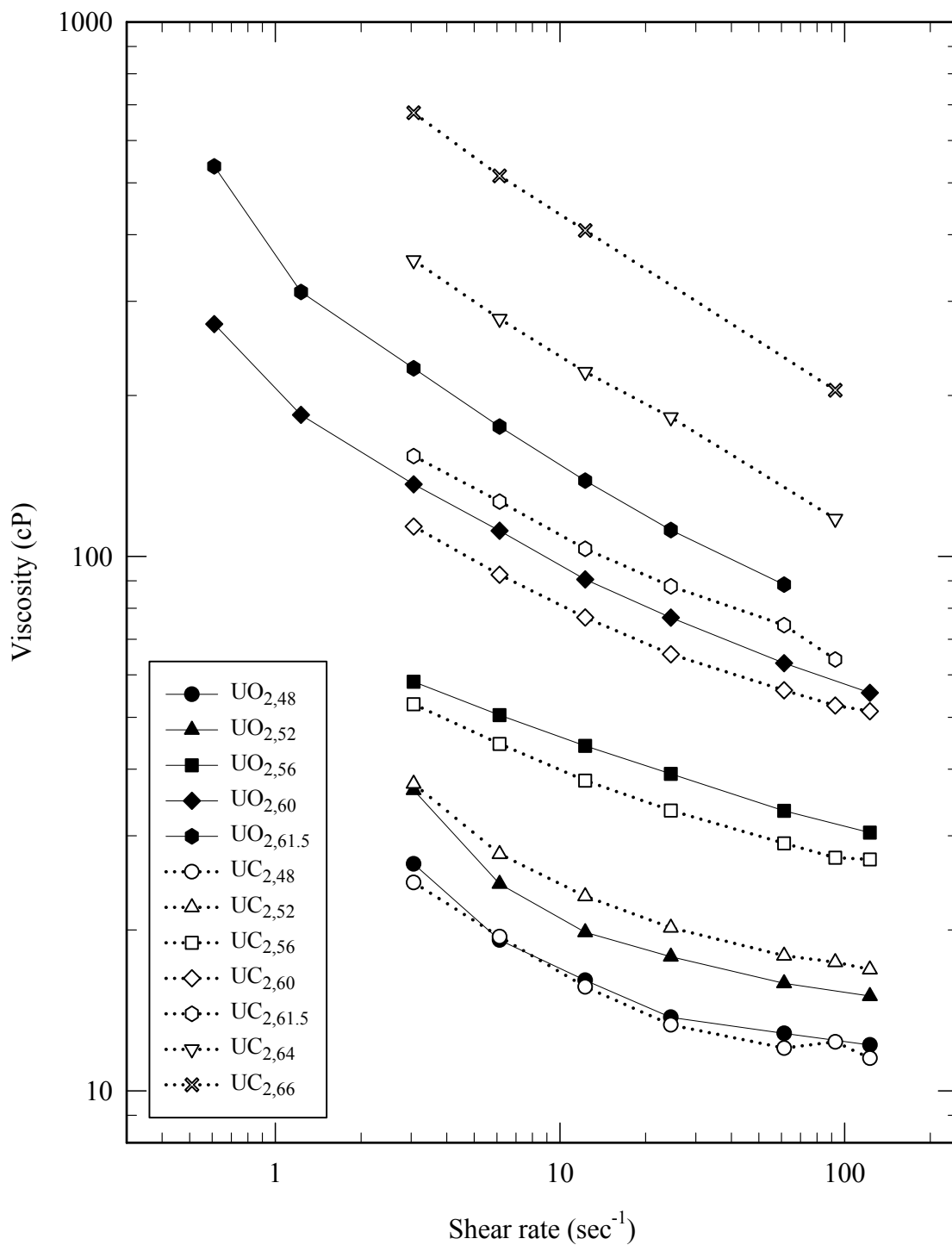


**Figure 4.11** A plot of viscosity at 25°C against shear rate of Udornthani lot 2 NRL concentrates at various TSC: UO<sub>2</sub> (closed symbols) and UC<sub>2</sub> (opened symbols)

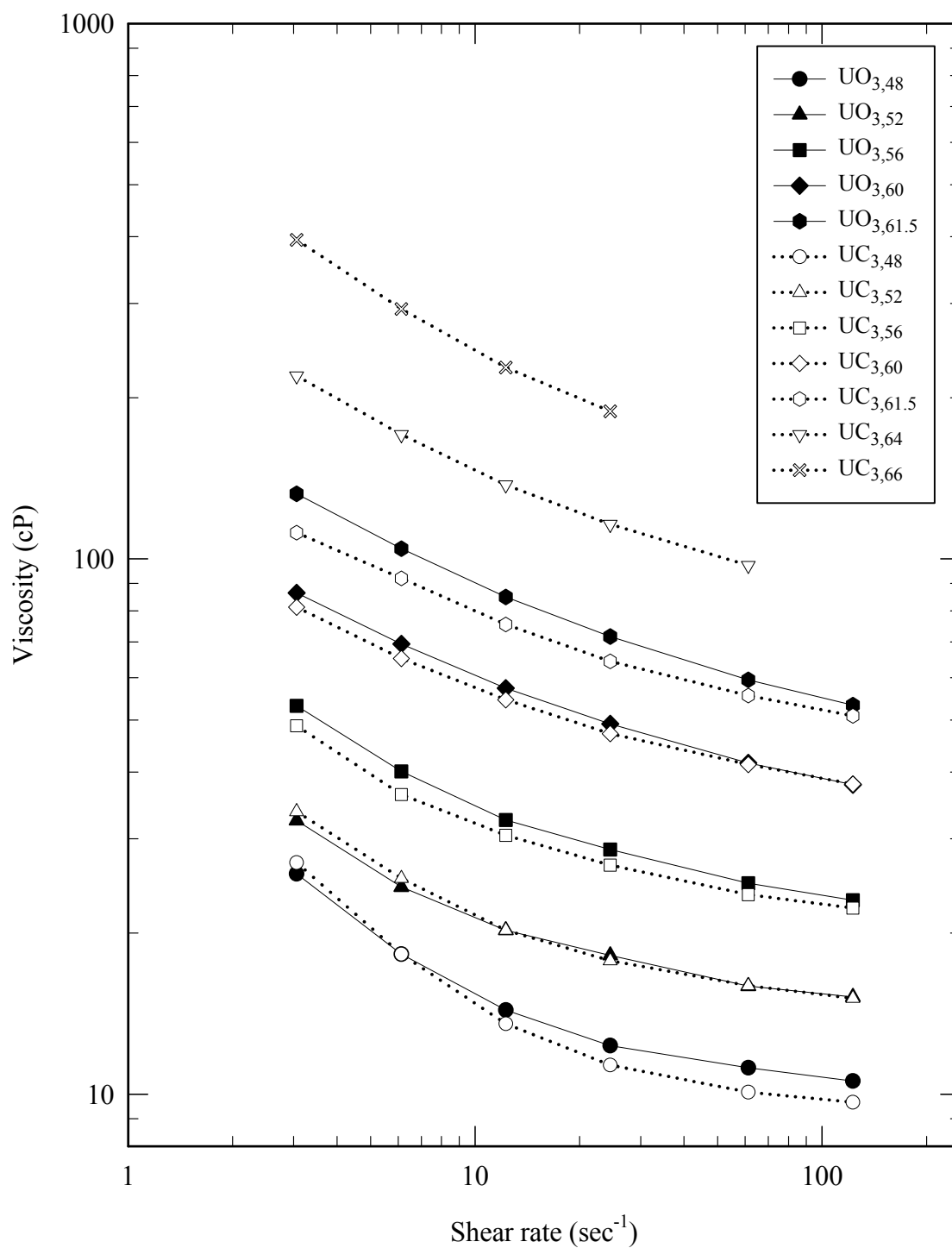


**Figure 4.12** A plot of viscosity at 25°C against shear rate of Udornthani lot 3 NRL concentrates at various TSC: UO<sub>3</sub> (closed symbols) and UC<sub>3</sub> (opened symbols)

#### 4.4 Effect of particle size and PSD on the latex viscosity

The latex viscosities at shear rates of 3.06, 6.13 and 12.26  $\text{sec}^{-1}$  were employed to present the effect of particle size and particles size distribution. Relative viscosity (equation 2.1), the ratio of viscosity of latex solution to the medium ( $\eta_0$ ), was used. In this study, water was assumed to be a latex medium in all samples. Density and viscosity of water at different temperatures were listed in Appendix A. Figure 4.13 shows the relative viscosity of NRL samples plotted against %TSC (by weight) at shear rate of 3.06  $\text{sec}^{-1}$  and temperature of 25°C. As it is shown, NRL samples are clearly divided into two groups of viscosity as drawn in gray areas. The same results are also observed at shear rate of 6.13 and 12.26  $\text{sec}^{-1}$  (Figure 4.14 and Figure 4.15). The separation of viscosity groups begins at 58-60% TSC. The first group with higher relative viscosity is composed of CO<sub>1</sub>, CC<sub>1</sub>, UO<sub>2</sub> and UC<sub>2</sub> and the second is composed of SO<sub>1</sub>, SC<sub>1</sub>, UO<sub>1</sub>, UC<sub>1</sub>, UO<sub>3</sub> and UC<sub>3</sub>. The relative viscosity of samples are in the order of CO<sub>1</sub>~UO<sub>2</sub> > CC<sub>1</sub>~UC<sub>2</sub> > UO<sub>1</sub>~UO<sub>3</sub> > SO<sub>1</sub> > UC<sub>3</sub>~UC<sub>1</sub> > SC<sub>1</sub>. The comparison of relative viscosity results with z-average diameter (in Table 4.3) was carried out to explain the experimental results. It is found that NRL samples in the upper gray have smaller particle size than that in the lower gray area. That is large particle showed lower relative viscosity than small particles. The results are agreed with the study of rheological behavior of synthetic latex (Johnson and Kelsey, 1958; Greenwood et al., 1998; Chu et al., 1998).

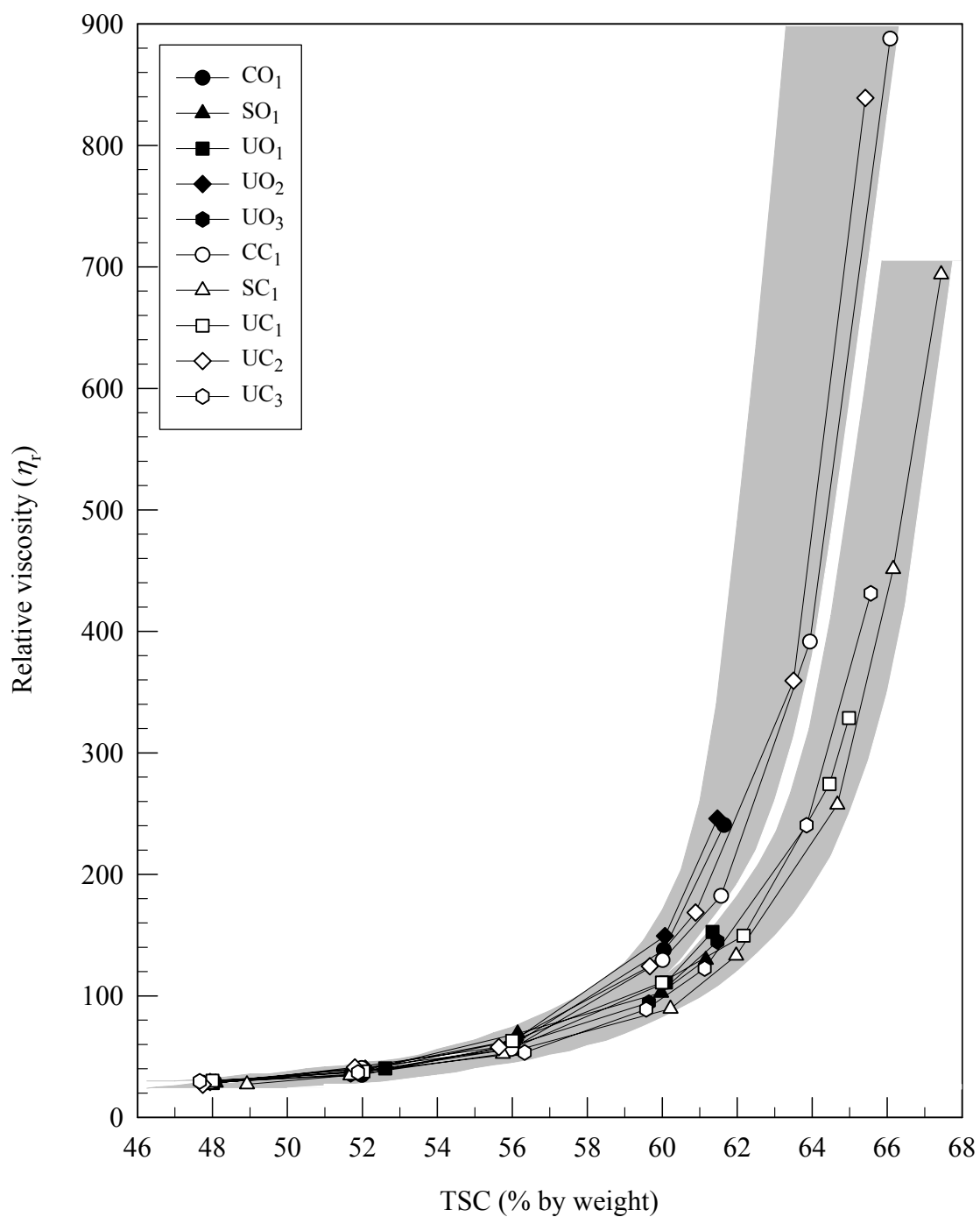


**Figure 4.13** Relative viscosity at various particle sizes as a function of TSC at shear rate of  $3.06 \text{ sec}^{-1}$  and temperature of  $25^\circ\text{C}$ : directly diluted samples (closed symbols) and diluted from re-centrifugation NRL (opened symbols)

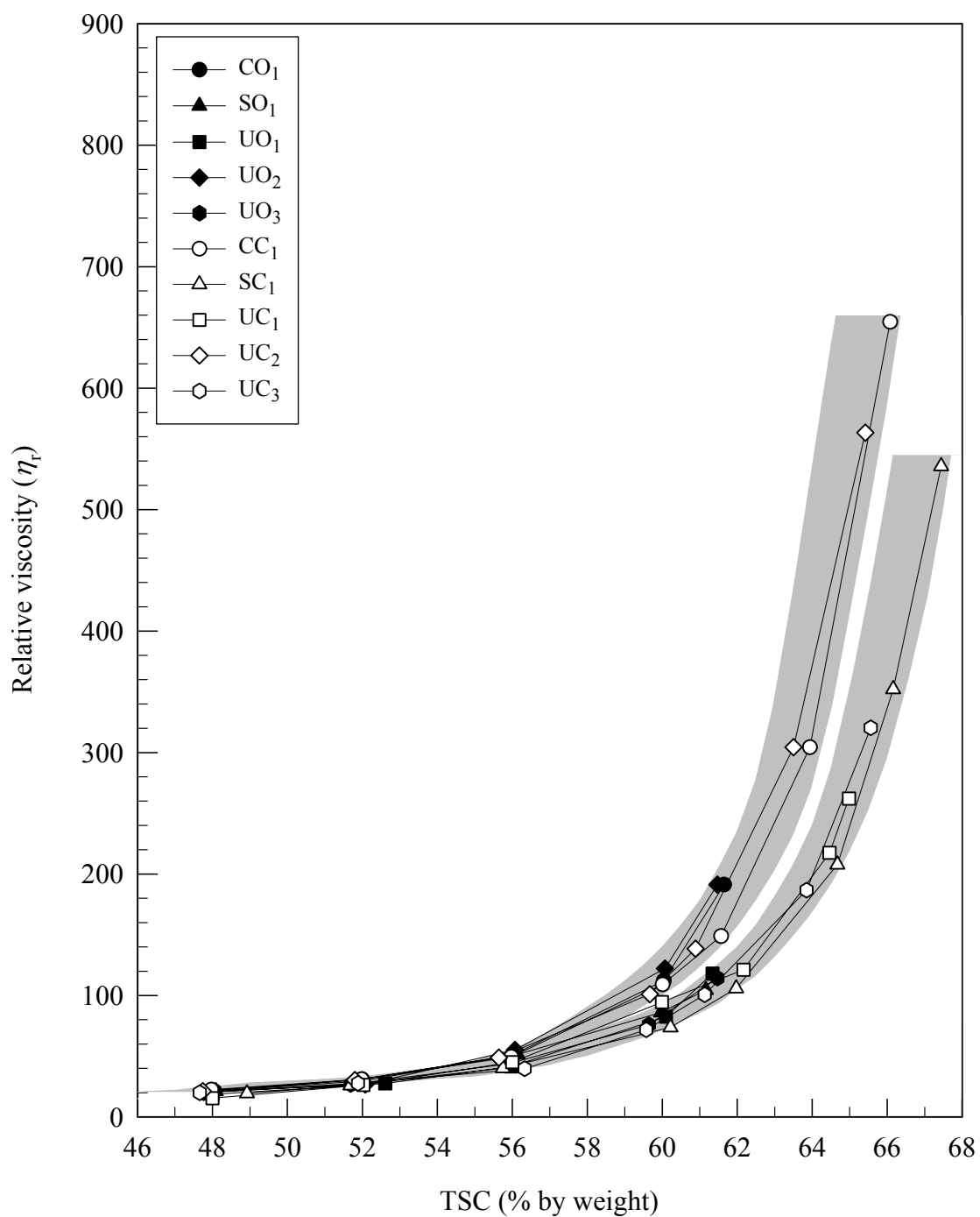


**Figure 4.14** Relative viscosity at various particle sizes as a function of TSC at shear rate of  $6.13 \text{ sec}^{-1}$  and temperature of  $25^\circ\text{C}$ : directly diluted samples (closed symbols) and diluted from re-centrifugation NRL (opened symbols)

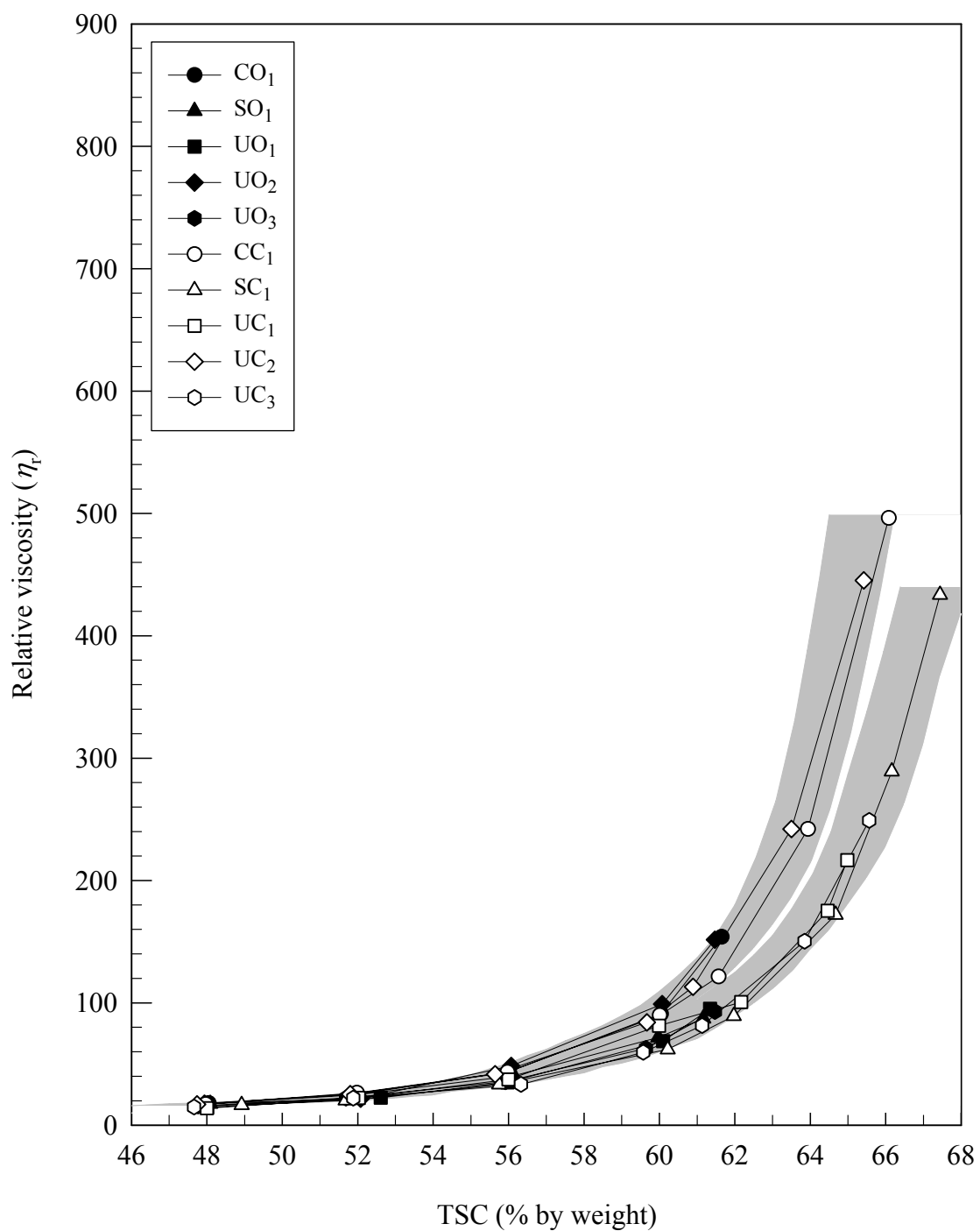


**Figure 4.15** Relative viscosity at various particle sizes as a function of TSC at shear rate of  $12.26 \text{ sec}^{-1}$  and temperature of  $25^\circ\text{C}$ : directly diluted samples (closed symbols) and diluted from re-centrifugation NRL (opened symbols)

Effect of particle size on latex viscosity can be explained by two reasons. First, increasing particle size or larger particle is expected to decrease the viscosity of latex, since the average distance between the surfaces of neighboring particles are increased (Blackley, 1997). The increasing of average distance between particles decreases the opportunity of particles to encounter and form of interparticle bonds (Johnson and Kelsey, 1958). Second, increasing particle size to decreases the surface area per unit volume (Blackley 1997). The normalized surface area per unit volume by CO<sub>1</sub> of NRL samples are shown in Table 4.5. Surface area per unit volume is calculated base on the spherical shape of particle. Surface area and volume of NRL particles were calculated according to equation (4.5) and equation (4.6), respectively.

$$\text{Surface area} = 4\pi \left(\frac{d_i}{2}\right)^2 \quad (4.5)$$

$$\text{Volume} = \frac{4}{3}\pi \left(\frac{d_i}{2}\right)^3 \quad (4.6)$$

As mentioned earlier, PSD does affect flow of latex. Polydisperse system shows lower viscosity than monodisperse system. In this work, it is difficult to clearly see the effect of PSD on latex viscosity. For natural latex, one cannot actually blend particles of specific sizes with a known proportion. However, among NRL studied, SO<sub>1</sub> with highest particle size does not show the lowest viscosity. This could be an example indicating the effect of PSD. For high polydisperse system, the small particles can be accommodated between the larger ones. This increases the packing efficiency (Blackley, 1997).

**Table 4.5** The normalized surface area per volume of NRL samples by surface area per volume of CC<sub>1</sub> sample

NRL samples	$D[4,3]$ , ( $\mu\text{m}$ )	Surface area ( $\text{m}^2$ )	Volume ( $\text{m}^3$ )	Surface area per unit volume ( $\text{m}^2/\text{m}^3$ )	Normalized surface area per volume
CO <sub>1</sub>	0.74	8.43E-11	1.04E-17	8.11E+06	1.00
SO <sub>1</sub>	0.93	1.33E-10	2.06E-17	6.45E+06	0.80
UO <sub>1</sub>	0.82	1.04E-10	1.42E-17	7.32E+06	0.90
UO <sub>2</sub>	0.78	9.37E-11	1.22E-17	7.69E+06	0.95
UO <sub>3</sub>	0.80	9.86E-11	1.31E-17	7.50E+06	0.93
CC <sub>1</sub>	0.81	1.01E-10	1.36E-17	7.41E+06	0.91
SC <sub>1</sub>	0.89	1.22E-10	1.81E-17	6.74E+06	0.83
UC <sub>1</sub>	0.89	1.22E-10	1.81E-17	6.74E+06	0.83
UC <sub>2</sub>	0.80	9.86E-11	1.31E-17	7.50E+06	0.93
UC <sub>3</sub>	0.83	1.06E-10	1.47E-17	7.23E+06	0.89

As a result, latex viscosity decreases. It is to mention that, the difference in viscosity between the different z-average sizes decreases with increasing shear rates. For example, 64% TSC (by weight) relative viscosities between CC<sub>1</sub>-UC<sub>1</sub> differ about 250, 140 and 90 cP at shear rates 3.06, 6.13 and 12.26  $\text{sec}^{-1}$ , respectively. This can be explained by shear thinning behavior. As the shear rate increased, the rubber particles become deformable and align with the direction of flow, so that the particles surface was less affected.

#### 4.5 Effect of the total solids content on viscosity

The NRL viscosity at 25°C as a function of TSC at various shear rates was investigated. The latex viscosity was converted into relative viscosity term to neglect the different medium of NRL and temperature as in section 4.4. Plot of relative viscosity of Chonburi NRL against total solids content at six shear rates are shown in Figure 4.16. Relative viscosity of CO<sub>1</sub> is presented by closed symbols and CC<sub>1</sub> is presented by opened symbols. As seen in Figure 4.16, the relative viscosity of both samples slowly increased with percent TSC until the critical point (~ 60% TSC), so called critical TSC (TSC<sub>c</sub>). At upper than TSC<sub>c</sub>, relative viscosities of both samples rapidly increased with increasing TSC. The rapid increasing of relative viscosity with TSC beyond the critical point was explained by correlation to the maximum packing volume ( $\phi_{\max}$ ) of the particles system (Hunter, 1993, Schneider et al., 2002). The similar results are also obtained in NRL from Suratthani, Udornthani lot 1, 2 and 3, as presented in Figure 4.17, 4.18, 4.19 and 4.20, respectively. Similar latex behavior is typically observed in both concentrated natural rubber latex (Rhodes and Smith, 1939; Cornish and Brichta, 2002) and in synthetic latex (Chu et al., 1998; Luckham and Ukeje, 1999; Schneider et al., 2002).

In this work, TSC<sub>c</sub> is defined as the intersection between slope of tangent at low TSC (slow increase viscosity) and tangent at high TSC (rapid increase viscosity). The exemplary determination of TSC<sub>c</sub> is shown in Figure 4.21. Figure 4.21 shows the determination of TSC<sub>c</sub> of CC<sub>1</sub> and UC<sub>1</sub> at shear rate 3.06 sec<sup>-1</sup>. The lines are drawn according to the slope of average relative viscosity with TSC in both of lower and higher of TSC<sub>c</sub> range. The intersection between slopes indicated the TSC<sub>c</sub> of CC<sub>1</sub> and UC<sub>1</sub> samples. TSC<sub>c</sub> of each NRL latex is obtained and summarized in Table 4.6.

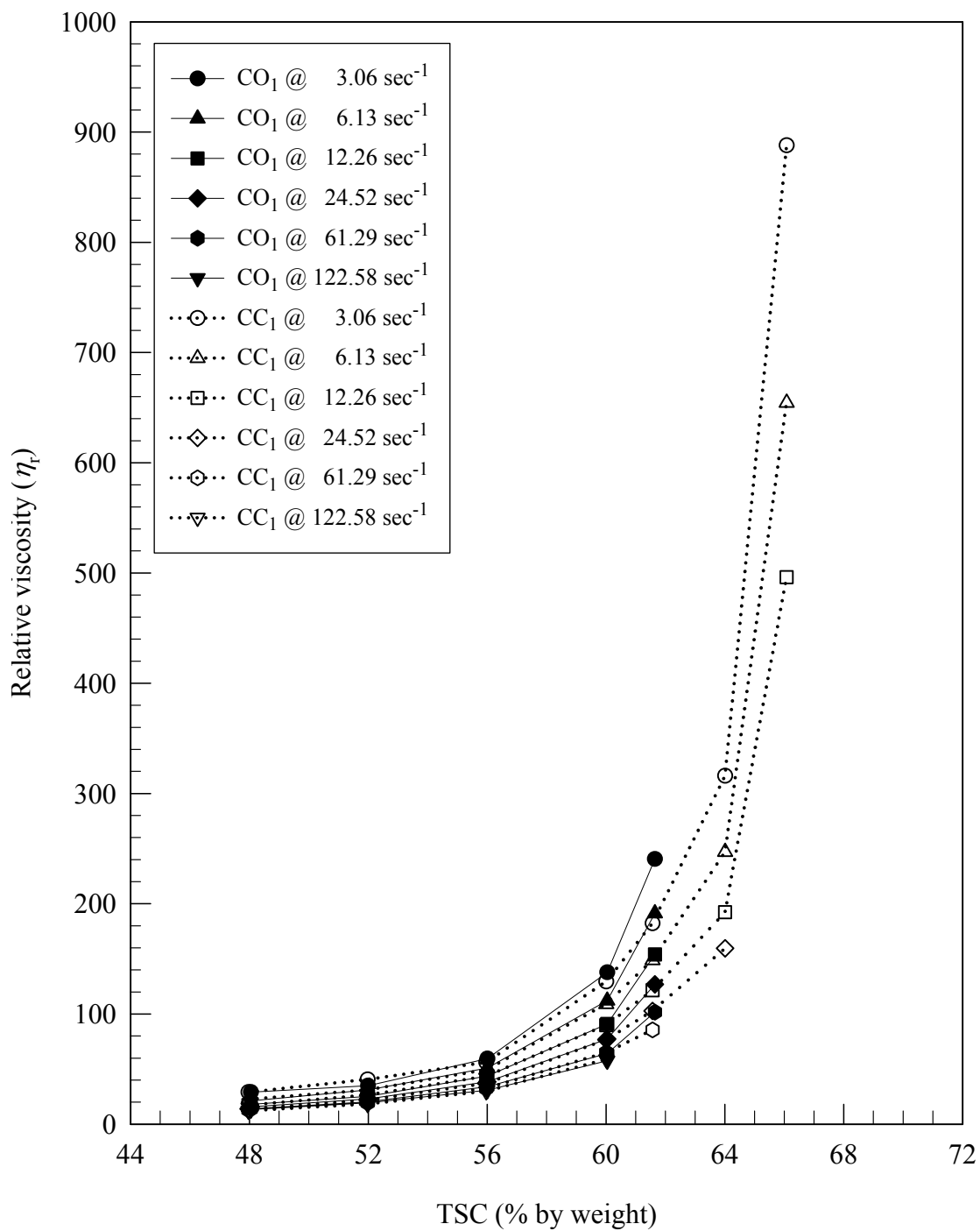


**Figure 4.16** Relative viscosity at various shear rates as a function of TSC of Chonburi NRL at 25°C: CO<sub>1</sub> (closed symbols) and CC<sub>1</sub> (open symbols)

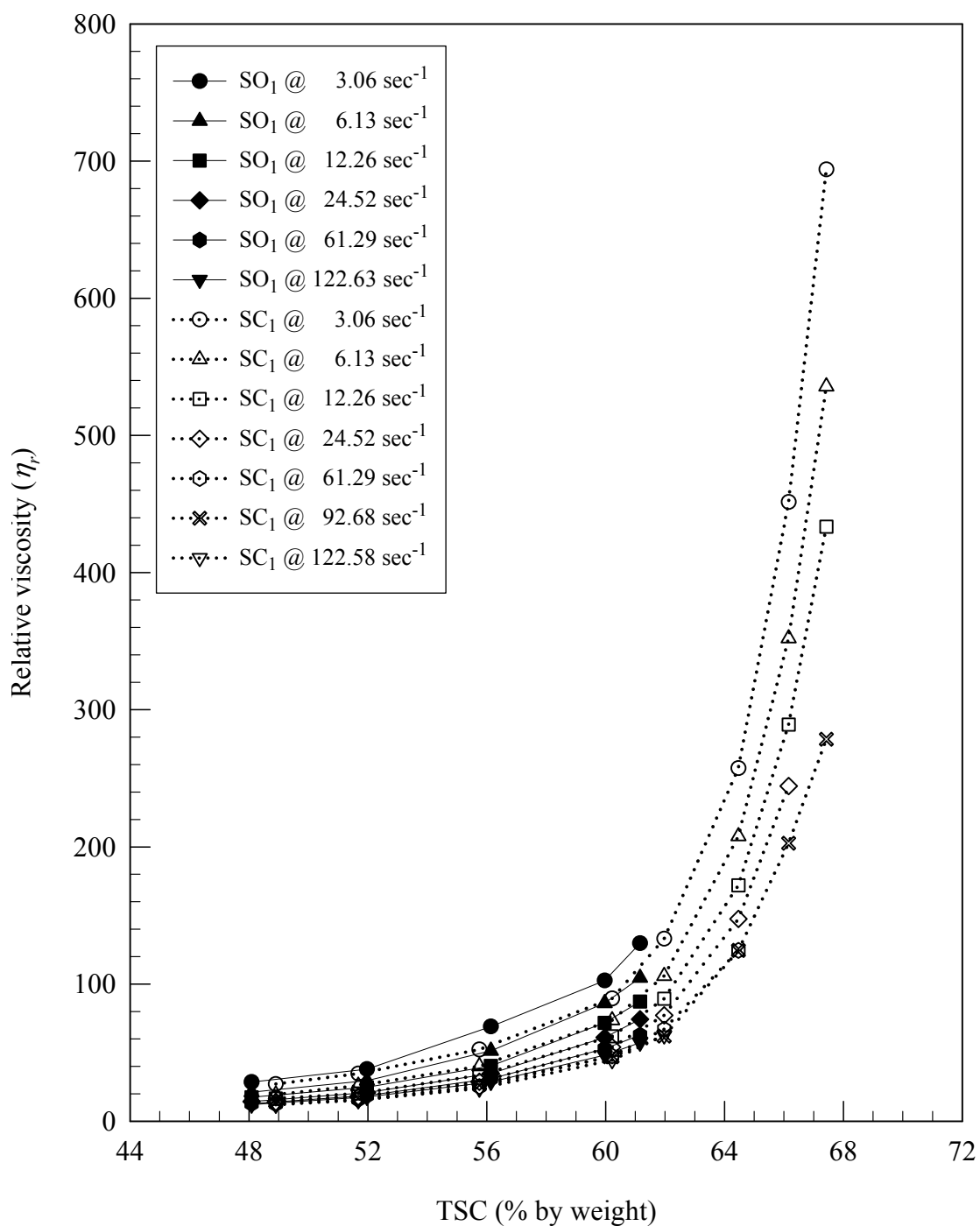


**Figure 4.17** Relative viscosity at various shear rates as a function of TSC of Suraththani NRL at 25°C: SO<sub>1</sub> (closed symbols) and SC<sub>1</sub> (opened symbols)

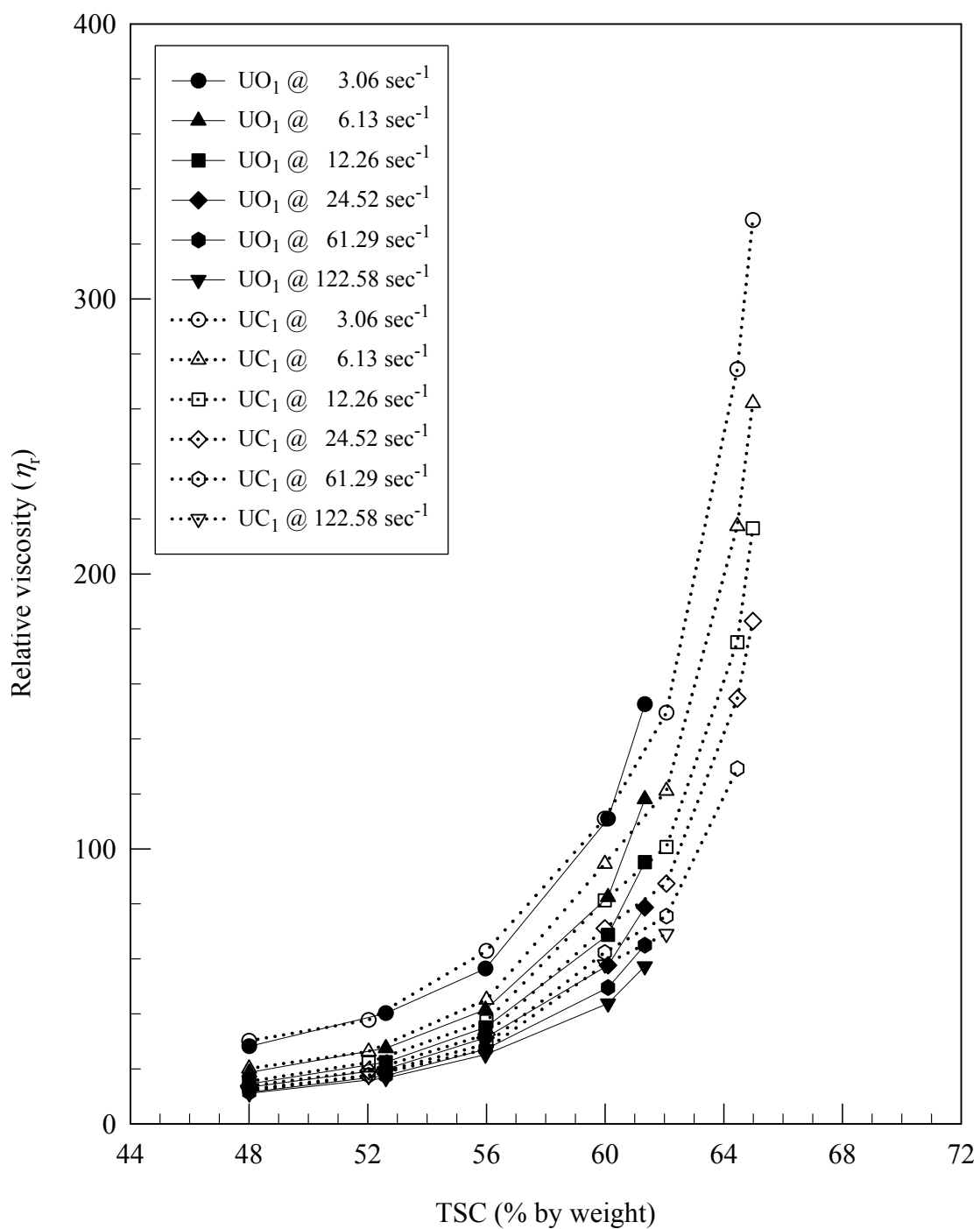


**Figure 4.18** Relative viscosity at various shear rates as a function of TSC of Udmnthani lot 1 NRL at 25°C: UO<sub>1</sub> (closed symbols) and UC<sub>1</sub> (open symbols)

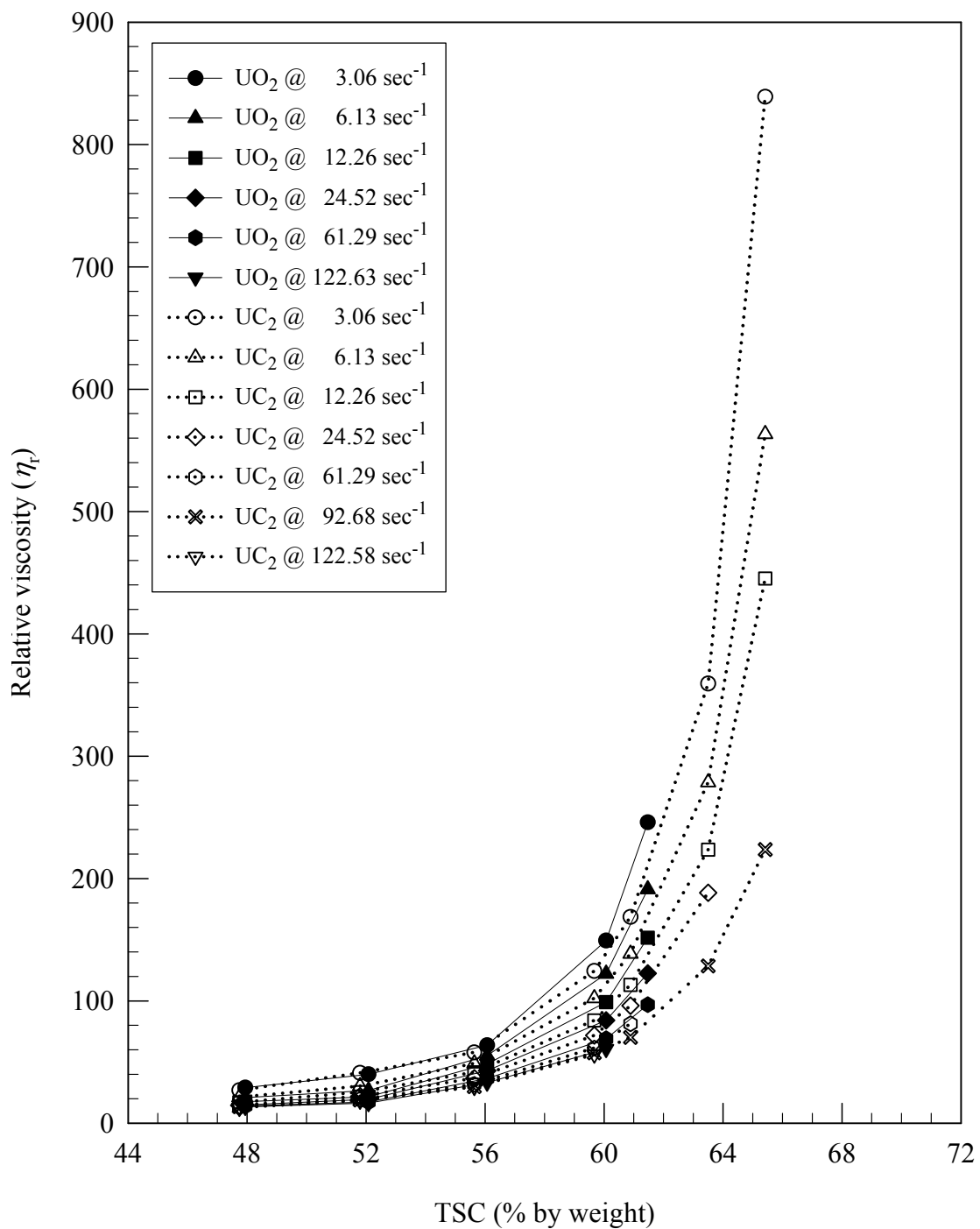


**Figure 4.19** Relative viscosity at various shear rates as a function of TSC of Udnrnthani lot 2 NRL at 25°C: UO<sub>2</sub> (closed symbols) and UC<sub>2</sub> (open symbols)

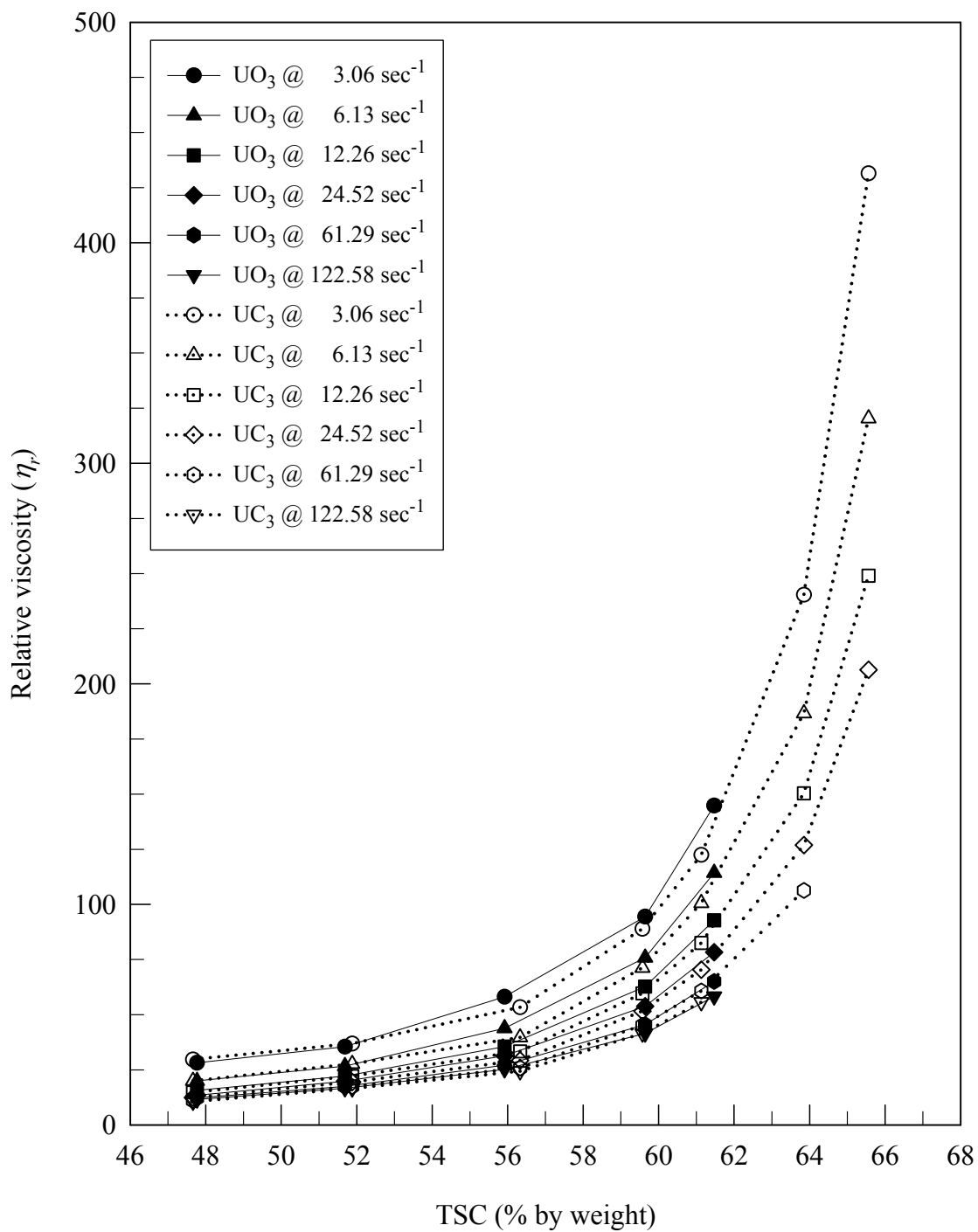


**Figure 4.20** Relative viscosity at various shear rates as a function of TSC of Udmnthani lot 3 NRL at 25°C: UO<sub>3</sub> (closed symbols) and UC<sub>3</sub> (open symbols)

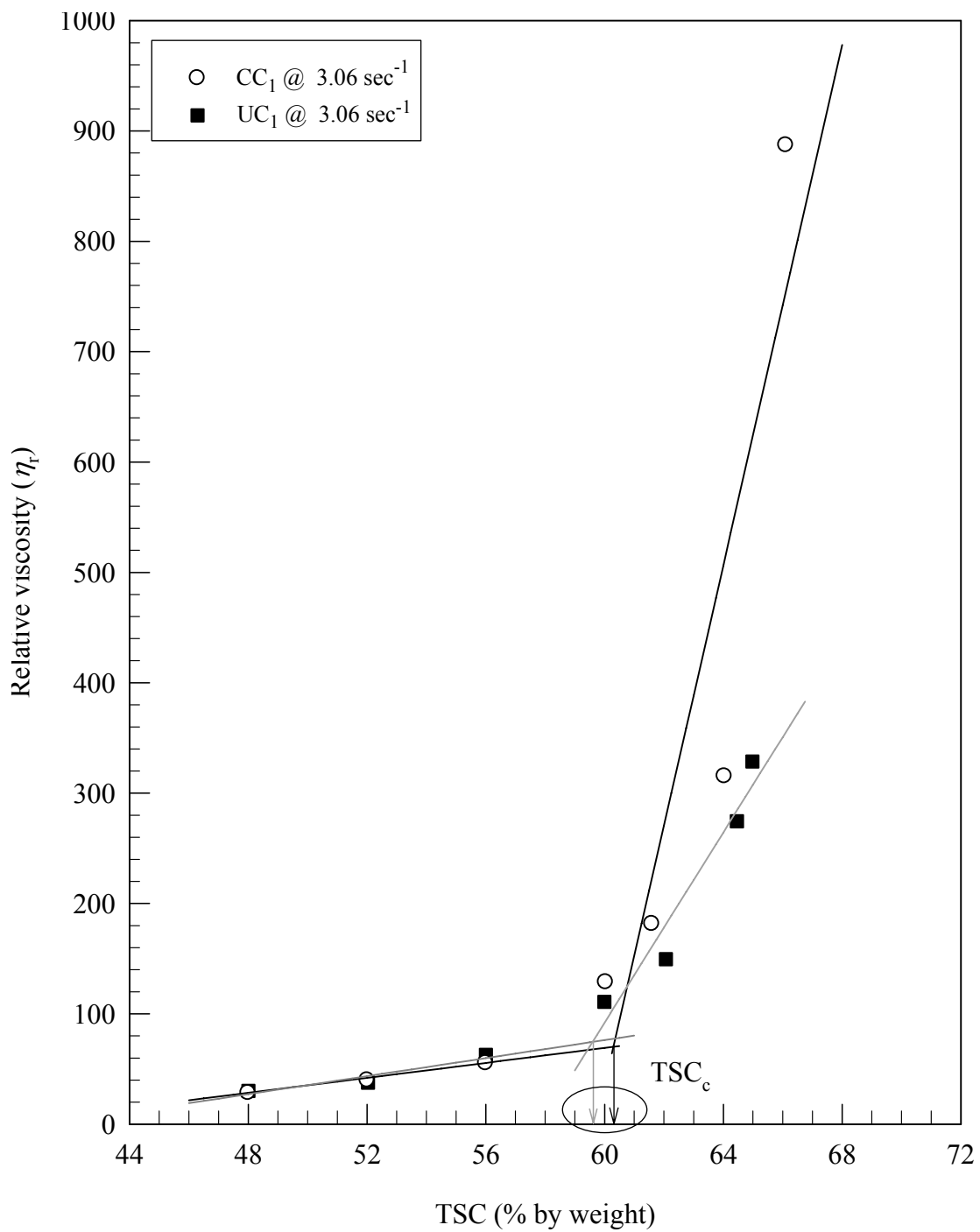


**Figure 4.21** The determination of critical total solid content (TSC<sub>c</sub>) is illustrated

**Table 4.6** The critical total solids content ( $TSC_c$ ) of NRL samples determined from slope intersection

NRL samples	Shear rate ( $\text{sec}^{-1}$ )	$TSC_c$	Average $TSC_c$
CC <sub>1</sub>	3.06	60.3	60.2 ± 0.1
	6.13	60.2	
	12.26	60.2	
SC <sub>1</sub>	3.06	60.8	60.7 ± 0.2
	6.13	60.8	
	12.26	60.7	
	24.52	60.3	
	92.68	60.7	
UC <sub>1</sub>	3.06	59.6	59.2 ± 0.3
	6.13	59.2	
	12.26	59.1	
	24.52	59.0	
UC <sub>2</sub>	3.06	59.9	59.7 ± 0.2
	6.13	59.7	
	12.26	59.7	
	92.68	59.4	
UC <sub>3</sub>	3.06	59.6	59.5 ± 0.1
	6.13	59.4	
	12.26	59.4	
	24.52	59.4	

As seen in Table 4.6, only  $TSC_c$  of diluted samples from re-centrifuged latex with sufficient data at high TSC are shown. For direct dilution of as received NRL concentrates samples, the determination of  $TSC_c$  from slope intersection was not

applied because of low viscosity data beyond the  $TSC_c$ . As seen in Table 4.6,  $TSC_c$  of all latex samples does not vary with applied shear rates. It suggests that  $TSC_c$  does not depend on the applied shear rates and represents an individual characteristic of each system. The  $TSC_c$ s of NRL samples (only from re-centrifuged) are in order of  $UC_1 < UC_3 < UC_2 < CC_1 < SC_1$ . It is proposed that  $TSC_c$  relates to the maximum packing volume ( $\phi_{max}$ ). It can be inferred that PS and PSD should affect  $TSC_c$ . As reviewed in chapter 2,  $\phi_{max}$  varies with particle size and PSD.

According equation (2.3) and (2.4), comparing high and low  $\phi_{max}$  systems, high  $\phi_{max}$  system gives lower latex viscosity. This high  $\phi_{max}$  system would benefit latex in manufacturing process since latex contains higher solids content with low viscosity.  $TSC_c$  of NRL would then be useful for NRL processes.

#### **4.6 Effect of temperature on the latex viscosity**

To investigate the influence of temperature on the viscosity, NRL samples with different  $TSC$ s from two preparation methods were employed. Temperature range of 10 to 40°C with the increment of 5°C was used. Figure 4.22 (a) shows a plot of latex viscosity of  $UO_{3,56}$  against temperature at six shear rates. The latex viscosity of  $UO_{3,56}$  decreased when temperature is increased at all shear rates. As for all liquids, latex viscosity decreases with increasing temperature. This result does not show a behavior of latex heat-sensitization (Blackley, 1997). The latex heat-sensitization behavior is a decrease of latex viscosity as temperature increased, until a certain temperature is attained at which a sudden increase in viscosity is evident and coagulation occurs. The decreasing behavior of viscosity with increasing temperature is also found in  $UO_{3,60}$  (Figure 4.23 (a)),  $UC_{3,56}$  (Figure 4.24 (a)),  $UC_{3,60}$  (Figure 4.24

(a)) and UC<sub>3,64</sub> (Figure 4.26 (a)). This behavior was also observed in other species of NRL (P. argentatum and F. elastica) (Cornish and Brichta, 2002) and synthetic rubber (Varkey et al., 1995). According to equation 2.1,

$$\eta_r (T) = \frac{\eta (T)}{\eta_0 (T)}$$

$\eta_r$  represents the latex viscosity when viscosity of medium ( $\eta_0$ ) is taken into consideration. As shown in Figure 4.22 (b) for UO<sub>3,56</sub>,  $\eta_r$  increases with temperature at all shear rates, opposite to the results shown in Figure 4.22 (a). This finding indicates that viscosity of the medium changes more dramatic than viscosity of the latex itself with temperature.

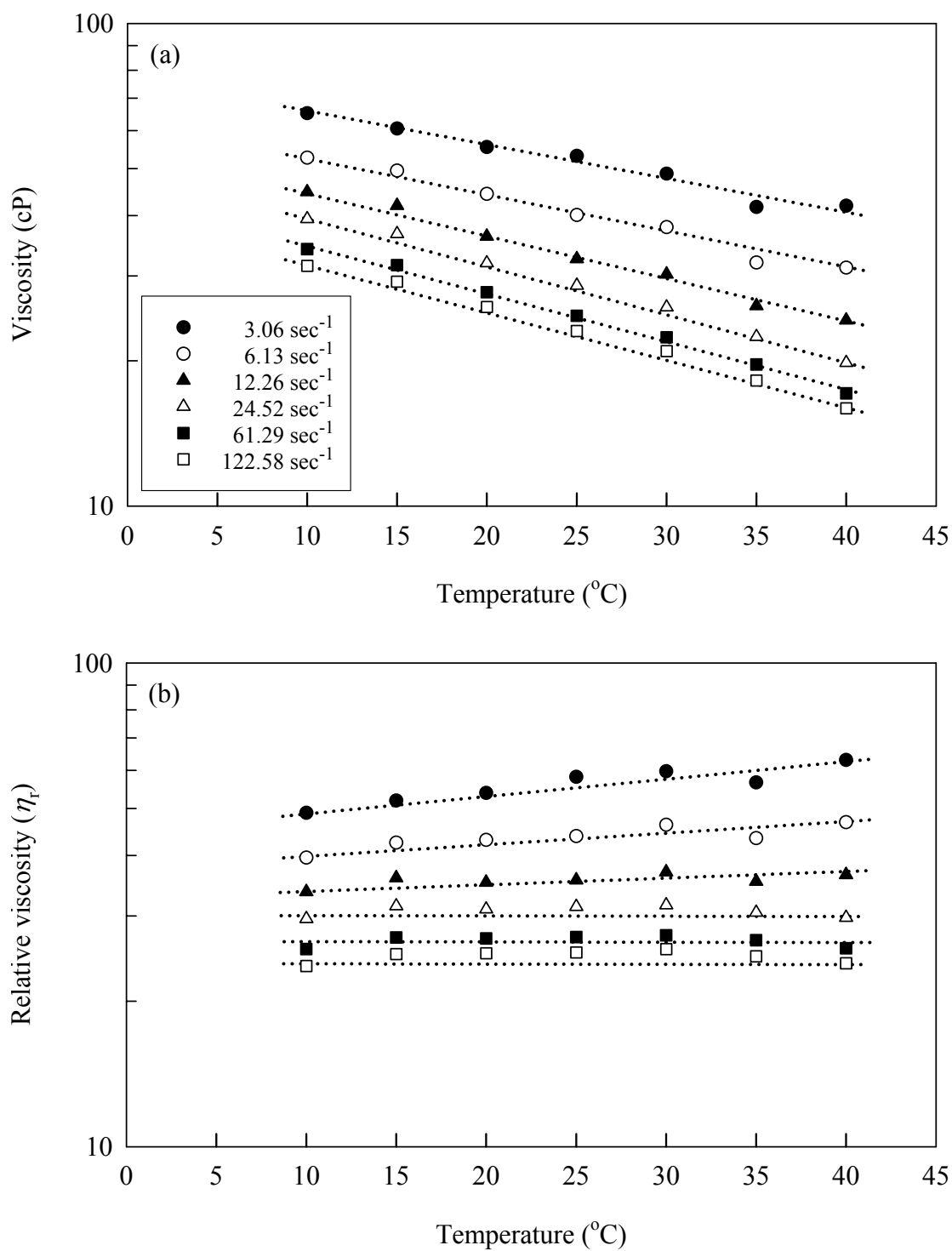


**Figure 4.22** Effect of temperature on (a) viscosity and (b) relative viscosity of  $\text{UO}_{3,56}$  at various shear rates

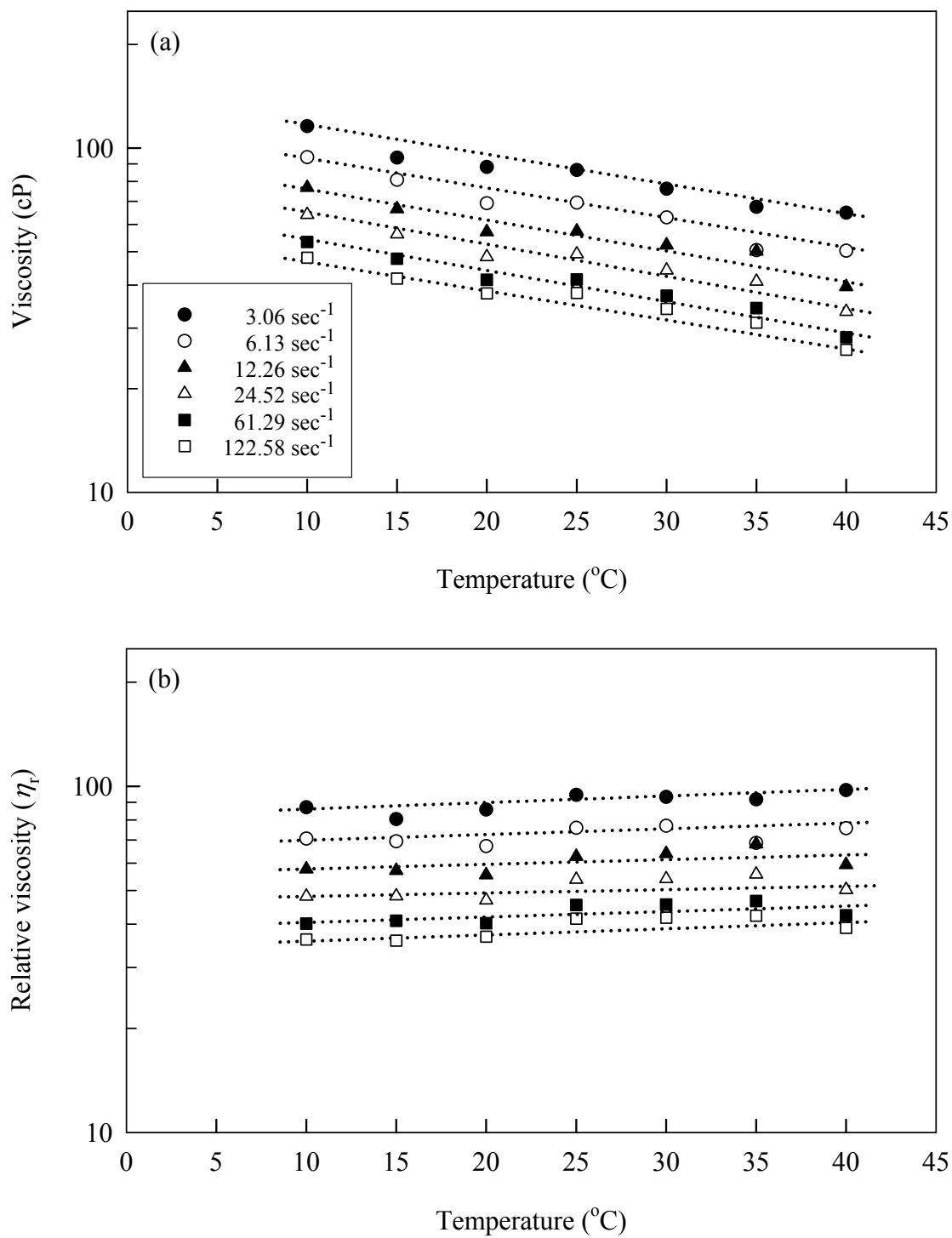


**Figure 4.23** Effect of temperature on (a) viscosity and (b) relative viscosity of  $\text{UO}_{3,60}$  at various shear rates

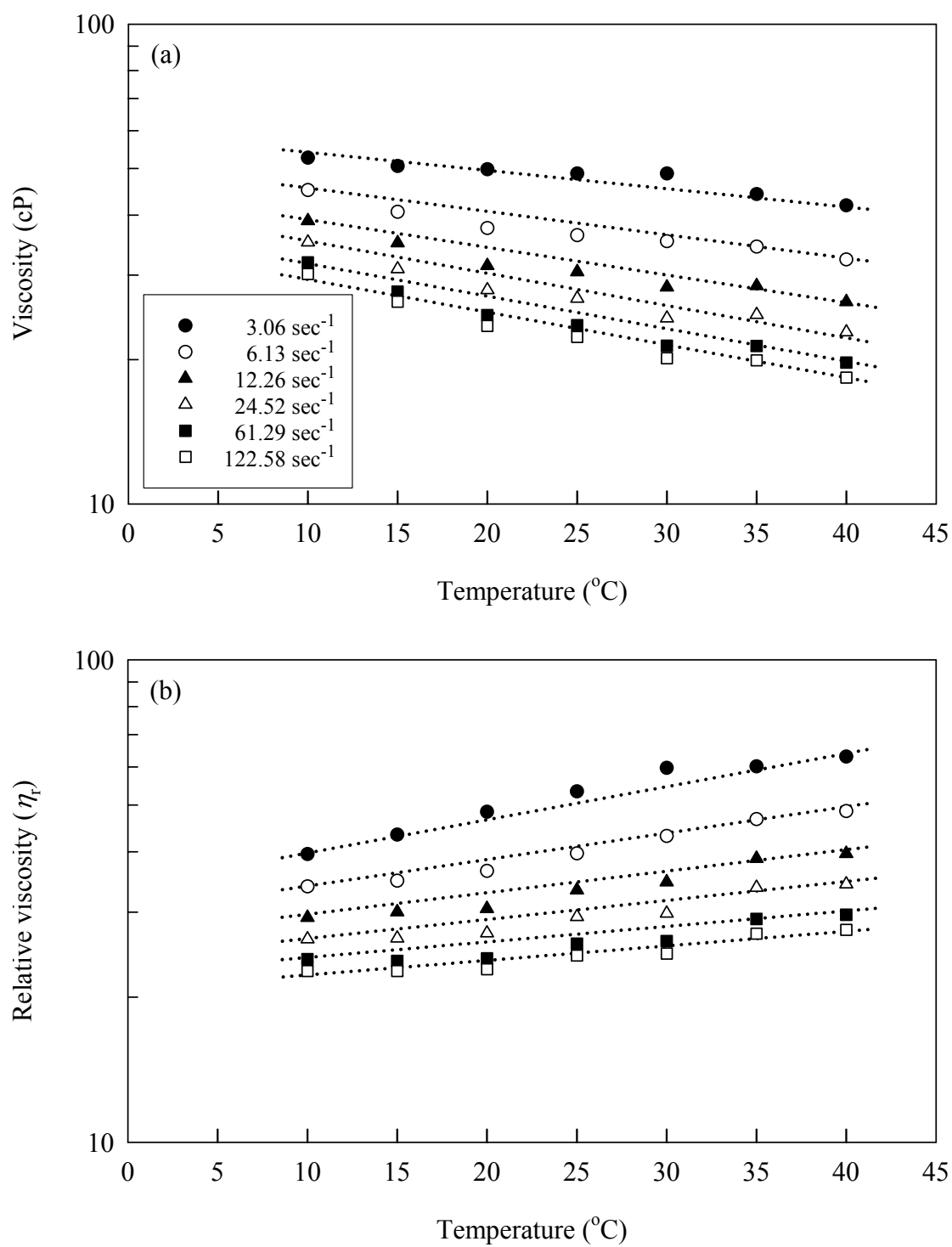


**Figure 4.24** Effect of temperature on (a) viscosity and (b) relative viscosity of UC<sub>3,56</sub> at various shear rates

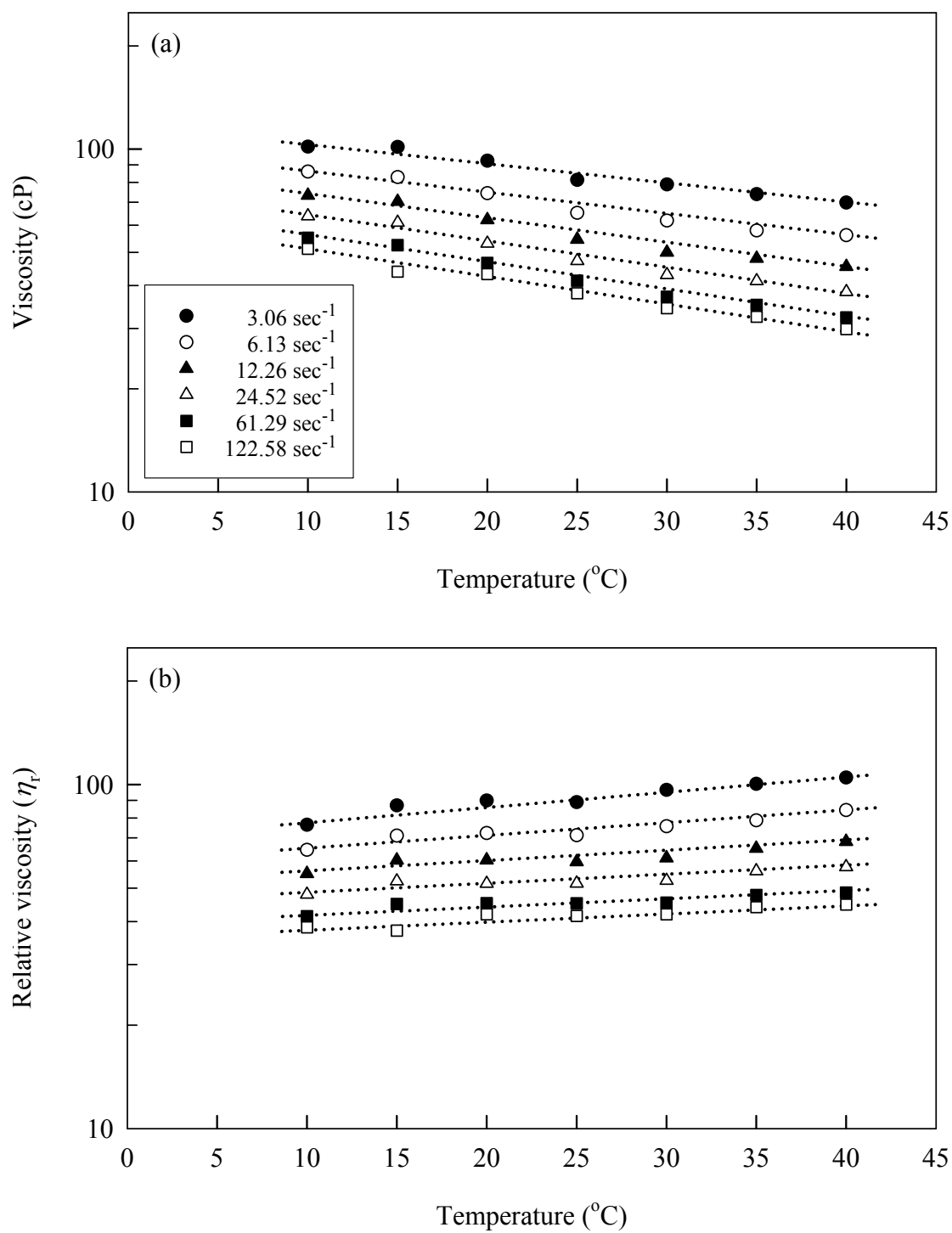


**Figure 4.25** Effect of temperature on (a) viscosity and (b) relative viscosity of UC<sub>3,60</sub> at various shear rates

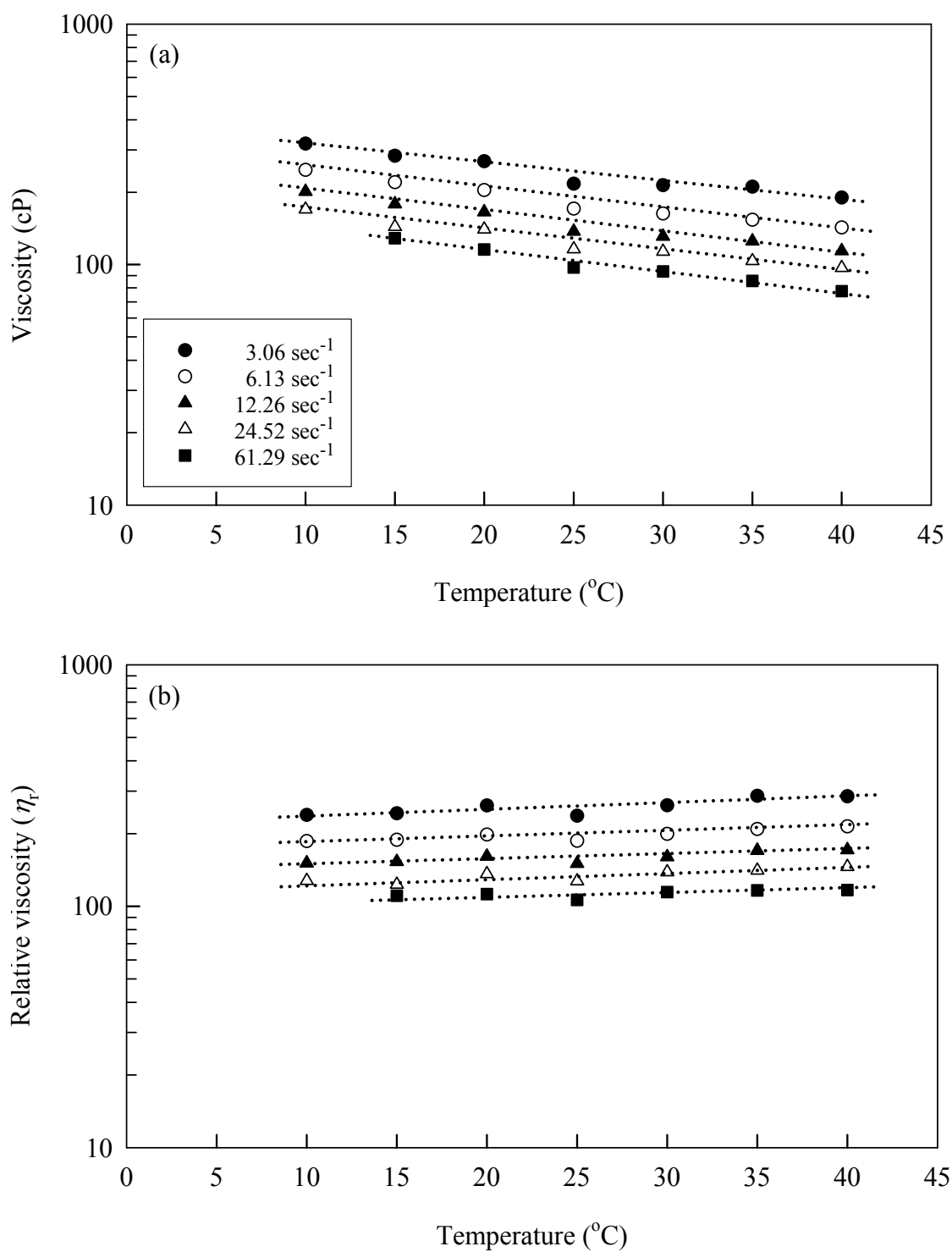


**Figure 4.26** Effect of temperature on (a) viscosity and (b) relative viscosity of UC<sub>3,64</sub> at various shear rates

#### 4.7 The viscosity model

Mathematical models have been developed for rheological behavior of colloidal suspension as mentioned in section 2.4. Two well-known viscosity models, namely Mooney and Krieger-Dougherty equation were employed. Mooney equation (equation 2.3) describes the relationship between relative viscosities of latex system with volume fraction of particle in exponential term. Krieger-Dougherty equation (equation 2.4) indicates the relationship between relative viscosity of latex system and volume fraction of polymer in power term of maximum volume fraction. Both equations are frequently employed in colloidal suspension of spherical particle system in volume fraction range of 0-0.70 (Quadrat et al., 2005, Bradna et al., 1996, Carlsson et al, 2006, Pishvaei et al., 2005). In this research, Mooney and Krieger-Dougherty equations were applied to deformable particles as NRL particles to investigate the applicability of both equations on NRL system.

Volume fraction of rubber particles ( $\phi_{\text{rubber}}$ ) can be calculated using equation 4.7. TSC (% by weight) was converted into volume fraction. TSC was assumed to represent mass of rubber particles.

$$\phi_{\text{rubber}} = \frac{\text{Volume of rubber}}{\text{Total volume}} \quad (4.7)$$

$$\phi_{\text{rubber}} = \frac{v_{\text{rubber}}}{v_{\text{rubber}} + v_{\text{water}}} \quad (4.8)$$

$$\text{Volume } (v_{\text{rubber}}) = \frac{\text{Mass } (m)}{\text{Density } (\rho)} = \frac{\text{TSC}}{\rho} \quad (4.9)$$

Equation 4.9 shows the relationship between volume with mass and density.

Substitution of equation 4.9 into 4.8 results in

$$\phi_{\text{rubber}} = \frac{\frac{\text{TSC}}{\rho_{\text{rubber}}}}{\frac{\text{TSC}}{\rho_{\text{rubber}}} + \left(\frac{100 - \text{TSC}}{\rho_{\text{water}}}\right)} \quad (4.10)$$

The volume fraction obtained from equation 4.10 was substituted into equation 2.3 for Mooney model and equation 2.4 for Krieger-Dougherty model. Experimental viscosity was fitted using CurveExpert<sup>®</sup> program version 1.34. The program can fit the data with math model and interpolate the data to find the constant value by Chi-square method. The  $[\eta]$  and  $\phi_{\text{max}}$  of NRL samples in both equations were obtained. Density of CC<sub>1</sub>, SC<sub>1</sub>, UC<sub>1</sub>, UC<sub>2</sub> and UC<sub>3</sub> used for calculation is listed in Table 4.7.

**Table 4.7** Density of natural rubber latexes

NRL samples	Density (g/cm <sup>3</sup> )
CC <sub>1</sub>	0.8975 ± 0.0023
SC <sub>1</sub>	0.8953 ± 0.0019
UC <sub>1</sub>	0.9002 ± 0.0023
UC <sub>2</sub>	0.8981 ± 0.0032
UC <sub>3</sub>	0.8953 ± 0.0009

Figures 4.27-4.31 show the illustration of relative viscosity at certain shear rates against volume fraction. By fitting, the dotted and solid lines are drawn according to Mooney and Krieger-Dougherty, respectively. Figure 4.27 displays the fitting of relative viscosity data of CC<sub>1</sub> at shear rate of 3.06 sec<sup>-1</sup> and 12.26 sec<sup>-1</sup>. The relative viscosity drawn according to Krieger-Dougherty equation showed better

fitting than Mooney equation at shear rate  $3.06 \text{ sec}^{-1}$  but no difference at  $12.26 \text{ sec}^{-1}$ . Figure 4.28 displayed the fitting of relative viscosity data of SC<sub>1</sub> sample with Mooney equation and Krieger-Dougherty equation at shear rate  $3.06 \text{ sec}^{-1}$ ,  $12.26 \text{ sec}^{-1}$  and  $92.68 \text{ sec}^{-1}$ . The fitting lines from both equations showed good fitting for relative viscosity data of SC<sub>1</sub>. Below 70% volume fraction, both equations gave insignificant difference in relative viscosity values. Above 70% volume fraction, both equations gave the small difference in relative viscosity. This is also observed in UC<sub>1</sub>, UC<sub>2</sub> and UC<sub>3</sub>.

The intrinsic viscosity  $[\eta]$  and maximum packing volume ( $\phi_{\text{max}}$ ) obtained from CurveExpert<sup>®</sup> fitting are listed in Table 4.8 using Mooney equation and Table 4.9 using Krieger-Dougherty equation. The correlation coefficient ( $R^2$ ) value is a statistical value that depicts the relationship between experimental data and regression model. If  $R^2$  equals to 1, the best fitting is obtained (Pongvichai, 2004).

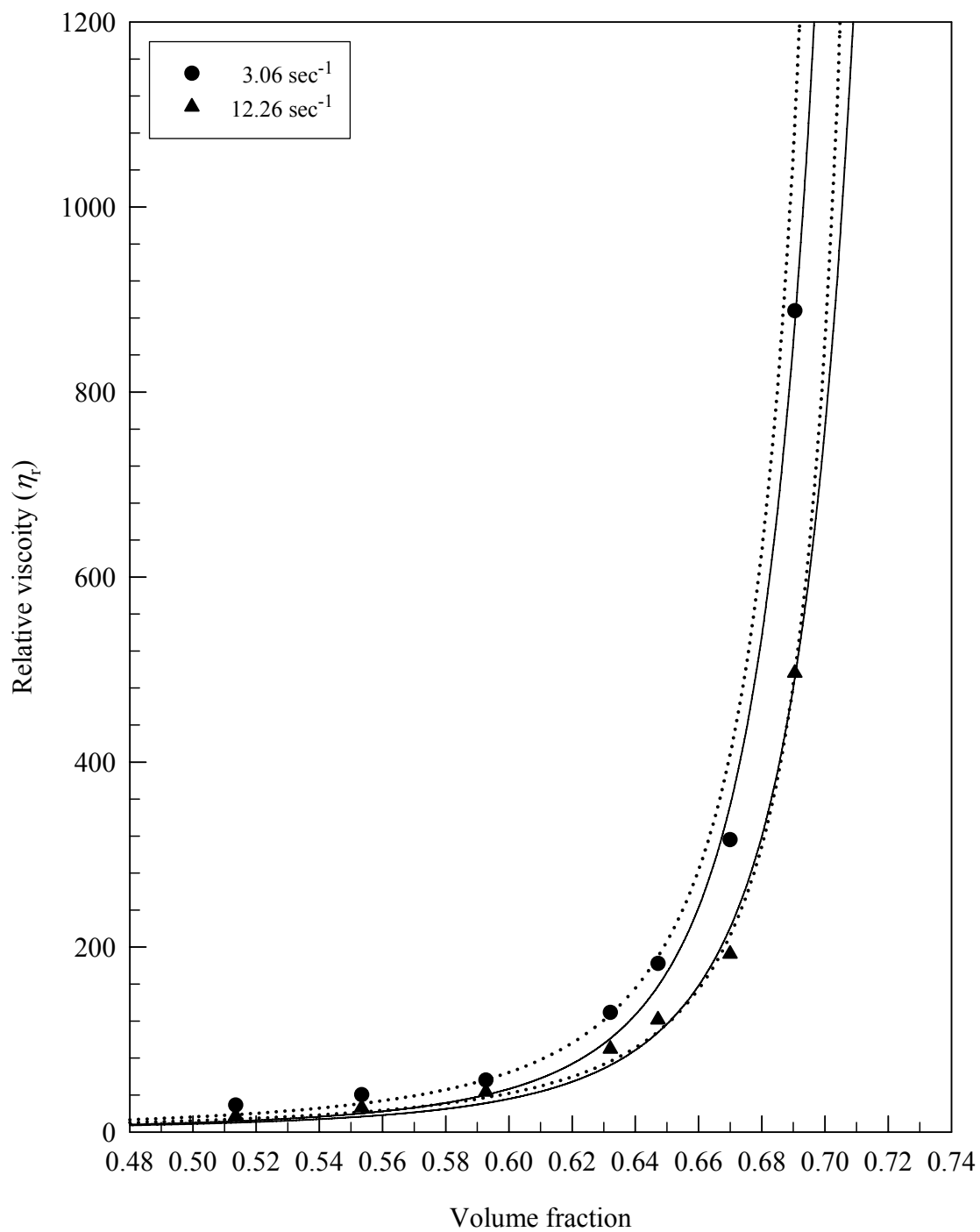


**Figure 4.27** Relative viscosity of  $\text{CC}_1$  at shear rate of 3.06 ( $\bullet$ ) and 12.26  $\text{sec}^{-1}$  ( $\blacktriangle$ ). The dotted lines are drawn according to Mooney equation. The solid lines are drawn according to Krieger-Dougherty equation.

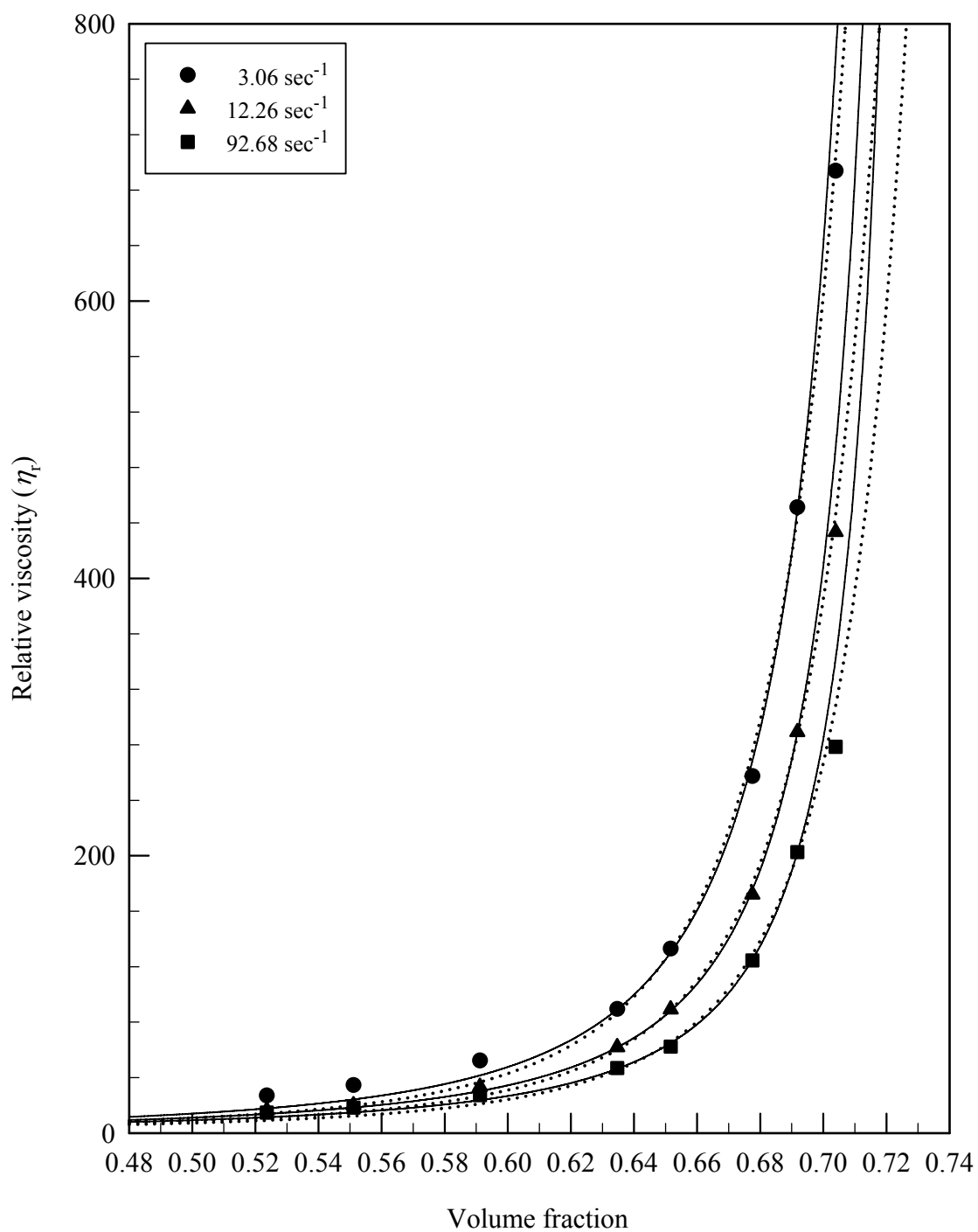


**Figure 4.28** Relative viscosity of  $\text{SC}_1$  at shear rate of 3.06 (●), 12.26  $\text{sec}^{-1}$  (▲) and 92.68  $\text{sec}^{-1}$  (■). The dotted lines are drawn according to Mooney equation. The solid lines are drawn according to Krieger-Dougherty equation.

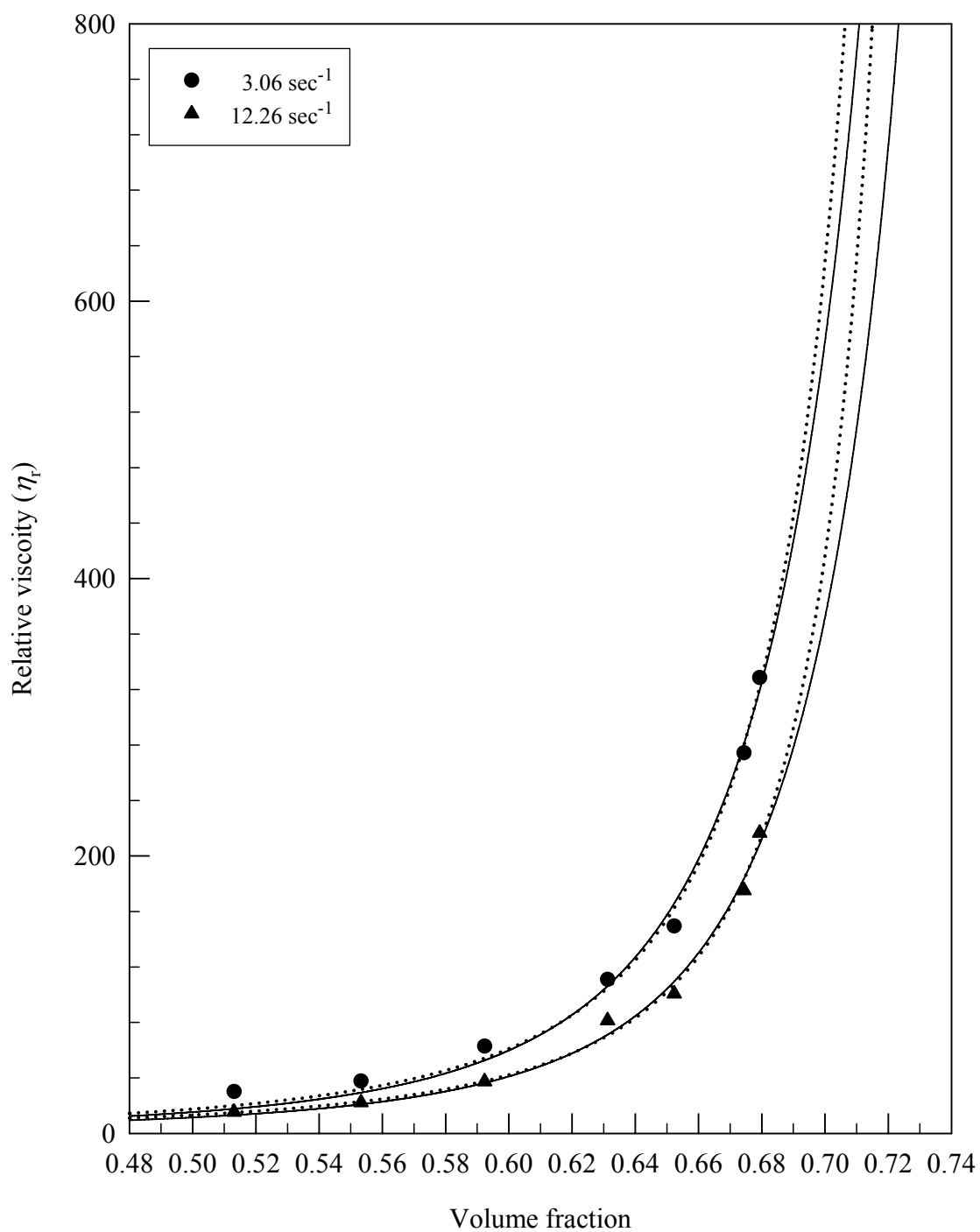


**Figure 4.29** Relative viscosity of UC<sub>1</sub> at shear rate of 3.06 (●) and 12.26  $\text{sec}^{-1}$  (▲). The dotted lines are drawn according to Mooney equation. The solid lines are drawn according to Krieger-Dougherty equation.

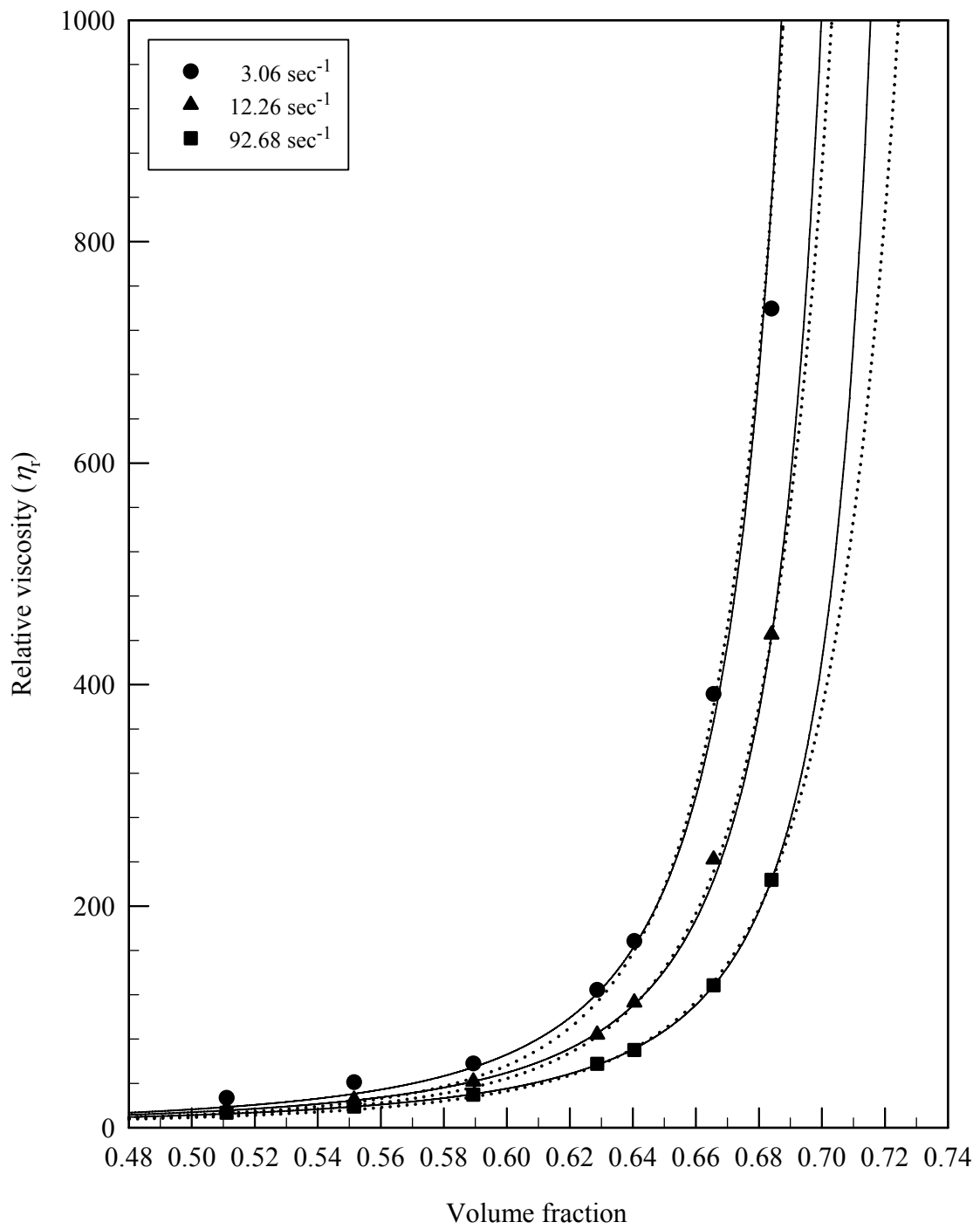


**Figure 4.30** Relative viscosity of UC<sub>2</sub> at shear rate of 3.06 (●), 12.26 sec<sup>-1</sup> (▲) and 92.68 sec<sup>-1</sup> (■). The solid lines are drawn according to Krieger-Dougherty equation. The dotted lines are drawn according to Mooney equation.

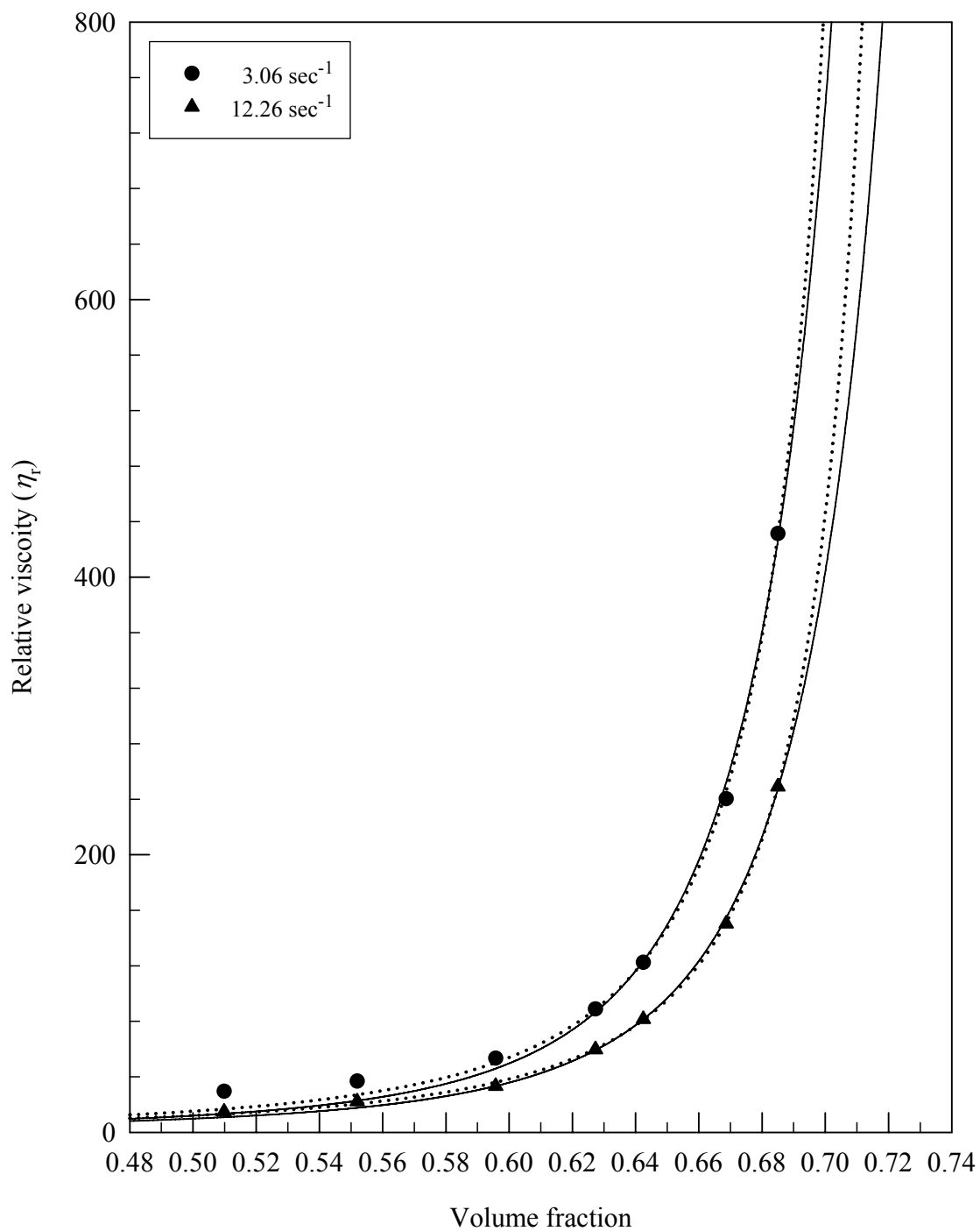


**Figure 4.31** Relative viscosity of  $\text{UC}_3$  at shear rate of  $3.06$  ( $\bullet$ ) and  $12.26 \text{ sec}^{-1}$  ( $\blacktriangle$ ). The dotted lines are drawn according to Mooney equation. The solid lines are drawn according to Krieger-Dougherty equation.

**Table 4.8** Maximum packing volume ( $\phi_{\max}$ ), intrinsic viscosity ( $[\eta]$ ) and correlation coefficient ( $R^2$ ) from graph fitting using Mooney equation

<b>NRL samples</b>	<b>Shear rate (sec<sup>-1</sup>)</b>	<b><math>\phi_{\max}</math></b>	<b><math>[\eta]</math></b>	<b><math>R^2</math></b>
CC <sub>1</sub>	3.06	0.8607	1.94	0.9965
	6.13	0.8685	1.92	0.9961
	12.26	0.8701	1.85	0.9952
SC <sub>1</sub>	3.06	0.9174	2.17	0.9965
	6.13	0.9124	2.05	0.9981
	12.26	0.9057	1.93	0.9985
	24.52	0.9022	1.85	0.9988
	92.68	0.8988	1.77	0.9975
UC <sub>1</sub>	3.06	1.0032	2.74	0.9955
	6.13	0.9820	2.51	0.9968
	12.26	0.9736	2.38	0.9955
	24.52	0.9704	2.29	0.9969
UC <sub>2</sub>	3.06	0.8646	2.05	0.9987
	6.13	0.8939	2.17	0.9994
	12.26	0.8893	2.06	0.9994
	92.68	0.9197	2.02	0.9994
UC <sub>3</sub>	3.06	0.9224	2.28	0.9973
	6.13	0.9267	2.19	0.9987
	12.26	0.9287	2.11	0.9993
	24.52	0.9268	2.03	0.9995

**Table 4.9** Maximum packing volume ( $\phi_{\max}$ ), intrinsic viscosity ( $[\eta]$ ) and correlation coefficient ( $R^2$ ) from graph fitting using Krieger-Dougherty equation

NRL samples	Shear rate ( $\text{sec}^{-1}$ )	$\phi_{\max}$	$[\eta]$	$R^2$
CC <sub>1</sub>	3.06	0.7316	3.32	0.9984
	6.13	0.7339	3.12	0.9982
	12.26	0.7340	2.99	0.9976
SC <sub>1</sub>	3.06	0.7517	3.21	0.9985
	6.13	0.7499	3.06	0.9995
	12.26	0.7473	2.92	0.9997
	24.52	0.7459	2.81	0.9999
	92.68	0.7444	2.69	0.9992
UC <sub>1</sub>	3.06	0.7758	3.57	0.9970
	6.13	0.7677	3.34	0.9970
	12.26	0.7638	3.18	0.9964
	24.52	0.7629	3.08	0.9974
UC <sub>2</sub>	3.06	0.7294	3.32	0.9997
	6.13	0.7395	3.37	0.9999
	12.26	0.7377	3.15	0.9999
	92.68	0.7478	2.94	0.9999
UC <sub>3</sub>	3.06	0.7497	3.30	0.9988
	6.13	0.7511	3.16	0.9996
	12.26	0.7517	3.03	0.9998
	24.52	0.7508	2.92	0.9999

The intrinsic viscosity values of latexes are in range of 1.5-2.8 cP for Mooney equation fitting and 2.6-3.6 cP for Krieger-Dougherty equation fitting. Both intrinsic viscosities obtained showed discrepancy from 2.5 as in Einstein equation. Einstein

equation was proposed for highly dilute suspension of non-interacting spheres and non-deformable particles in a Newtonian fluid (Lovell and El-Aasser, 1997). However, NRL particles are polydisperse and deformable. In addition, NRL viscosity was studied at high concentration. Thus higher intrinsic viscosity obtained than that in Einstein equation can be explained by high interaction and deformability of NRL system. Ammonia ( $\text{NH}_3$ ), tetramethyl thiuram disulphide (TMTD) and zinc oxide (ZnO) are normally added into commercial NRL concentrates to inhibit bacterial and latex coagulation. These stabilizers gave the stronger repulsive interaction among the particles and thus increased the intrinsic viscosity system (Staicu et al., 2005).

As seen in Table 4.8 and 4.9, maximum packing volume ( $\phi_{\max}$ ) is of 0.85-1.00 for Mooney equation fitting and of 0.73-0.77 for Krieger-Dougherty equation fitting. From purely geometric arguments, the maximum packing volume is estimated to lie between 0.52 to 0.74 (Carlsson et al., 2006). High  $\phi_{\max}$  in both equations could be the influence of degree of the deformability of rubber particles and degree of particle size distribution. The rubber particles are deformed upon the applied shear forces to accommodate in the space between the particles, similar to the penetration of small particles into the space between large particles. Thus the packing efficiency of rubber particles is high. Higher  $\phi_{\max}$  than that based on purely geometric arguments was also observed in multimodal synthetic latex (Schneider et al., 2002). In this experiment, unrealistic of  $\phi_{\max}$  value ( $\phi_{\max} > 1$ ) according to Mooney fitting was observed in UC<sub>1</sub>. This is explained by the effect of stabilizer in latex system. Mooney equation was not developed for multimodal system with potential particle-particle interaction (due to stabilizer) (Schneider et al., 2002).

From Table 4.8 and Table 4.9,  $\phi_{\max}$  of each latex sample showed insignificant

differences although the applied shear rates were changed. It suggests that  $\phi_{\max}$  is independent on the applied shear rates and represents an individual characteristic of each sample. The average maximum packing volume data was calculated and shown in Table 4.10. The average  $\phi_{\max}$  is found in order of  $UC_1 > UC_3 > SC_1 > UC_2 > CC_1$  for both fitting.

**Table 4.10** Average maximum packing volume calculated from Mooney equation and Krieger-Dougherty equation

NRL samples	Average maximum packing volume	
	Mooney equation	Krieger-Dougherty equation
CC <sub>1</sub>	0.8664 ± 0.0050	0.7332 ± 0.0014
SC <sub>1</sub>	0.9073 ± 0.0076	0.7478 ± 0.0029
UC <sub>1</sub>	0.9823 ± 0.0148	0.7676 ± 0.0059
UC <sub>2</sub>	0.8918 ± 0.0226	0.7386 ± 0.0075
UC <sub>3</sub>	0.9262 ± 0.0027	0.7508 ± 0.0008

By fitting the viscosity with both equations, it was found that correlation coefficients ( $R^2$ ) are greater than 0.99. It means that both equations can be used in polydisperse and deformable system such as in NRL concentrates. Based on higher correlation coefficient, Krieger-Dougherty equation is more suitable to apply to NRL concentrates.

## **CHAPTER V**

### **CONCLUSIONS**

The aim of this research work was to investigate the effect of particle size, PSD, TSC and temperature on the viscosity of NRL concentrates. The samples used in this study can be classified into two categories: (i) NRL concentrates samples were directly diluted from received latex and (ii) NRL re-centrifuged samples were diluted from re-centrifuged latex. From laser diffraction, the z-average diameter is in range of 0.74-0.93  $\mu\text{m}$  for directly diluted NRL samples and 0.81-0.89  $\mu\text{m}$  for diluted re-centrifuged NRL. The NRL concentrates showed polydisperse system, with the particle size distribution index ( $P_d$ ) ranging from 1.08-1.13 for directly diluted NRL samples and 1.09-1.14 for diluted re-centrifuged NRL. TEM micrographs showed the spherical shape and polydisperse rubber particles.

All NRL samples showed the shear thinning behavior at shear rate range of 3.06-122.58  $\text{sec}^{-1}$ . As the shear rate increased, the rubber particles became deformable and aligned with the direction of flow, resulting in the decrease in viscosity. High TSC samples showed strong change with shear rate than low TSC. Preparation methods showed no significant difference in latex viscosity at the same TSC (in range of 48-60% TSC).

Large particles gave lower viscosity than small particles. Increasing particle size increased the average distance between the surfaces of neighboring particles and decreased the surface area per unit volume of particle. Thus the viscosity decreased. In the polydisperse system, the small particles can be accommodated between

the larger ones, reducing the average distance between neighboring particles. This increased the strength between the particles and the packing efficiency. As a result, the viscosity increased. The less effect of particle size and PSD on latex viscosities was observed when applied shear rates were increased. As the shear rate increased, the rubber latexes became deformable and aligned with the direction of flow. Then the effect of particles surface could be reduced.

The relative viscosity of all NRL samples increased as a function of TSC. The viscosity slowly increased with increasing TSC until the  $TSC_c$  limit. Upper than  $TSC_c$  limit, the viscosity rapidly increased with increasing TSC. In addition,  $TSC_c$  showed the independence of the applied shear rates. The rapid increase of viscosity at upper than  $TSC_c$  is explained by the close to the maximum packing volume ( $\phi_{max}$ ) of particle system. The  $TSC_c$  was observed in range of 58-60% (by weight) TSC for directly diluted NRL and 59-61% TSC (by weight) for diluted re-centrifuged NRL.  $TSC_c$  of large rubber particle system was observed at lower value than that of the small particle system. This is due to the higher chance of small particles to penetrate into the space between the large particles to approach the maximum packing volume ( $\phi_{max}$ ).

The latex viscosity decreased with temperature in range of 10-40°C. This may be because of the decrease of the interaction forces between particles or a disappearance of the water bridges due to evaporation. However, the relative viscosity of latex showed an increase with temperature. It indicates that the viscosity of medium changes more dramatic than viscosity of latex itself with temperature.

Mooney and Krieger-Dougherty equations showed the good fitting in latex viscosity. The correlation coefficients ( $R^2$ ) obtained from both equations are higher

than 0.99. The intrinsic viscosity values of latexes are in range of 1.5-2.8 cP for Mooney fitting and 2.6-3.6 cP for Krieger-Dougherty fitting. Higher intrinsic viscosities from both equations than Einstein equation can be explained by high concentration of latex particles and deformability of latex particles. The average maximum packing volumes are observed in range of 0.86-0.82 for Mooney fitting and 0.73-0.77 for Krieger-Dougherty fitting. With the higher  $R^2$  obtained in Krieger-Dougherty equation, it suggests that Krieger-Dougherty equation is more suitably applied to NRL concentrated than Mooney equation.

## REFERENCES

- Berend, K., and Richtering, W. (1995). Rheology and diffusion of concentrated monodisperse and bidisperse polymer latexes. **Colloids and Surfaces**. 99: 101-119.
- Blackley, D.C. (1997). **Polymer latexes: Science and technology**. (2<sup>nd</sup> ed.). New York: Chapman & Hall.
- Bozzola, J.J., and Russell, L.D. (1999). **Electron microscopy: principles and techniques for biologists** (2<sup>nd</sup> ed.). Miami: Jones and Bartlett Publishers, Inc.
- Bradna, P., Stern, P., Quadrat, O., and Snuparek, J. (1996). Thickening of electrostatically stabilized latexes by ethyl acrylatemethacrylic acid copolymers with various molecular weights. **Colloids and Surfaces**. 113: 1-10.
- Cacioli, P. (1997). Introduction to latex and the rubber industry. **Rev. fr. Allegol**. 37 (8): 1173-1176.
- Carlsson, G., Jarnstrom, L., and Stam, J.V. (2006). Latex diffusion at high volume fractions studied by fluorescence microscopy. **J. Colloid and Interface Science**. 298 (1): 162-171.
- Chu, F., Guillot, J., and Guyot, A. (1998). Rheology of concentrated multi-sized poly (St/BA/MMA) latexes. **Colloid Polym Sci**. 276: 305-312.

- Cornish, K., and Brichta, J.L. (2002). Some rheological properties of latex from *Parthenium Argentatum* Gray compared with latex from *Hevea brasiliensis* and *Ficus elastica*. **J. Poly and Envi.** 112: 13-18.
- Crowther, B.G. (1982). **Processing Technology in Rubber Technology and Manufacture.** London: Plastics and Rubber Institute.
- Elizalde, O., Leal, G.P., and Leiza, J.R. (2000). Particle size distribution measurements of polymeric dispersions: a comparative study. **Particle and particle size characterization journal: Part. Syst. Charact.** 17: 236-243.
- Greenwood, R., Luckham, P.F., and Gregory, T. (1995). The effect of particle size on the layer thickness of a stabilizing polymer adsorbed onto two different classes of polymer latex, as determined from rheological experiments. **Colloids and Surfaces.** 98: 117-125.
- Greenwood, R., Luckham, P.F., and Gregory, T. (1998). Minimizing the viscosity of concentrated dispersions by using bimodal particle size distributions. **Colloids and Surfaces.** 144: 139-147.
- Hall, R.J. (2000). **Statistics-Introductions to basic concepts.** [Online]. Available: <http://bobhall.tamu.edu/FiniteMath/Module8/Introduction.html>
- Horsky, J., Quadrat, O., Porsch, B., Mrkvickova, L., and Snuparek, J. (2001). Effect of alkalization on carboxylated latexes prepared with various amount of a non-ionogenic hydrophilic co monomer 2-hydroxyethyl methacrylate. **Colloids and Surfaces.** 180: 75-85.
- Hunter, R.J. (1992). **Foundations of colloid science Volume I.** New York: Oxford University Press Inc.

- Hunter, R.J. (1992). **Foundations of colloid science Volume II**. New York: Oxford University Press Inc.
- Hunter, R.J. (1993). **Introduction to modern colloid science**. New York: Oxford University Press Inc.
- Hyams, D.G. (1997). CurveExpert (version 1.34) [Computer software] Mississippi.
- Israelachvili, J. (1997). **Intermolecular and surface forces**. San Diego: Academic Press Inc.
- Johnson, P.H., and Kelsey, R.H. (1958). **Rubber world** 138: 877.
- Jones, A.R., Leary, B., and Boger, D.V. (1991). The rheology of a concentrated colloidal suspension of hard spheres. **J. Colloid and Interface Science**. 147: 479-495.
- Kroschwitz, I. and Jacqueline, I. (1990). **Concise encyclopedia of polymer science and engineering**. New York: John Wiley and Sons, Inc.
- Krieger, I.M. and Dougherty, T.J. (1959). **Trans. Soc. Rheol.**, 3: 137
- Larson, R.G. (1999). **The structure and rheology of complex fluids**. New York: Oxford university press.
- Lovell, P.A., and El-Aasser, M.S. (ed.) (1997). **Emulsion polymerization and emulsion polymers**. New York: John Wiley and Sons, Inc.
- Luckham, P.F., and Ukeje, M.A. (1999). Effect of particle size distribution on the rheology of dispersed systems. **J. Colloid and Interface Science**. 220: 347-356.
- Matthan, R.K. (ed.) (1998). **Rubber engineering**. New York: McGraw-Hill.
- Malvern Instrument Ltd. (1999). Sizer<sup>®</sup> (version 2.19) [Computer software] England.

- Mewis, J., and Vermant, J. (2000). Rheology of sterically stabilized dispersions and latexes. **Progress in Organic Coatings** 40: 111-117.
- Mooney, M. (1951). **J. Rheol.**, 2: 210.
- Ngothai, Y., Bhattacharya, S.N., and Coopes, I.H. (1995). Effect of temperature on the flow behavior of polystyrene latex-gelatin dispersions. **J. Colloid and Interface Science.** 172: 289-296.
- Nopnit, V. (1985). **Practical TEM for biological scientists.** Bangkok: Chulalongkorn Publication.
- Pishvaei, M., Graillat, C., McKenna, T.F., and Cassagnau, P. (2005). Rheological behavior of polystyrene latex near the maximum packing fraction of particles. **Polymer.** 46: 1235-1244.
- Pongvichai, S. (2004). **Statistical analysis by using computer.** Bangkok: Chulalongkorn Publication.
- Press, W.H., Teukolsky, S.A., Vetterling, W.T., and Flannery, B.P. (2002). **Numerical recipes in C++: The art of scientific computing (2<sup>nd</sup>).** New York: Cambridge university press.
- Quadrat, O., Snuparek, J., Mikesova, J., and Horsky, J. (2005). Effect of “hard” co monomers styrene and methyl methacrylate in ethyl acrylate/acrylic acid latexes on their thickening with associative thickener. **Colloids and Surfaces.** 253: 163-168.
- Quemada, D., and Berli, C. (2002). Energy of interaction in colloids and its implications in rheological modeling. **Advances in Colloid and Interface Science.** 98: 51-85.

- Rat, P., and Sirin, C (1986). Para rubber **Thai Junior Encyclopedia Project**. Bangkok: Chulalongkorn Publication.
- Rawle, A. (2000). **Basic principles of particles size analysis**. [Online]. Available: [http://www.malvern.co.uk/malvern/kbase.nsf/0/5E3F5A148D336B048D3360480256BF2006E2195/\\$file/Basic\\_principles\\_of\\_partilce\\_size\\_analysis\\_MRK034-low\\_res.pdf](http://www.malvern.co.uk/malvern/kbase.nsf/0/5E3F5A148D336B048D3360480256BF2006E2195/$file/Basic_principles_of_partilce_size_analysis_MRK034-low_res.pdf)
- Rhodes, E., and Smith, H.F. (1939). The viscosity of preserved and concentrated latex. **The India-Rubber Journal**. 7: 241.
- Rippel, M.M., Lee, L., Leite, C.A.P., and Galembeck, F. (2003). Skim and crem natural rubber particles: colloidal properties, coalescence and film formation. **J. Colloid and Interface Science**. 268: 330-334.
- Rodriguez, B.E. and Kaler E.W. (1992). Binary mixture of monodisperse latex dispersions. 2. viscosity. **Langmuir**. 8: 2382-2389.
- Rouilly, A., Rigal, A., and Gilbert, R.G. (2004). Synthesis and properties of composites of starch and chemically modified natural rubber. **Polymer**. 45: 7813-7820
- Sanguansap, K., Suteewong, T., Saendee, P., Buranabunya, U., and Tangboriboonrat, P., (2005). Composite natural rubber based latex particles: a novel approach. **Polymer**. 46: 1373-1378.
- Schneider, M., Claverie, J., Grailliat, C., and Mckenna, T.F. (2002). High solids content emulsions. I. A study of the influence of the particle size distribution and polymer concentration on viscosity. **J. Appl Polym Sci**. 84 (10): 1878-1896.

- Schneider, M., and Mckenna, T.F. (2002). Comparative study of methods for the measurements particle size and size distribution of polymeric emulsions. **Particle and particle size characterization journal: Part. Syst. Charact.** 19: 28-37.
- Schramm, L.L. (2001). **Dictionary of colloid and interface science (2<sup>nd</sup>)**. New York: John Wiley and Sons, Inc.
- Staicu, T., Micutz., M., and Leca, M. (2005). Electrostatically and electrosterically stabilized latexes of acrylic copolymers used as pressure-sensitive adhesives. **Progress in organic coatings.** 53: 56-62.
- Stimson, D. (2000). **The mastersizer S – flexibility in particle sizing.** [Online]. Available:<http://www.malvern.co.uk/common/downloads/MRK366-0LLR.pdf>
- Tantatherdtam, R. (2003). **Reinforcement of natural rubber latex by nanosize montmorillonite clay** [Online]. Ph.D. Dissertation, The Pennsylvania state university, America. Available:<http://etda.libraries.psu.edu/theses/approved/WorldWideFiles/ETD-350/Rattana.pdf>
- Rubber Research Institute of Thailand (2006). **Economic and Marketing of rubber in Thailand** [Online]. Available: <http://www.rubberthai.com/information/info/econ.pdf>
- Varkey, J.T., Rao, S.S., and Thomas, S. (1995). Rheological behavior of natural and synthetic rubber latexes in the presence of surface active agents. **Plastics, Rubber and Composites processing and Applications** 23: 249-257.
- Westall, B. (1968). The molecular weight distribution of natural rubber latex. **Polymer.** 9: 243-248.

## **APPENDIX A**

# **DENSITY AND VISCOSITY OF WATER AT DIFFERENT TEMPERATURES**

**Table A.1** Density and viscosity of water at different temperatures (Yaws, 1999)

<b>Temperature (°C)</b>	<b>Density, <math>\rho</math> (g/cm<sup>3</sup>)</b>	<b>Viscosity, <math>\eta</math> (cP)</b>
5	1.0456	1.5304
10	1.0412	1.3308
15	1.0367	1.1661
20	1.0321	1.0292
25	1.0276	0.9144
30	1.0230	0.8177
35	1.0184	0.7356
40	1.0138	0.6654
45	1.0091	0.6051

## **APPENDIX B**

### **POSTER PRESENTATIONS**

**Poster presentations presented in Thailand.**

1. Jatuporn Sridee, Chantima Deeprasertkul and Chaiwat Rusakulpiwat (10-11 August 2004). “Effect of total solids content on the viscosity of natural rubber latex concentrated”, Poster Presentation, **The 4<sup>th</sup> National Symposium on Graduate Research**, Lotus Hotel Pang Suan Kaew, Chiang Mai, Thailand.
2. Jatuporn Sridee, Chantima Deeprasertkul and Chaiwat Rusakulpiwat (18-20 October 2005). “Applicability of Mooney and Krieger-Dougherty equations to natural rubber latex”, Poster Presentation, **31<sup>st</sup> Congress on Science and Technology of Thailand**, Suranaree University of Technology, Nakhon Ratchasima, Thailand.

## **BIOGRAPHY**

Mr. Jatuporn Sridee born in Suphanburi, Thailand on Tuesday July 31<sup>st</sup>, 1979. He graduated with his Bachelor Degree in Chemical Engineering from Suranaree University of Technology in 2001. Then he continued his Master Degree in School of Polymer Engineering at institute of Engineering, Suranaree University of Technology. His research studied in the topic of the rheological properties of natural rubber latex. While he studying in Master Degree, he presented two posters entitled of “Effect of total solids content on the viscosity of natural rubber latex concentrated” and “Applicability of Mooney and Krieger-Dougherty equations to natural rubber latex (Appendix B).